

IMPACT OF LATERAL SWELL PRESSURE ON
RETAINING STRUCTURE DESIGN USING
EXPANSIVE COHESIVE BACKFILL

by

MARK G. THOMAS

Presented to the Faculty of the Graduate School of The University of Texas at Arlington
in Partial Fulfillment of the Requirements for the Degree of

MASTER OF SCIENCE IN CIVIL ENGINEERING

THE UNIVERSITY OF TEXAS AT ARLINGTON

MAY 2008

Copyright © by Mark G. Thomas 2008

All Rights Reserved

ACKNOWLEDGEMENTS

I wish to take this opportunity to thank the many people who supported and encouraged me throughout this endeavor after a 20-year hiatus from academic life. I extend particular gratitude and appreciation to my wife Ginger for her support, encouragement and, above all, patience during these most challenging last few years; and also to my mother Sandi for her unwavering support.

I would also like to express my sincerest thanks to my advisor and friend, Dr. Anand J. Puppala, Ph.D., P.E., for suggesting the research topic in this largely unexplored area of geotechnical study; and for his direction, insight and advice during the research and preparation of this paper for presentation. In addition, I wish to thank the geotechnical faculty of the University of Texas at Arlington, Drs. Puppala, Laureano Hoyos, Ph.D., P.E., and M. Sahadat Hossain, Ph.D., P.E., for providing me with the educational tools necessary to pursue this endeavor.

Further, I would like to thank my colleagues and friends at Fugro Consultants, Inc., who have supported me during this pursuit, especially Mr. David Lutz, P.E., for his vigilant concern and unswerving friendship; Ms. Karen Pimsner, likewise for her concern and friendship, and not least for her editing prowess and for consenting to serve as proofreader; and Mr. Saad Hineidi, P.E., for approving company financial support for the first 3 years of graduate studies.

Finally, I would like to thank Messrs. Aubrey D. (Pete) Henley, P.G., and John W. Johnston, P.E., my former employers at Henley-Johnston and Associates, Inc., for providing me my first real opportunity to serve in the geotechnical/engineering consulting field. Their educational and practical insights I gained during my tenure with them are too numerous to mention.

April 11, 2008

ABSTRACT

IMPACT OF LATERAL SWELL PRESSURE ON RETAINING STRUCTURE DESIGN USING EXPANSIVE COHESIVE BACKFILL

Mark G. Thomas, M.S.

The University of Texas at Arlington, 2008

Supervising Professor: Anand J. Puppala

Since cohesive soils are difficult to drain once becoming saturated, in order to reduce lateral earth pressures exerted by saturated cohesive soils on retaining structures, retaining wall designs most always specify use of drainable granular backfill. However, costs for the importation of granular backfill materials continues to increase due to depletion of these materials in certain areas, and to the ever-increasing costs for material transportation, largely related to increased labor and fuel prices. These factors, together with the costs of removing replaced cohesive materials, and coupled with resource and environmental conservation concerns, are driving efforts to develop reasonable and prudent design methods for retaining structures using on-site cohesive soil backfill.

Traditional design using non-expansive cohesive backfill is well established. However, certain cohesive fill materials exert lateral swell pressures as soil moisture contents increase. If these pressures are not accommodated in the structure design, the stability of the structure will be reduced, potentially to the point of failure.

This thesis study reviews certain properties of cohesive soils and their impact on retaining structure design, reviews relevant research pertaining to the determination of lateral swelling pressure performed by others, and attempts to correlate the implications of the previous research with the properties of cohesive soils in order to assess the impact of lateral swelling pressure on external structure stability. This effort was undertaken as a precursor to the development of a method for predicting the magnitude of the lateral swelling pressure component of lateral earth pressure for use in developing new and prudent design methodologies for retaining structures. The recommendations resulting from this thesis work have been formulated with this end result as the central focus.

TABLE OF CONTENTS

ACKNOWLEDGEMENTS	iii
ABSTRACT	v
LIST OF ILLUSTRATIONS.....	x
LIST OF TABLES.....	xiv
Chapter	Page
1. INTRODUCTION	1
1.1 General.....	1
1.2 Research Objectives.....	4
1.3 Organizational Outline.....	5
2. PROPERTIES OF COHESIVE SOILS	6
2.1 Introduction.....	6
2.2 Clay Chemistry	10
2.2.1 General.....	10
2.2.2 Kaolinite, Illite, Smectite	12
2.3 Plasticity and Atterberg Limits	17
2.3.1 Definitions and Relevance	17
2.3.2 Atterberg Limits.....	18
2.4 Activity	21

2.5 Capillarity and Matric Suction.....	22
2.5.1 Capillarity	22
2.5.2 Matric Suction.....	24
2.6 Time-Dependent Considerations	24
3. SWELL PRESSURE MEASUREMENTS: BACKGROUND	26
3.1 Introduction.....	26
3.2 Laboratory Measurements of Swell and Swell Pressure.....	27
3.2.1 One-Dimensional Swell Tests.....	27
3.2.2 Three-Dimensional Swell Tests.....	33
3.2.2.1 General.....	33
3.2.2.2 Previous Research – Modified Oedometer Tests	34
3.2.2.3 Previous Research – Modified Triaxial Cell Tests.....	39
3.2.2.4 Previous Research – Other Investigations	41
3.2.3 Comparisons and Implications of Laboratory Tests	42
3.3 Field Measurements of Swell and Swell Pressure	44
3.3.1 Instrumented Field Studies	44
3.3.2 In situ Test Apparatus	50
3.3.3 Large-scale Study.....	53
3.3.4 Pilot-scale Study	59
3.4 Comparisons of Laboratory and Field Measurements	64
3.5 Summary of Literature Review Findings.....	65
4. TRADITIONAL RETAINING WALL DESIGN	68

4.1 Introduction.....	68
4.2 Basic Concepts.....	69
4.3 Rigid Walls	74
4.3.1 Lateral Earth Pressures Acting on Rigid Walls Using Granular Backfill.....	75
4.3.2 Lateral Earth Pressures Acting on Rigid Walls Using Cohesive Backfill	77
4.3.3 Wall Stability Calculations	79
4.4 Flexible (MSE) Walls	92
4.4.1 Lateral Earth Pressures Acting on Flexible Walls Using Granular Backfill.....	93
4.4.2 Lateral Earth Pressures Acting on Flexible Walls Using Cohesive Backfill	94
4.4.3 Wall Stability for Flexible Walls	95
5. EFFECTS OF LATERAL SWELL PRESSURE ON CALCULATED FACTORS OF SAFETY	101
5.1 Introduction.....	101
5.2 Lateral Swell Pressure Effect on External Stability Calculations	101
5.3 Local Case Study – MSE Wall	109
6. FINDINGS AND CONCLUSIONS	116
7. RECOMMENDATIONS FOR FUTURE RESEARCH.....	118
REFERENCES	124
BIOGRAPHICAL SKETCH	130

LIST OF ILLUSTRATIONS

Figure		Page
1.1	Wall Failure Along Dam Spillway	2
1.2	MSE Wall Failure Along Highway.....	2
1.3	Severe Wall Distress	3
1.4	Severe Wall Distress	3
2.1	Grain-size Classification Systems.....	7
2.2	Pavement Heave.....	8
2.3	Pavement Heave and Cracking.....	9
2.4	Structural Distress.....	9
2.5	Brick Facia Cracking	10
2.6	Clay Mineralogical Crystal Structure	11
2.7	Structure of 1:1 Clay Minerals.....	13
2.8	Structure of Micalike Clay Minerals.....	13
2.9	Structure of Smectite Minerals	13
2.10	Four States of Cohesive Soil Behavior	18
2.11	Plasticity Chart.....	21
2.12	Capillary Rise versus Meniscus Radii	23
3.1	Conventional Lever Arm Consolidometer.....	28
3.2	Series of Lever Arm Consolidometers.....	29

3.3	Pneumatic Consolidometer and Sample Confining Ring	30
3.4	Direct Load Consolidometer.....	31
3.5	Thin-walled Consolidation Ring.....	34
3.6	Lateral Swell Pressure Ring Mark II (LSP MK II).....	35
3.7	LSP MK II and Equipment Setup.....	36
3.8	Relationship Between Initial Water Content, Lateral Swell Pressure and Vertical Swell.....	38
3.9	Triaxial Swell Test Cell	40
3.10	Triaxial Swell Test Apparatus	41
3.11	Measured Heave versus Predicted Heave	43
3.12	Retaining Wall Instrumentation Plan View	45
3.13	Retaining Wall Instrumentation Profile	46
3.14	Lateral Earth Pressure Development Over Time For Selected Earth Pressure Cells.....	47
3.15	Lateral Earth Pressure Development With Depth.....	48
3.16	Field Instrumentation for Heave Measurements.....	49
3.17	Test Site Measured Data. Vertical Swell, Moisture Content and Suction Changes.....	50
3.18	In situ Swelling Pressure Probe MK II System	51
3.19	In situ Swelling Pressure Probe MK II	52
3.20	Large-scale Experiment Setup	54
3.21	Large-scale Experiment Instrumentation	55
3.22	Lateral Pressure Development versus Depth	57
3.23	Lateral Swell Pressure versus Depth Using CNS Backing.....	58

3.24	Experimental Retaining Wall.....	60
3.25	Minimum Moisture Content to Avoid Swelling versus PI	63
3.26	Interpreted Lateral Swell Pressure Distribution.....	67
4.1	Common Types of Retaining Walls.....	69
4.2	Lateral Earth Pressures From the 3 Main Pressure Components: Soil, Surcharge and Water	70
4.3	At-Rest, Active and Passive Pressures on Retaining Structures.....	71
4.4	Lateral Earth Pressures on Conventional Rigid or Flexible Walls	75
4.5	Rankine Active Force (P_a) and Point of Application.....	76
4.6	Coulomb Active Force (P_a) and Point of Application	77
4.7	Rankine Lateral Earth Pressure Distribution and the Location of Tensile Crack Development With Cohesive Soil Backfill	79
4.8	Four Common Modes of Retaining Structure Failure	80
4.9	Generalized Rigid Wall Geometry.....	83
4.10	Factors of Safety With Respect to Sliding (Based on Data From Table 4.1).....	87
4.11	Factors of Safety With Respect to Sliding Using a Keyway (Based on Data From Table 4.2).....	89
4.12	Factors of Safety With Respect to Sliding Using a Keyway and Assuming a Moderate Water Level (Based on Data From Table 4.3).....	91
4.13	Comparison of Factors of Safety with Respect to Sliding for a 25-foot Tall Wall (Based on Data From Tables 4.1 Through 4.3)	91
4.14	Block and Stepped MSE Walls.....	92
4.15	Lateral Earth Pressure on MSE Wall. Soil and Surcharge Only.....	94

4.16	Failure Plane for MSE Wall Reinforcement Length Determination	96
4.17	Bi-Linear Potential Failure Plane for Inextensible Reinforcements.....	96
4.18	Variable Vertical Reinforcement Spacing	99
5.1	Interpreted Lateral Swell Pressure Distribution.....	103
5.2	Generalized Rigid Wall Geometry.....	103
5.3	Factors of Safety With Respect to Sliding Using a Keyway, Assuming a Moderate Water Level and Lateral Swell Pressure (Based on Data From Table 5.1).....	106
5.4	Comparison of Factors of Safety With Respect to Sliding for a 25-foot Wall (Based on Data From Tables 4.3 and 5.1)	107
5.5	Comparison of Factors of Safety With Respect to Sliding for a 25-foot Wall (Based on Data From Table 4.2).....	109
5.6	Local MSE Wall Failure Due to Sliding.....	110
5.7	Lateral Earth Pressure on MSE Wall	111

LIST OF TABLES

Table		Page
2.1	Clay Mineral Particle Size and Specific Area.....	16
2.2	Liquid and Plastic Limits of Well-known Clays.....	20
3.1	Lateral Swell Pressure Variation With Surcharge	37
3.2	Lateral Swell Pressure Variation With Initial Water Content	38
3.3	Average Lateral Swell Pressure Developed During Pilot-scale Test	62
3.4	Literature Review Conclusions.....	66
4.1	Soil Parameter and Geometric Definitions for Examples.....	84
4.2	Factors of Safety versus Wall Height and Footing Heel Width.....	86
4.3	Comparisons of Factors of Safety Against Sliding With and Without 4-foot Deep Keyway Below Base of Footing	88
4.4	Comparison of Factors of Safety Against Sliding With Differing Water Levels	90
5.1	Factors of Safety vs. Wall Height and Footing Heel Width	105
5.2	Factors of Safety With Respect to Sliding for Differing Magnitudes of Lateral Swell Pressure Development.....	108

CHAPTER 1

INTRODUCTION

1.1 General

Most retaining wall designs, both rigid and flexible, specify the use of granular materials (sand and/or gravel) as the backfill behind those structures, primarily because the methods for calculating earth pressures on the walls are relatively simple and well established (Coulomb, 1776; Rankine, 1857). This simplicity is due, in part, to the relatively inert nature of granular materials, i.e., the particles do not appreciably interact chemically with each other, with the surrounding soil particles, or with water.

While a considerable majority of retaining wall systems designed and constructed in the USA and around the world perform satisfactorily, a significant number of retaining wall failures occur each year. Examples of some types of wall failure and wall distress can be seen in Figures 1.1 through 1.4. Some of these failures can be attributed to construction outside of the original design criteria (Marsh and Walsh, 1996), particularly the use of cohesive backfill as a substitute for granular backfill materials. The main reasons that cohesive materials are ever considered for use in these situations are almost always economic.



Figure 1.1 – Wall Failure Along Dam Spillway



Figure 1.2 – MSE Wall Failure Along Highway



Figure 1.3 – Severe Wall Distress (wall at left). Note rotated light standards, deformed guardrail, sunken pavement and curb separation.



Figure 1.4 – Severe Wall Distress. Note bulge at bottom.

Because of the attributes of cohesive soils, prediction of realistic values of earth pressures against retaining structures when using these materials as backfill is difficult. If appropriate design methods can be established for using cohesive backfill materials behind retaining structures, it may be possible that the increased costs for providing sufficient internal and external wall stability will be more than offset by the savings realized by using on-site materials rather than having to import backfill materials from off-site sources (Carder, 1988). The present research is motivated by the need to develop a reasonable design methodology for using potentially expansive cohesive backfill materials behind retaining structures.

1.2 Research Objectives

The primary purpose of this study is to examine the phenomenon of lateral swelling pressure development in clay soils and to develop useful means to predict the magnitude of those pressures for use in retaining structure design. As part of this study, the following efforts are undertaken:

- Review of relevant properties of clays pertaining to retaining structures.
- Review of published literature regarding laboratory and field measurements of swell pressure and swell strain.
- Examination of traditional retaining structure design methods using both granular and cohesive backfill.
- Correlation of the selected clay properties to the observations published by others.
- Development of a predictive method of lateral swelling pressure for use in retaining structure design.

1.3 Organizational Outline

A brief description of each chapter included in this study is presented in below.

Chapter 1 introduces this Thesis topic, including the need for the present research, and briefly describes the contents of each chapter.

Chapter 2 presents a review of clay properties of particular concern to retaining structure design, and discusses the various implications of each.

Chapter 3 discusses the findings from published research exploring laboratory and field measurements of swell pressure and swell strain.

Chapter 4 examines and compares traditional retaining wall design methods using both granular and cohesive backfill and discusses the difficulties and shortcomings of those methods using cohesive materials.

Chapter 5 presents suggestions for analysis and design of retaining structures using cohesive backfill based on this current research, with particular emphasis on the lateral swell pressure component of earth pressure.

Chapter 6 summarizes the findings and conclusions of this research.

Chapter 7 offers recommendations for future related research.

CHAPTER 2

PROPERTIES OF COHESIVE SOILS

2.1 Introduction

Soil materials are typically classified as either coarse-grained or fine-grained, depending on the predominant particle size or sizes present. The Unified Soil Classification System (ASTM D 2487) identifies a coarse-grained soil as one with less than 50% of the total soil material passing a U.S. No. 200 Standard Sieve with a mesh opening of 0.075mm. Terminology of soil types in this classification system is largely based on particle size. Gravels (75mm to 4.75mm) and sands (4.75mm to 0.075mm), are common coarse-grained soil constituents. Fine-grained soils are those composed primarily of silt and clay-sized particles, those smaller than 0.075 mm. Figure 2.1 graphically illustrates various adopted soil particle-size divisions.

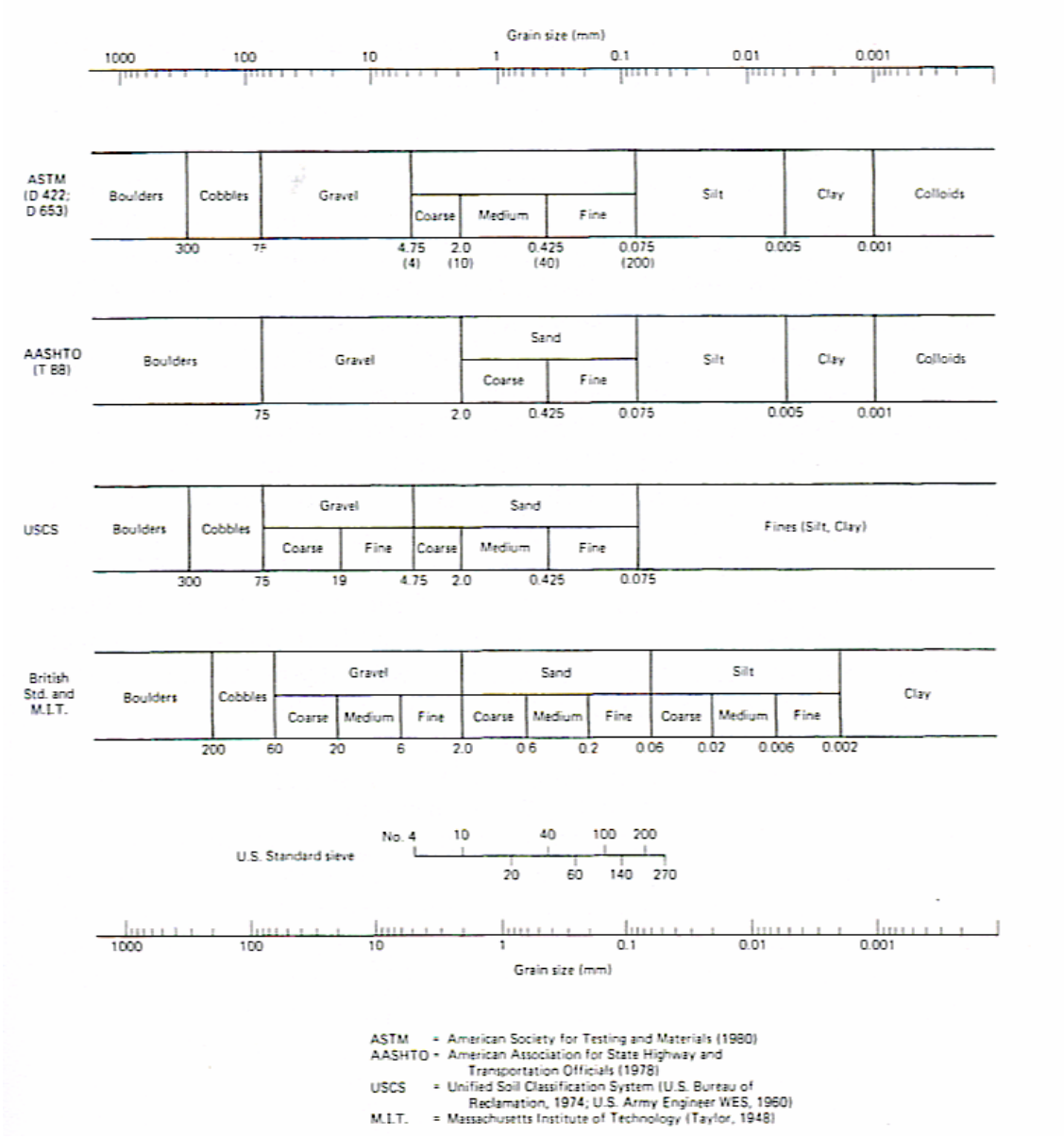


Figure 2.1 - Grain-size Classification Systems (from: Holtz and Kovacs, 1981)

To paraphrase Holtz and Kovacs (1981), “cohesive”, in the context of soil materials, refers to those materials having an appreciable clay mineral content, having plasticity (a state of consistency dependent on water content), and having cohesion (interparticle electrochemical attraction). Silts, though fine-grained, generally exhibit

little plasticity; and like sands and gravels, are essentially independent of water content and have little or no electrochemical interparticle attraction, except when particle sizes are very small. Silts, sands and gravels are often termed “cohesionless”.

The phenomenon of soil swelling and the potential for structural damage has been recognized since at least the 1930’s (Simpson, 1934; Mindlin, 1936). Structural distress due to expansive cohesive soils has been reported in several areas in the western and southwestern USA and many other countries around the World (Chen, 1988). Figures 2.2 through 2.5 below illustrate some examples.



Figure 2.2 - Pavement Heave



Figure 2.3 – Pavement Heave and Cracking



Figure 2.4 – Structural Distress



Figure 2.5 – Brick Facia Cracking

The areas most affected typically have a semi-arid climate and the soils are unsaturated to varying degrees. In this chapter we will examine some of properties of cohesive (clay) soils that contribute to the expansive characteristics of these materials, and how these characteristics impact the design and performance of retaining structures using cohesive materials for backfill.

2.2 Clay Chemistry

2.2.1 General

Clay mineral particles are very active electrochemically, especially with water. This affinity for water leads to soil mass volume changes with changes in soil moisture content – often termed expansive soil behavior. As a cohesive soil mass hydrates, the materials experience a volume change (termed swelling or heaving), the magnitude of which depends on the clay chemistry and the initial degree of saturation. Conversely,

desiccation or drying of those materials typically results in soil mass shrinkage. This activity is due to the nature and structure of clay minerals.

Clay minerals belong to a family of minerals called phyllosilicates, or layered silicates (Hurlbut and Klein, 1982). This family also includes other layered silicate minerals such as mica, talc, serpentine and chlorite. The basic clay mineral atomic crystalline structure consists of vertically layered combinations of two simple structural units: a tetrahedral-shaped silica sheet made of silicon and oxygen atoms with a general composition of $(\text{Si}_4\text{O}_{10})^{4-}$; and an octahedral-shaped sheet with primarily aluminum cations (gibbsite sheet) or magnesium cations (brucite sheet) connected to hydroxyl anions as illustrated in the figures below. The general composition of the gibbsite sheet is $\text{Al}_2(\text{OH})_6$ and of the brucite sheet is $\text{Mg}_3(\text{OH})_6$.

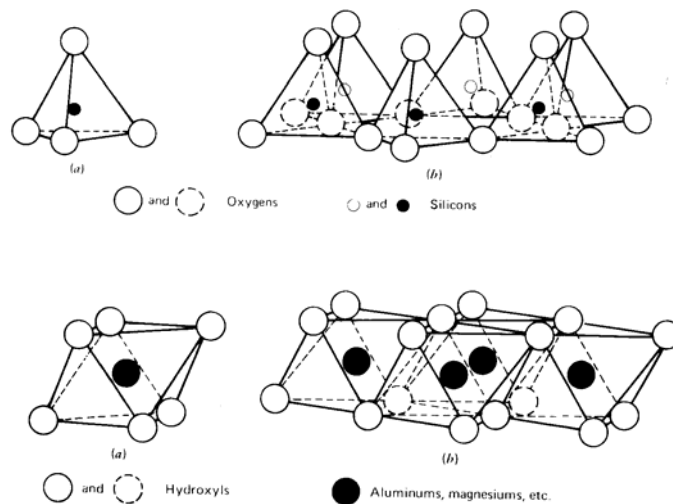


Figure 2.6 – Clay Mineralogical Crystal Structure. Silica Sheet Above; Brucite – Gibbsite Sheet Below (from: Mitchell, 1993)

The different groups of clay minerals result primarily from the layer-stacking arrangements and the type of chemical bonding present between successive layer sheets. Because of the sheet-like structure of clay minerals, these materials appear “plate-like” under the microscope and in hand specimens. Differences of behavior between various clay minerals are largely due to atomic isomorphous substitution within the crystalline structures of the sheets and the degree of crystal development (Mitchell, 1993). The unbalanced electrical charges resulting from certain cationic substitutions and the net electronegative polarity resulting from sheet stacking arrangements gives rise to a number of mechanical phenomena, including cohesion and water absorption.

Because of the almost endless possibilities for substitution and crystal development, the study of clays is a detailed science unto itself. For the purposes at hand, we will only consider three of the most common types of clay minerals.

2.2.2 Kaolinite, Illite, Smectite

The bulk of clay minerals found in nature can be classified as one of three types: 1:1 clay minerals, mica-like clay minerals and smectite clay minerals (commonly referred to as montmorillonite). The clay structures of each type are illustrated in Figure 2.2. This classification is dependent on the particular sheet layering and layer bonding present in each. Specific mineral classification depends on the composition of the octahedral sheet, whether gibbsite(G) or Brucite (B).

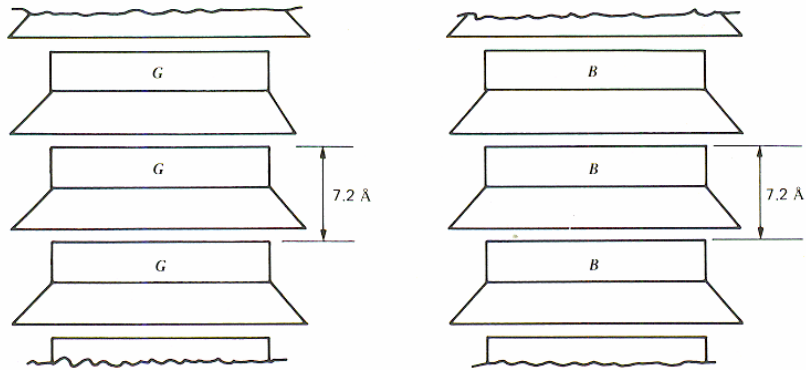


Figure 2.7 - Structure of 1:1 Clay Minerals. Kaolinite (left), Serpentine (right) (from: Mitchell, 1993)

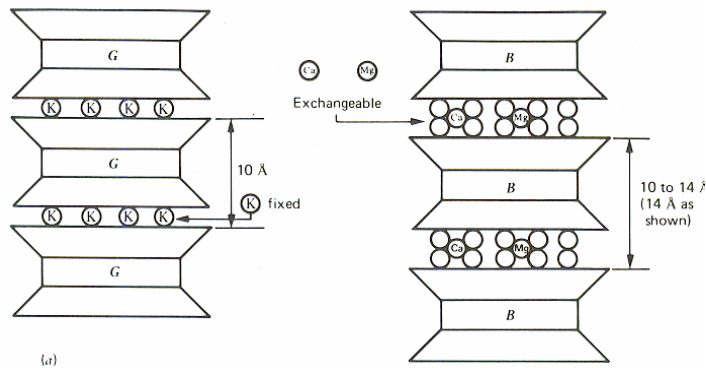


Figure 2.8 - Structure of Micalike Clay Minerals. Illite / Muscovite (left), Vermiculite (right) (from: Mitchell, 1993)

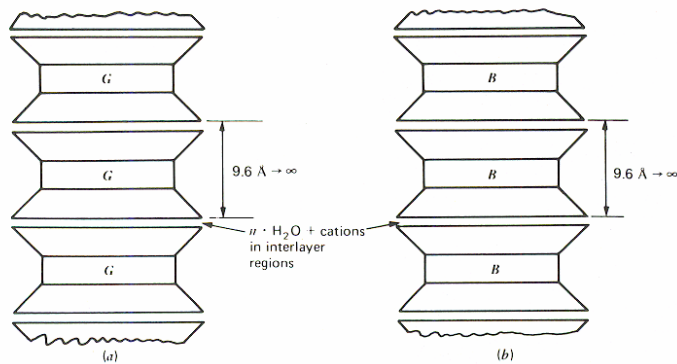



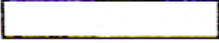
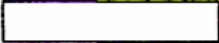

Figure 2.9 - Structure of Smectite Minerals. Montmorillonites (left), Saponites (right) (from: Mitchell, 1993)

Kaolinite minerals are formed of successive layers of one tetrahedral and one octahedral sheet. As such, kaolinite and related minerals are often termed 1:1 minerals. Very little, if any, ionic substitution within either sheet in these minerals and cation exchange capacity is very low, typically in the range of 3 to 15 meq /100gm. The layers are connected by very strong hydrogen bonds between hydroxyl ions of the octahedral sheet and oxygen ions of the tetrahedral sheet. These strong bonds resist hydration and swelling in the presence of water and allows the layers of sheets to stack up to form of rather large crystals (Holtz and Kovacs, 1981). Specific surface area, or the surface area per unit mass of material, of kaolinite is generally in the range of 10 to 20 m²/gm.

Illite is the most common clay mineral encountered in near-surface soils. It is structurally similar to the mica mineral “muscovite” and is sometimes referred to as hydrous mica (Mitchell, 1993). Illites are composed of layers consisting of one octahedral sheet sandwiched between two silica tetrahedral sheets, and are designated 2:1 minerals. Extensive ionic substitutions occur in illite, primarily in the silica tetrahedral layer. The resulting electrical charge deficiency is partially balanced by potassium ions that fit very snugly, and thus are non-exchangeable, in the space between the layers. The electrochemical bonds generated by the presence of non-exchangeable interlayer potassium ions are very strong. These bonds are so strong in illite that the interlayer spacing remains constant even in the presence of water (Mitchell, 1993). Cation exchange capacity in illites typically ranges from 10 to 40 meq /100gm, and would be much greater if the potassium ions were not present. Illites occur as very small, flaky particles. The specific surface area of illites generally range from about 65 to 100 m²/gm

Smectite clay minerals are similar in structure to illite (2:1 structure), but do not contain interlayer potassium ions. As such, bonding between layers in smectites is very weak, consisting of van der Waals forces between the tetrahedral sheets, allowing water and exchangeable ions to enter and separate the layers. Because of the degree of substitution of ions in both the tetrahedral and the octahedral sheets, and the absence of potassium ions, a large amount of unbalanced charge is generated and results in a high cation exchange capacity, generally in the range of 80 to 150 meq /100gm. These factors give rise to tremendous potential for expansion (swelling) when exposed to water. Compounding this potential is the extremely small size of smectite particles (crystals). With interlayer forces so weak, the particles often are so thin as to exist as mere “films” (Mitchell, 1993). The specific area of smectite clays can be as much as 840 m² /gm. Figure 2.6 illustrates clay mineral particle size ranges. Note the increase in specific area (in km²/kg) with decreasing particle size.

**Table 2.1 – Clay Mineral Particle Size and Specific Area
(from: Holtz and Kovacs, 1981)**

Edge View	Typical Thickness (nm)	Typical Diameter (nm)	Specific Surface (km ² /kg)
 Montmorillonite	3	100-1000	0.8
 Illite	30	10 000	0.08
 Chlorite	30	10 000	0.08
 Kaolinite	50-2000	300-4000	0.015

The extremely small particle sizes of clay minerals consequently results in small pore spaces between the particles. Holtz and Kovacs (1981) indicate that in soil studies, it is common to assume an effective pore diameter of 20 percent of the effective particle size, D_{10} , where D_{10} is the particle diameter at which 10 percent of the particles in a soil mass are smaller. This has tremendous implications in soil mass water absorption capability, as explained later in section 2.5 – Capillarity and Matric Suction.

2.3 Plasticity and Atterberg Limits

2.3.1 Definitions and Relevance

Earlier it was noted that one of the characteristics of a cohesive soil was that it possessed plasticity. According to Das (2002), plasticity is the puttylike property of clays that contain a certain amount of water. Perhaps a more explicit definition comes from the word plastic, in the context of physics, for which Webster (1982) states: “capable of continuous and permanent change in shape in any direction without breaking apart”. Clay materials certainly conform to both definitions under most conditions found in nature.

The plasticity of soil is caused by the adsorbed water surrounding the individual clay particles. The magnitude of plasticity is dependent on the type of clay minerals present and the relative quantities present. The plasticity property of clay soils was investigated, defined and quantified in the early 1900’s by Swedish soil scientist A. Atterberg (1911).

Though the concepts and ultimate testing procedures developed from and subsequent to Atterberg’s work, especially Casagrande (1932, 1958), are nearly universally accepted and implemented by the geotechnical community worldwide, it will be useful here to revisit the basic principles, inasmuch as we will attempt to use Atterberg Limits as one component of correlation in predicting lateral swell pressure exerted on retaining structures by use of cohesive backfill.

2.3.2 Atterberg Limits

Atterberg defined six boundaries of clay (or cohesive) soil consistency based on the water content required to produce that consistency, or condition. Three of these boundary moisture content “limits” are in common usage in geotechnical practice and provide a framework for describing cohesive soil behavior as a solid, a semi-solid, a plastic or a liquid as illustrated in Figure 2.10.

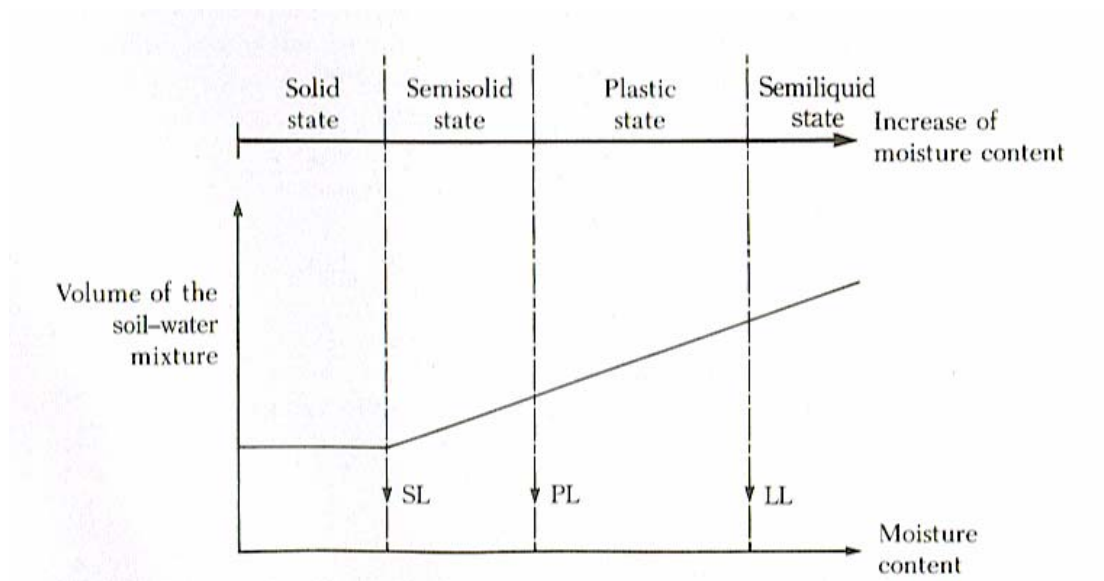


Figure 2.10 – Four States of Cohesive Soil Behavior (from: Das, 2004)

The first boundary state of consistency, and perhaps the most critical to this current research, is the Liquid Limit (LL or W_L), defined as the gravimetric water content of a material above which that material begins to behave as a viscous liquid with very low shear strength (2.5 kPa as defined by Casagrande, 1932) and below which that material behaves as a plastic substance. The Liquid Limit of clay minerals is largely governed by the ability of water to penetrate the crystal interlayers and to adsorb onto the crystal surfaces and/or hydrate interlayer cations present. Since water is a polar

molecule, the net negative charges on clay crystal surfaces, as a result of intracrystalline electrical charge imbalances, readily attract water onto those surfaces. Consequently, minerals with larger specific surface areas can adsorb more water than minerals with smaller specific surface areas. Experimental results confirm this. Kaolinite clays (small specific area) have liquid limits that typically range from 35 to 100 percent, whereas smectite clays (large specific area) have liquid limits generally ranging from 100 to 900 percent. Illites and mixtures of different clay and non-clay minerals have Liquid Limits that fall between these values.

The second boundary state of consistency commonly used in geotechnical practice is the Plastic Limit (PL or W_p). The Plastic Limit is considered to be the gravimetric water content above which a material behaves as a plastic material and below which it behaves as a semi-solid. It is also the moisture content at which a soil crumbles when rolled into threads 1/8 inch in diameter (Das, 2002). The range of Plastic Limit values within each clay mineral group is less than the range of Liquid Limit values. For kaolinite clays, the Plastic Limit is generally between 20 and 40 percent; and for smectite clays it generally ranges from about 50 to 100 percent. Again, the values for illites and clay mixtures are intermediate between these values.

Table 2.2 – Liquid and Plastic Limits of Well-known Clays (from: Das, 2004)

Description	Liquid limit	Plastic limit
Kaolinite	35–100	25–35
Illite	50–100	30–60
Montmorillonite	100–800	50–100
Boston Blue clay	40	20
Chicago clay	60	20
Louisiana clay	75	25
London clay	66	27
Cambridge clay	39	21
Montana clay	52	18
Mississippi gumbo	95	32
Loessial soils in north and northwest China	25–35	15–20

Shrinkage Limit (SL) is the third boundary state of consistency commonly used in worldwide geotechnical practice. This limit defines the gravimetric water content below which a soil mass becomes a brittle solid and experiences no further volume decrease upon increased drying. Above this point the materials behave as a semi-solid. Smectite clays, with their extremely small size and very large specific surface area typically have very low shrinkage limits compared to illite and kaolinite clays.

Plasticity Index (PI) is defined as the moisture content difference between the Liquid and Plastic Limits, or the range of water content where a material behaves plastically (Holtz and Kovacs, 1981). Fine-grained (cohesive) soils are classified as either low or high compressibility materials based on the results of Atterberg Limits tests. This classification can be determined graphically by plotting PI versus LL as shown in Figure 2.11.

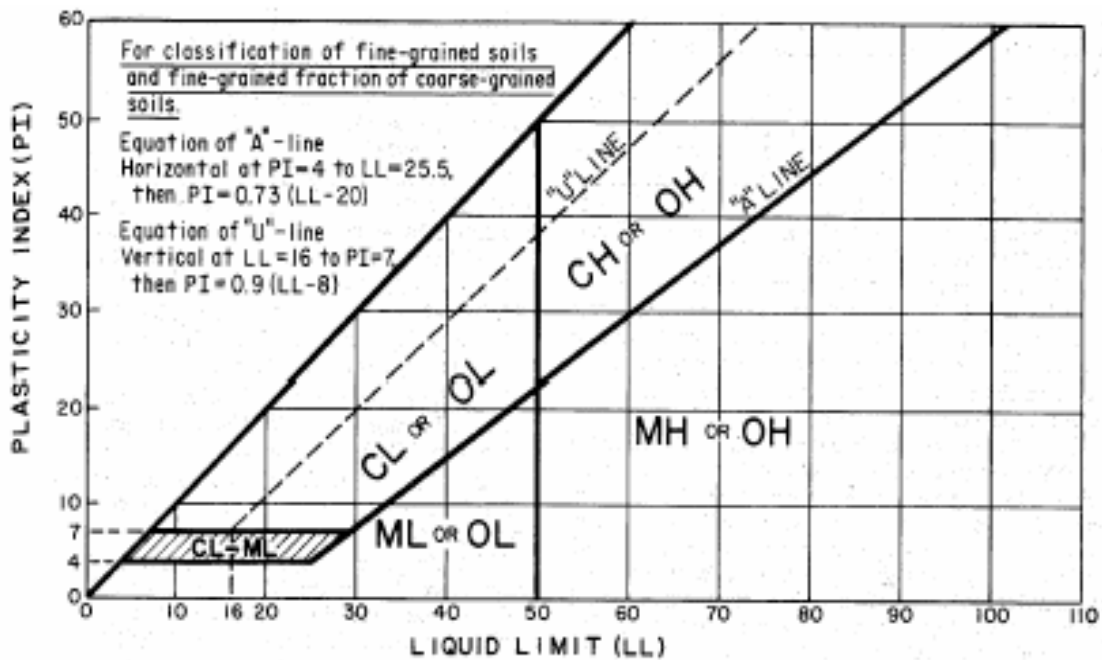


Figure 2.11 – Plasticity Chart (from: ASTM, 2004)

Plasticity Index has been related to swell strain by several authors (Holtz, 1959; Seed, et al, 1962; Chen, 1975; and Mitchell, 1993). Mitchell (1993) developed the following relationship for compacted natural soils:

$$S = 2.16 \times 10^{-3} (PI)^{2.44} \quad (2.1)$$

with an accuracy of +/- 35 percent, where S is the percent swell. Despite the relatively large uncertainty, this relationship can provide valuable initial guidance regarding potential swell-related risks.

2.4 Activity

As indicated earlier, plasticity of a soil mass is dependent on the clay minerals present and their relative quantities in the mass. Skempton (1953) published observations that the PI of a soil mass increases linearly with increasing clay-size fraction, the

percentage of material finer than 0.002 mm by weight (C). He defined the term “activity” as

$$A = PI / \% \text{ clay-size fraction (or } A = \Delta PI / \Delta C) \quad (2.2)$$

This value is often used as an indicator of swelling potential of clay-bearing soils.

Similar to the relationship noted for PI, Mitchell (1993) developed the following relating swell potential (S) to activity (A) and percent clay fraction (C) based on the data obtained by Seed et al (1962):

$$S = 3.6 \times 10^{-5} A^{2.44} C^{3.44} \quad (2.3)$$

It should be clear from the foregoing discussions that both PI and activity are important parameters to consider in determining the magnitude of swell pressure in a clay soil mass.

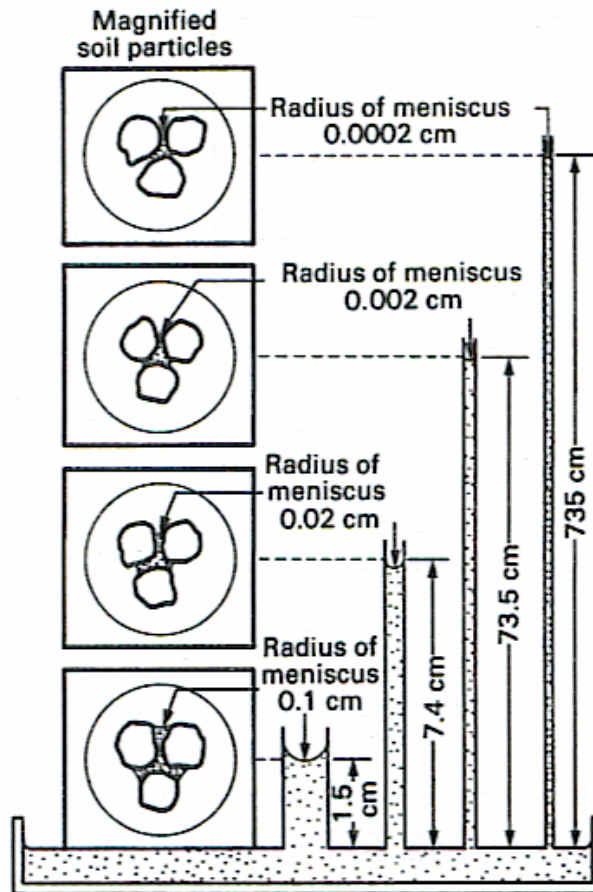
2.5 Capillarity and Matric Suction

2.5.1 Capillarity

For a variety of reasons, material workability in particular, backfill is nearly always placed in an unsaturated condition. In order to more fully understand the complex soil-water interactions of clay-bearing soils and the resulting soil mass volume and pressure changes associated with these interactions, one needs to examine the phenomena of capillarity and soil suction in unsaturated cohesive soils.

Capillarity is often related to the height of fluid rise in tubes of varying diameter. A meniscus is developed in the water column as a result of adhesion at the water-tube interface. The meniscus radius is directly proportional to the tube diameter. However, the observed fluid rise and the resultant capillary pressure are both inversely proportional to the tube diameter, i.e., small diameter tubes exhibit large capillary rises and pressures

as shown in Figure 2.12. Water pressure at the free water surface is zero and hydrostatic below the free water surface. By this convention, capillary pressures are negative.



**Figure 2.12 – Capillary Rise versus Meniscus Radii
(from: Fredlund and Rahardjo, 1993)**

Capillarity in unsaturated soil masses occurs because of surface tension that is developed between water, soil particles and air. In a soil mass, the pore spaces between particles behave somewhat like small diameter tubes. Adhesion between the water and the soil particles causes a meniscus to form. Similar to the tube analogy, in the unsaturated condition the resulting soil capillary water pressure (negative) is proportional to the radius of the menisci that develop as illustrated Figure 2.12.

2.5.2 Matric Suction

The concept of soil suction was developed in the early 1900's, primarily for use in agricultural-type businesses. Applications to geotechnical engineering studies were first introduced in the mid-1900's at the Road Research Laboratory in England (Croney and Coleman, 1948, 1954). Total suction of a soil mass, in a geotechnical sense, consists of two components: matric suction, defined as the difference between pore-air pressure (u_a) and pore-water pressure (u_w); and osmotic suction, related to the salt content in the soil pore-water. Osmotic suction is typically assumed to remain constant in most geotechnical applications; hence, total suction is commonly interchangeable with matric suction (Fredlund and Rahardjo, 1993). The capillary phenomenon described above is essentially the matric suction of the soil. This suction has been referred to as the free energy of the soil water in a soil mass (Edlefsen and Anderson, 1943; Aitchison, 1965a). In more general terms, matric suction can be described as the ability of a soil mass to absorb and hold water.

Since matric suction is a function of pore size, it is not surprising the suction values in excess of 10,000 kPa have been measured in cohesive soils. As a soil mass approaches saturation, the effective radii of the menisci increases and the resulting suction decreases to a value of zero at full saturation. For the purposes of this research, matric suction measurements are relevant in that they may be used to aid in the prediction of the magnitude of the potential swell in a soil mass, including swell pressure.

2.6 Time-Dependent Considerations

Whereas clay mineralogy, particle size and PI are intrinsic properties of any given cohesive soil mass, permeability, pore water pressure, soil fabric and matric suction are

interdependent properties that change over time. Furthermore, these changes occur very slowly with the mass. Thorough treatment of the implications of time-dependence is beyond to scope of this study. However, the writer wishes to convey that consideration of this issue is necessary to predict the long-term behavior and performance of retaining structures constructed using cohesive materials for backfill.

CHAPTER 3

SWELL PRESSURE MEASUREMENTS: BACKGROUND

3.1 Introduction

In January 2007, a search of worldwide engineering databases was initiated for published research pertaining to lateral swell pressure and expansive soils associated with earth retaining structures. A further review of widely available geotechnical-related engineering textbooks, and the REFERENCES contained therein, was conducted and provided much of the framework for Chapter 2.

The database search yielded a limited number of published works, presumably because of the difficulty in measuring lateral swell pressure and the complex nature of and uncertainties involved with traditional retaining wall analyses using cohesive soil materials for backfill. In all, only about 36 technical papers were obtainable through the database search, dating from 1965 through 2006. At least 11 papers cited in REFERENCES were unobtainable, either by conventional or unconventional means. The papers, and associated REFERENCES, varied widely in applicability to this research, from none to much. Of the 28 papers considered applicable, 21 addressed laboratory aspects of measuring swell strain and/or swell pressure, mainly three-dimensional tests. The other 7 involved field measurements of these parameters either in whole, or in part.

This chapter will present the principal findings from the earlier laboratory and field research and present a comparison of the findings to aid the development of a

method to reliably predict the lateral swelling pressures generated on retaining structures using cohesive backfill.

3.2 Laboratory Measurements of Swell and Swell Pressure

3.2.1 One-Dimensional Swell Tests

Since expansive cohesive soils were recognized to constitute a potential threat to engineered structures, a number of methods have been introduced to measure the magnitude of swell in the laboratory. Yesil, et al., 1993, describe that the first methods for estimating soil swell pressure were one-dimensional laboratory tests that used a rigid soil confining ring in an oedometer (consolidometer) apparatus to measure the vertical stress and strain components of swell. To this day, one-dimensional tests are by far the most widely used means to estimate expansive soil swell pressures worldwide, largely due to the simplicity of the procedures and the ready availability of the testing equipment. In fact, the current testing procedure ASTM D 4546 is based on the one-dimensional principles developed early on. Figures 3.1 through 3.4 show a variety of laboratory oedometer equipment.

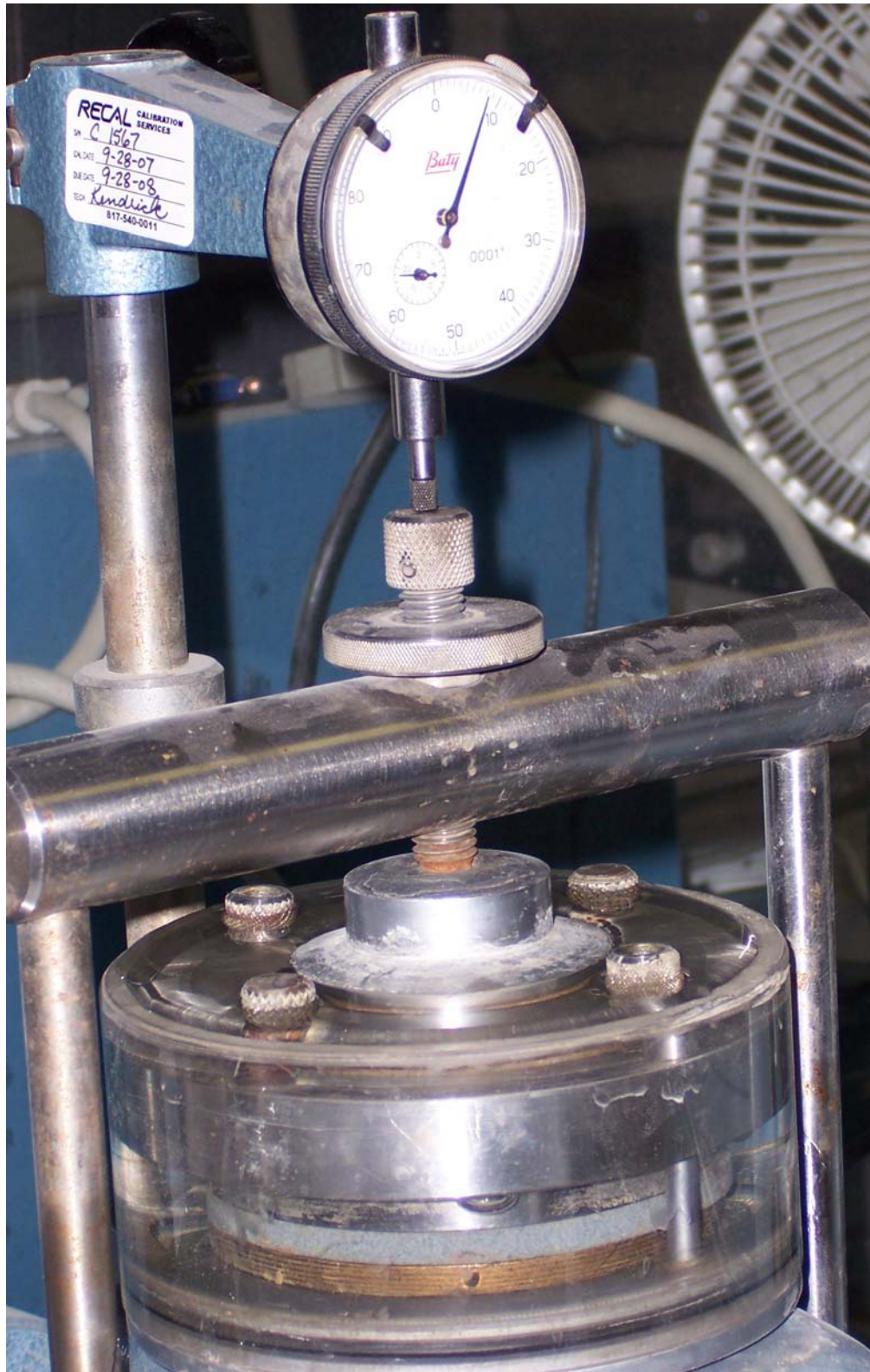


Figure 3.1 – Conventional Lever Arm Consolidometer



Figure 3.2 – Series of Lever Arm Consolidometers



Figure 3.3 – Pneumatic Consolidometer and Sample Confining Ring



Figure 3.4 – Direct Load Consolidometer

Typically in this test, a soil sample is trimmed into a rigid confining ring and placed in a consolidometer, a known vertical load is applied to the top of the specimen and the sample is then inundated with water and allowed to swell. Since the confining ring is very rigid, all of the swell strain occurs in the vertical direction. Vertical strain is usually measured with a dial gauge. For measuring the swell pressure, generally one of two different procedures is employed, ASTM D 4546 Method B or Method C.

In the first procedure (Method B), incremental vertical load is applied to the specimen as needed to prevent any vertical swell strain (heave). Stability is assumed to

occur when no further applied load is required to restrict vertical strain. This generally is achieved within 24 to 48 hours for most clay soils in the USA. Similar findings have been observed elsewhere (Ofer, 1981). The swell pressure (p_s) is then concluded to be the applied load required to prevent swell strain (p_v) divided by the cross-sectional area of the specimen (A) as shown below.

$$p_s = \frac{p_v}{A} \quad (3.1)$$

Swell strain is then determined by removing load, either all at once, or incrementally, to some predetermined value, often 200 pounds per square foot (psf), and measuring the resultant heave after reaching stability (no further increase in sample height with time).

The total heave is simply

$$\frac{\Delta h}{h_o} \quad (3.2)$$

where h_o is the original trimmed sample height.

In the second procedure (Method C), after a small vertical seating load is applied to the specimen, the sample is inundated with water and allowed to swell fully to stability. The total vertical swell strain is measured, then the sample is loaded vertically until the specimen returns to its original height (original void ratio). The applied load required to achieve this state, divided by the cross-sectional area of the specimen is taken as the swell pressure. This method generally yields larger values of swell pressure for a given sample than does Method B. The author presumes this is because that in going from drier to wetter during the first part of the test, the matric suction of the sample decreases. During the second part of the test, as water is forced out of the soil mass void

spaces to return to the original sample void ratio, the original high level of matric suction is restored. One can almost envision this added force as a type of friction as the water molecules are forced past the many clay particles trying to electrochemically retain them. This condition is not present in an unswelled specimen.

3.2.2 Three-Dimensional Swell Tests

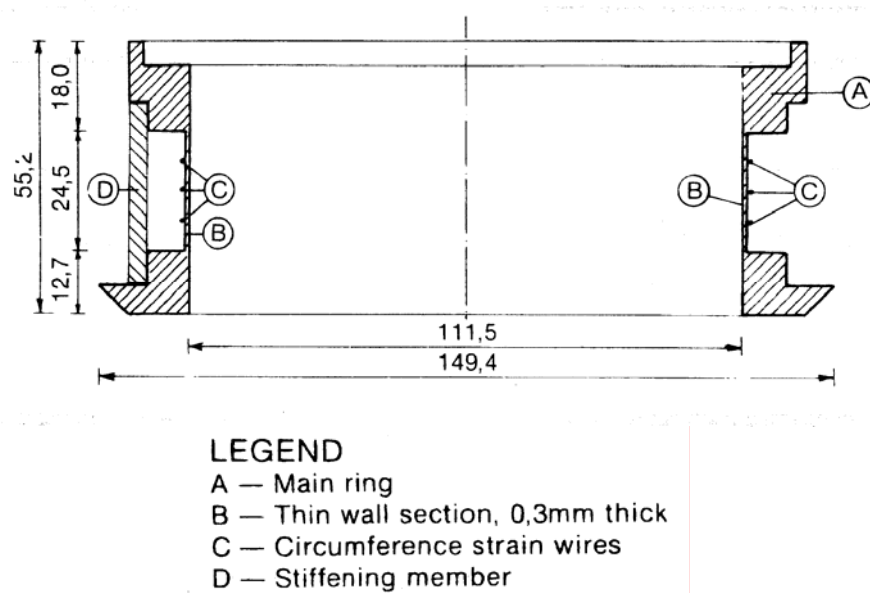
3.2.2.1 General

Because of the rigid nature of the confinement ring in a one-dimensional swell test, (zero lateral deformation), all of the swell strain in this type of test is forced to occur in the vertical direction. However, this condition is not representative of conditions in nature, where the vertical swell strain is only a portion of the total volume change (Al-Shamrani and Dhowian, 2003). Many engineers recognized early in the study of expansive soils that the behavior of these materials is a three-dimensional phenomenon and that information from one-dimensional tests is not based on realistic conditions (McDowell, 1956). Observations during actual projects revealed that one-dimensional tests often overpredict vertical strain due to heave by factor of 3 (Erol et al., 1987). McDowell (1956), in his Potential Vertical Rise method, also assumed that only one-third of the total volume change occurs vertically (Al-Shamrani, 2004). However, Crilly et al. (1992) indicate that use of a single swell reduction factor would tend to overestimate heave near the surface and underestimate it at depth. As such, data derived from this type of test is marginally useful, at best, in predicting swell parameters in the field. A number of researchers have recognized this limitation and have devised methods to simulate more realistic natural conditions as we will see below. These methods generally fall into two categories: modified oedometer tests or modified triaxial cell tests.

As presented later in this chapter, it was discovered that the results of swell parameter measurements obtained from three-dimensional tests are much more comparable to those obtained from instrumented field studies than are the results from traditional one-dimensional tests.

3.2.2.2 Previous Research – Modified Oedometer Tests

Komornik and Zeitlen (1965) developed a laboratory test method to measure, in addition to the axial parameters, the lateral swell pressure using a modified (thin-walled) consolidation ring equipped with pressure strain gauges (Figure 3.5).

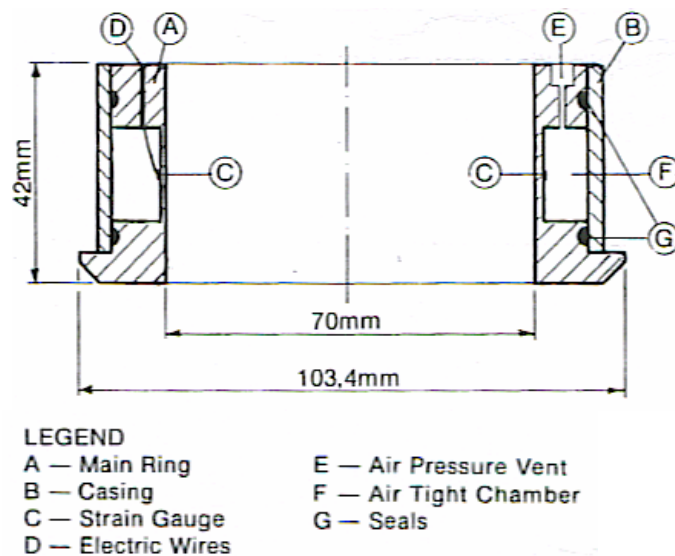


**Figure 3.5 – Thin-walled Consolidation Ring
(from: Komornik and Zeitlen, 1965)**

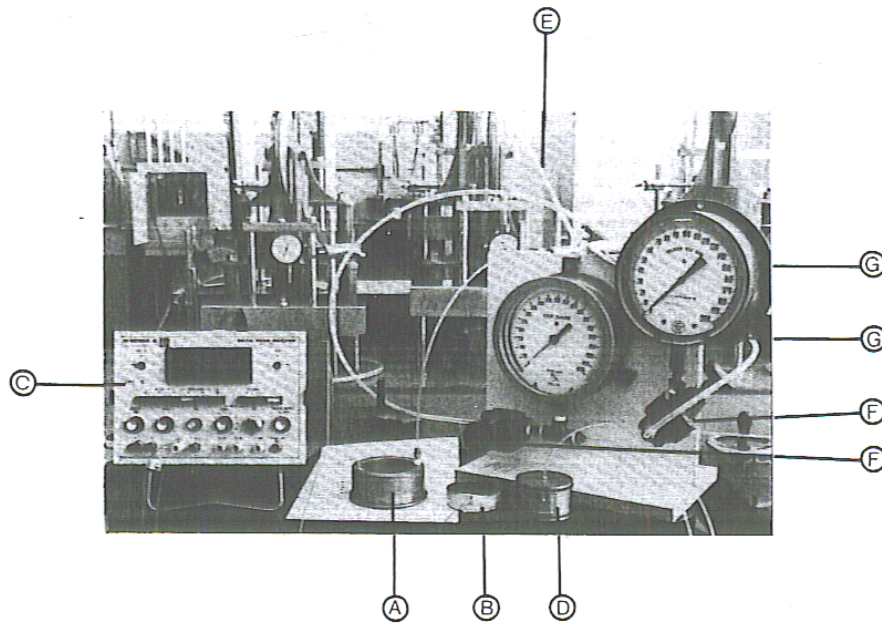
By determining the elastic properties of the modified ring, the lateral swell pressure exerted by the expanding soil can be determined by measuring the lateral, or hoop strain in the ring.

However, Ofer (1981) determined that significant errors in lateral pressure measurement can result with this apparatus if even small lateral strains are allowed to occur. He goes on to describe a modified oedometer apparatus using a conventional oedometer base, sleeve and loading frame, and a new method that measures lateral swell pressure by compensating for lateral swell strain.

In this method lateral swelling pressure is measured without allowing lateral strain using a modified and instrumented thin-walled confining ring as did Komornik and Zeitlen. The difference between the two methods is that air pressure is introduced into the modified ring to counterbalance any lateral swell strain (null test), though laboratory tests can be conducted varying the compensating air pressure, thereby allowing different measures of lateral ring strain. This ring has been dubbed the Lateral Soil Pressure ring MKII (LSP MK II) and is illustrated in Figure 3.6. The overall test equipment and setup is similar to that of the one-dimensional test setup as shown in Figure 3.7.



**Figure 3.6 – Lateral Swell Pressure Ring Mark II (LSP MK II)
(from: Ofer, 1981)**



LEGEND

- A — lateral Soil Pressure Ring
- B — Temperature Compensator
- C — Digital Strain Indicator
- D — Calibration Piston
- E Air Pressure Pipe
- F — Air Pressure Regulator
- G — Pressure Gauge

Figure 3.7 – LSP MK II and Equipment Setup (from: Ofer, 1981)

The LSP Mk II system is calibrated as chamber air pressure versus lateral ring strain. The required air pressure to maintain zero ring strain can be regarded as the actual lateral swell pressure being applied to the ring by the swelling soil.

Of the various characteristics noted during this and a subsequent investigation (Ofer and Komornik, 1982), the authors observed that vertical swell strain and lateral pressure development is time-dependent, and that the response times of these parameters depend on the amount of applied vertical pressure. Further, they determined that the maximum lateral swell pressures were developed in specimens compacted at optimum moisture content to maximum density, and that either a decrease or increase in moisture

content with an associated decrease in density results in a decrease in developed lateral swelling pressure.

Additionally, Ofer and Komornik (1982) found that even small amounts of lateral strain affect the lateral swell pressure considerably; and found that lateral swell pressure is much greater for samples restrained from lateral strain than those where small amounts of lateral strain are permitted. Finally, they determined that clays of similar mineralogy and physical properties exhibit similar lateral swelling characteristics when tested under similar conditions, despite the presumed differences in location, origin and history of those materials.

Using apparatus similar to that developed by Ofer, Edil and Alanzy (1992) conducted a series of laboratory experiments investigating a number parameters influencing the lateral swell pressures exerted by expansive cohesive soils. In this study, three of the researchers' stated conclusions are particularly relevant to this work. First, they conclude that lateral pressures induced by soil swelling is much greater than the lateral pressures generated as the result of increased vertical loading. In fact, K , the ratio of lateral pressure to vertical pressure, increases with increasing surcharge pressure. Further, the rate of this increase decreases with increasing surcharge. This behavior is illustrated in Table 3.1.

**Table 3.1 – Lateral Swell Pressure Variation With Surcharge
(from: Edil and Alanzy, 1992)**

Surcharge Pressure (psi)	1.0	2.0
Lateral Swelling Pressure (psi)	2.2	4.6
K	2.2	2.3
Vertical Swell (%)	16	13

1 psi= 6.9 kPa

Second, as the initial water content increases, the lateral swelling pressure decreases; however, not as much as the vertical pressure decreases. Table 3.2 presents the data developed for this part of the study, while Figure 3.8 graphically illustrates this relationship.

**Table 3.2 – Lateral Swell Pressure Variation With Initial Water Content
(from: Edil and Alanazy, 1992)**

Water Content (%)	15	20	30	40
Vertical Pressure (psi)	1.0	1.0	1.0	1.0
Lateral Pressure (psi)	2.8	2.2	1.4	1.0
K	2.8	2.2	1.4	1.0
Vertical Swell (%)	27	16	10	4

1 psi= 6.9 kPa

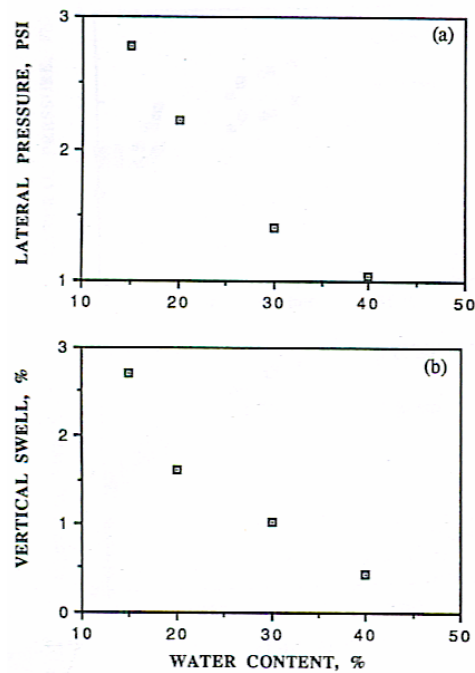


Figure 3.8 – Relationship Between Initial Water Content, Lateral Swell Pressure and Vertical Swell (from: Edil and Alanazy, 1992)

And third, the method of soil compaction influences the lateral swelling pressure behavior of a specimen. Specimens compacted to the same water content and dry

density, but by different methods (kneading versus static compaction) exhibit different degrees of swelling, including different lateral swell pressures when tested under similar conditions. In this study, specimens compacted statically exhibited higher swell parameters than those compacted by kneading.

3.2.2.3 Previous Research – Modified Triaxial Cell Tests

More recently Fourie (1989), Yesil et al., (1993) and Wattanasanticharoen, et al., (2007) have developed triaxial-type testing apparatus to measure swelling parameters. The Yesil et al., study only measures axial parameters, whereas the other two indicate a means to measure both axial and lateral swell pressures and the associated lateral strains. In the Yesil study, results from tests using varying confining pressures are used to interpret three-dimensional swelling behavior. However, the general total strain equations derived require determination of various constants for each specific soil type and do not lend themselves to general predictive use.

The Fourie study uses an approach based on the “Method of Equilibrium Void Ratios” after Sridharan et al. (1986). This method employs provisions for radial, as well as top and bottom drainage, or water entry, and uses a lateral strain belt similar to that described by Bishop and Henkel (1962).

Using this approach, any ratio of vertical-to-horizontal stress may be imposed on a specimen. Furthermore, this procedure allows vertical displacement to occur, simulating a condition of constant vertical total stress. By varying the lateral confining pressure for a given axial load, the lateral swell pressure is interpreted graphically as the lateral confinement required to achieve a net zero ultimate lateral strain. One additional advantage to this technique is that since lateral strains are measured directly, real-time

lateral swell pressures may be estimated on retaining structures where deflections are known.

In the Wattanasanticharoen et al. study, three-dimensional anisotropic stress conditions are approximated using modified triaxial cell equipment and measuring axial and vertical pressures and strains. In this test procedure, a sample is placed in a membrane, then into an airtight triaxial cell where a confining pressure is applied via water pressure. Vertical load is applied using a conventional consolidometer system of weights and lever arms. Figure 3.9 shows the triaxial cell and Figure 3.10 illustrates the complete test configuration.

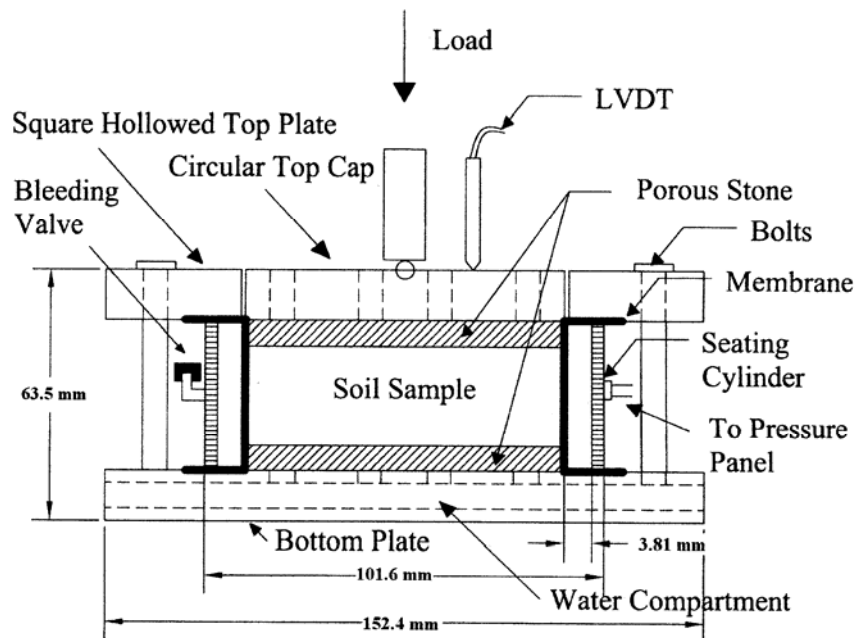
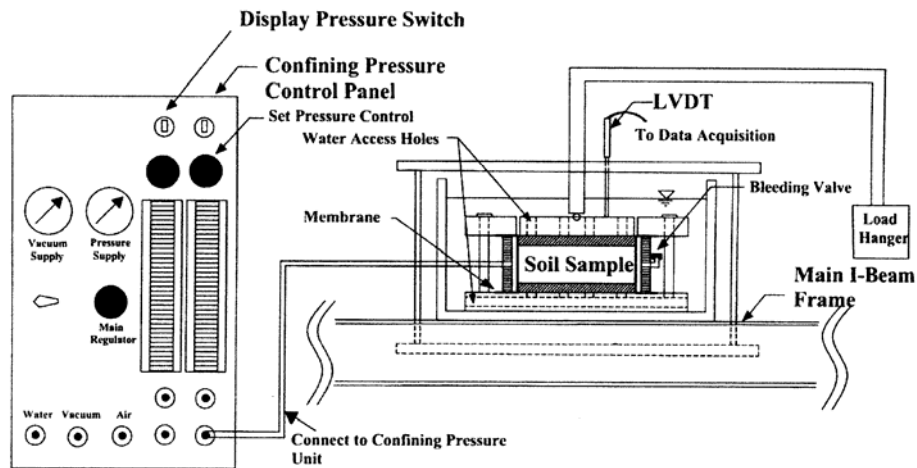


Figure 3.9 – Triaxial Swell Test Cell
(from: Wattanasanticharoen et al, 2007)



**Figure 3.10 – Triaxial Swell Test Apparatus
(from: Wattanasanticharoen et al, 2007)**

Swell strains in the diametral direction are measured immediately at the completion of the test by measuring the sample with vernier calipers. By using relatively high confining pressures and lower vertical pressures, the conventional directions of axial and lateral pressure are rotated 90 degrees, with vertical swell occurring in the diametral direction and lateral swell occurring in the axial direction. This apparatus can be modified to perform matric suction based characterizations by incorporation of suction transducers. As swell strains were the main focus of this research, only those parameters were investigated.

3.2.2.4 Previous Research – Other Investigations

Windal and Shahrour (2002) used instrumented calibrated confining rings of varying stiffness to measure vertical and lateral stresses and strains. They found that for a given initial axial stress, the axial strain and lateral swell pressure is higher for stiffer confining rings. Further, for a given increase in axial stress, the lateral stress increases more for a stiff ring than for a less stiff ring.

Dhawan, et al (1982), building on the works of others investigated the effect of lateral confinement on the swell pressure in expansive soils using modified triaxial cell equipment after Lal and Palit (1969). They demonstrated that under different confinement pressures, lateral swell pressures can exceed the vertical swell pressure generated.

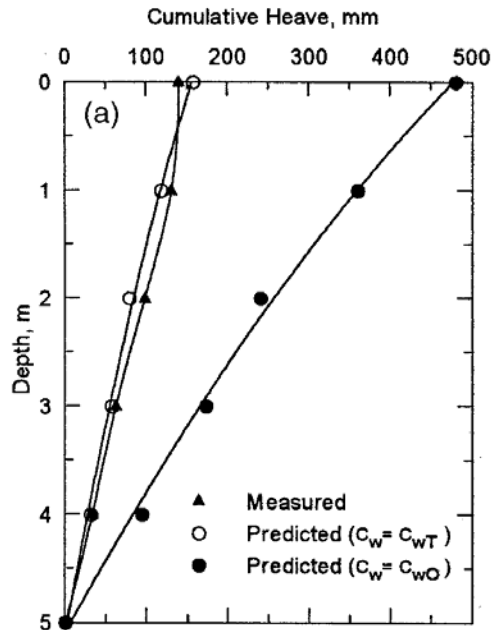
Similar studies have been performed by other researchers resulting in similar conclusions. These studies also focused on other aspects of research, and are thus described in subsequent sections.

3.2.3 Comparisons and Implications of Laboratory Tests

Dhawan, et al. (1982), Al-Shamrani and Dhowian (2002), Windal and Shahrour (2002) and Al-Shamrani (2004), investigated the effect of lateral confinement on the swell pressure in expansive soils by comparing the results from one-dimensional tests to those from three-dimensional tests performed on similar samples prepared in similar fashion. In general, they determined that swell strain measured in the laboratory by one-dimensional tests far exceeded those observed in three-dimensional tests. They determined that considerable swell strain occurs in lateral directions and that the lateral components of swell were being forced into the axial (vertical) direction, because of the rigidity of the confining rings used in the oedometer test apparatus.

Al-Shamrani and Dhowian (2003) conducted an extensive study comparing results from one- and three-dimensional tests with the results obtained from a rather large-scale field investigation. They concluded that one-dimensional tests typically overestimated the heave observed in the field by a factor of about 3. Figure 3.11 compares the results of field measurements of soil heave with heave predictions based on

laboratory tests using conventional oedometer and three-dimensional triaxial test methods.



**Figure 3.11 – Measured Heave (triangles) versus Predicted Heave (circles – open are from triaxial tests)
(from: Al-Shamrani and Dhowian, 2003)**

It seems clear, based on the foregoing discussions, that test data developed from one-dimensional swell test methods are of limited value, since these methods are not representative of actual conditions in nature. Additionally, these types of tests are unable to provide information on lateral swell strain or lateral swell pressure, the focus of this study. On the other hand, three-dimensional swell test methods appear to be more reflective of natural conditions.

Of the different types of three-dimensional tests and methods examined, both the modified consolidometer and modified triaxial cell-type tests appear capable of providing quality swell parameter data for both the axial and lateral directions. The modified

consolidometer test apparatus developed by Ofer (1981) and the modified triaxial cell apparatus described by Fourie (1989) seem especially promising for determining axial and lateral swell parameters. With the Ofer setup and method, it seems an easy jump to investigate the effects of wall yielding on lateral swell pressure. The modified triaxial apparatus developed by Wattanasanticharoen et al. also holds promise for a variety of studies, including suction based investigations.

3.3 Field Measurements of Swell and Swell Pressure

Limited research has been published where field measurements of lateral swell pressure have been attempted. Those available and reviewed for this work are divided into three types and are briefly summarized below.

3.3.1 Instrumented Field Studies

In an effort to further understand the complex interactions between expansive soils undergoing moisture changes and structures built against such materials, Richards and Kurzeme (1973) and Richards (1977) describe the installation of instrumentation, the recorded measurements, and the observations and analyses conducted on a retaining wall constructed in 1971 against expansive soil in Adelaide, Australia. In this study, a 7.5 m high (about 25-feet) reinforced-concrete basement wall was to be constructed against a highly expansive stiff fissured clay and a marl that was known to seep water. Because of concerns of potential heaving of the clay soils subsequent to any wetting, it was decided to conduct an extensive study investigating the performance of the wall over time through the installation and monitoring of a test section comprised of twelve vertical series of psychrometers and six vertical series of earth pressure cells spaced across a 25 m length of the wall. The earth pressure cells were installed at the back face of the retaining wall

to directly measure the applied lateral soil pressures generated as the soil moistures increased. The psychrometers were installed to measure changes in soil suction as the soil moisture increased at different distances from the back of the wall. However, the psychrometer installations nearest to the wall were a full 2 m away. A diagram of the overall wall and monitoring layout is shown in Figures 3.12 and 3.13.

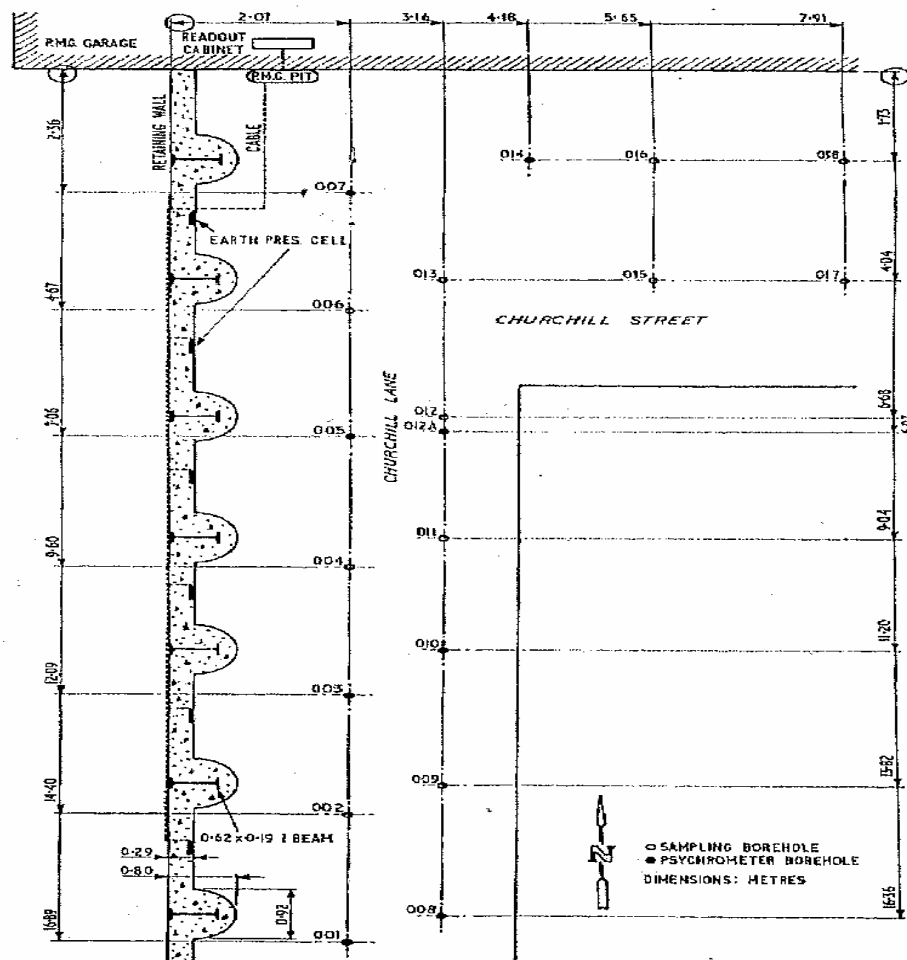
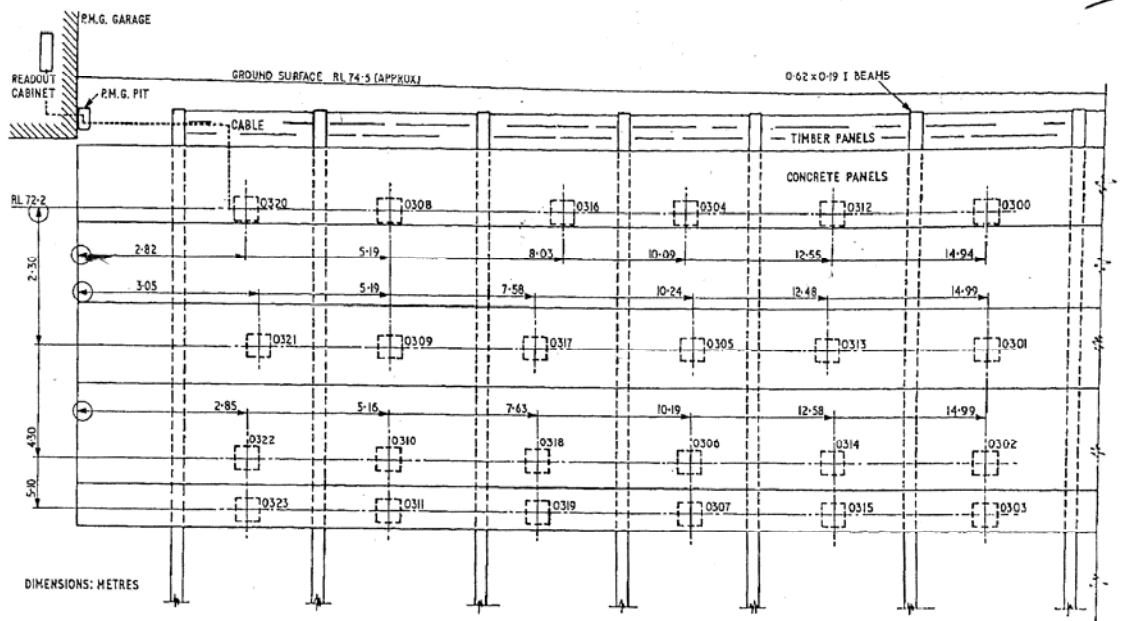


Figure 3.12 – Retaining Wall Instrumentation Plan View
(from: Richards and Kurzeme, 1973)



**Figure 3.13 – Retaining Wall Instrumentation Profile
(from: Richards and Kurzeme, 1973)**

Instrumentation measurements were obtained at regular intervals from the time of installation in mid-1971 at least through mid 1975. Though significant or consistent decreases in soil suction were not measured in the psychrometers, the dramatic increase in the lateral earth pressures of up to five times the vertical overburden pressure, as measured in the lower levels of earth pressure cells, indicates that water seeping from above migrated down the soil-concrete interface, resulting in soil swelling at the bottom of the wall. As the first row of psychrometers behind the wall registered no significant or consistent changes in soil suction values, it was apparent that the wetting front had not yet penetrated that far behind the wall. Further, it was found that the lateral earth pressure increases that were measured migrated upward over time (Figure 3.15).

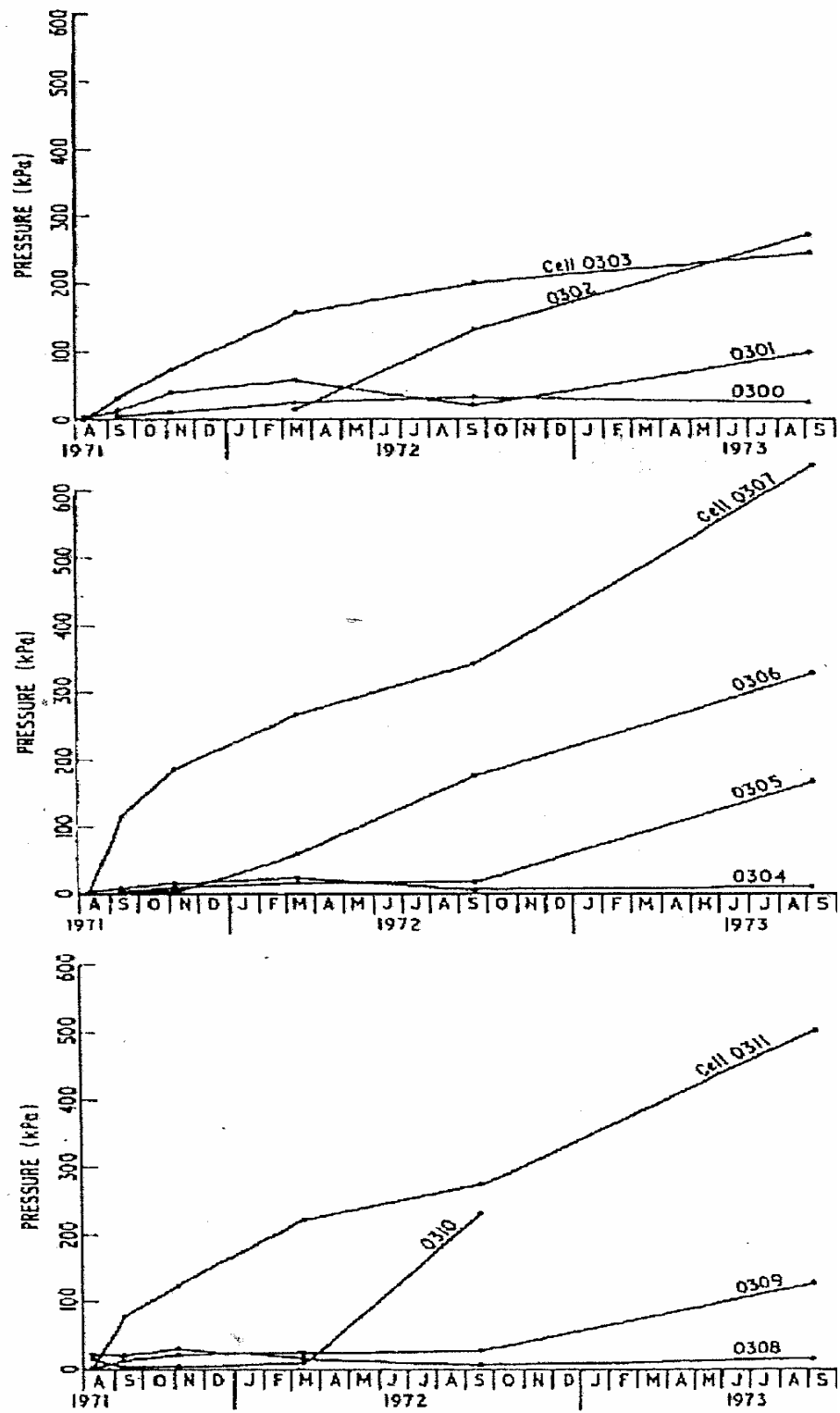
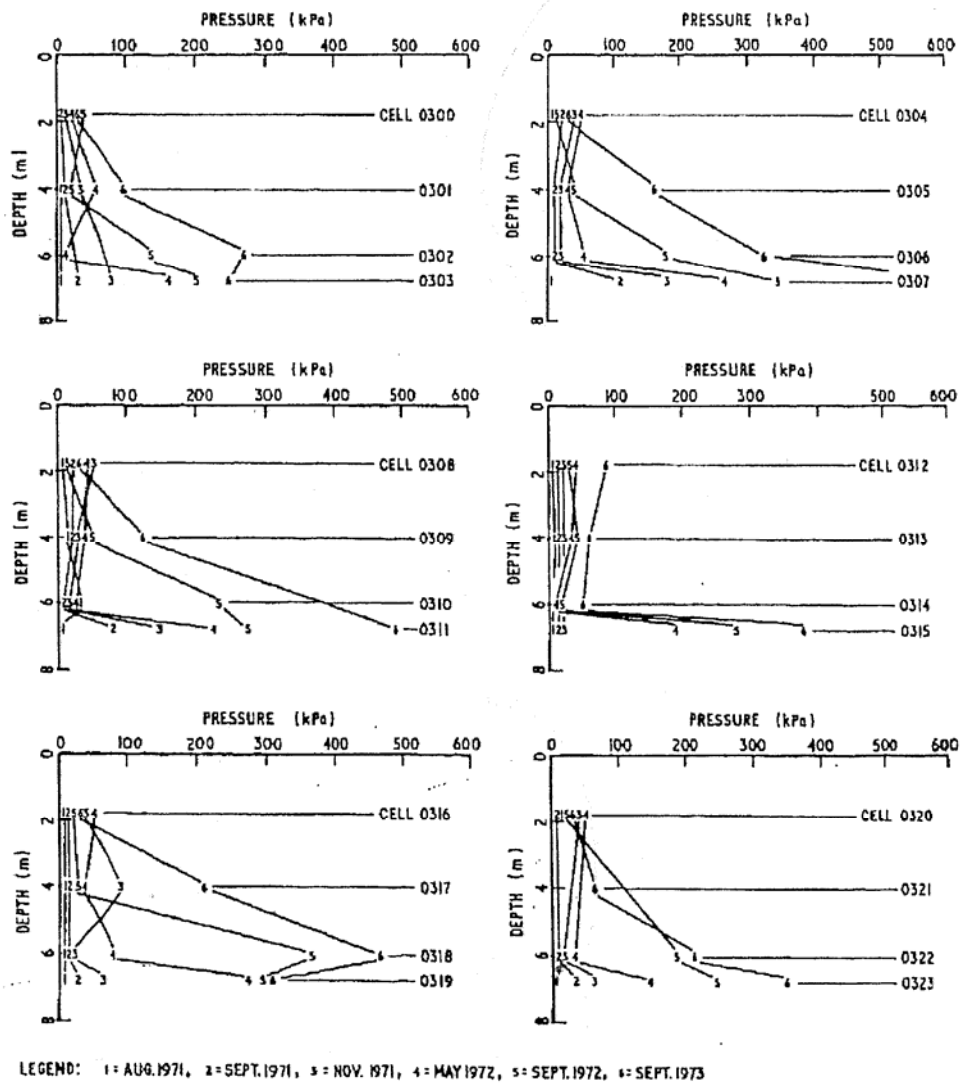


Figure 3.14 – Lateral Earth Pressure Development Over Time For Selected Earth Pressure Cells (from: Richards and Kurzeme, 1973)



**Figure 3.15 – Lateral Earth Pressure Development With Depth
(from: Richards and Kurzeme, 1973)**

To explain this phenomenon for this project, it is suggested that as the water seepage from above reached the lowest soils, those soils swelled laterally against the wall and sealed the water migration path along back face of the wall at those levels. By progressive repetition of this process, the lateral pressure increases migrate upward with time. It was also postulated that when free water is no longer available, soil suction

decreases would eventually dissipate through the surrounding soil mass, resulting in an overall total reduction of lateral earth pressure.

Al-Shamrani and Dhowian (2003) conducted a direct comparative study between laboratory measurements of swell parameters (summarized previously) from soils from Al-Ghatt in the central region of Saudi Arabia and observations and measurements at an instrumented field experimental station at that location subjected to increasing soil moisture conditions. Al-Ghatt, Saudi Arabia is an area of expansive materials where extensive distress to structures has occurred. The field experimental station was constructed over an area 20 m x 20 m, consisting of six units containing psychrometer stacks, with psychrometers placed vertically at 1 m intervals, heave plates placed at different depths, and an artificial saturation system to facilitate water entry into the subsurface. Figure 3.16 shows a schematic of the field instrumentation.

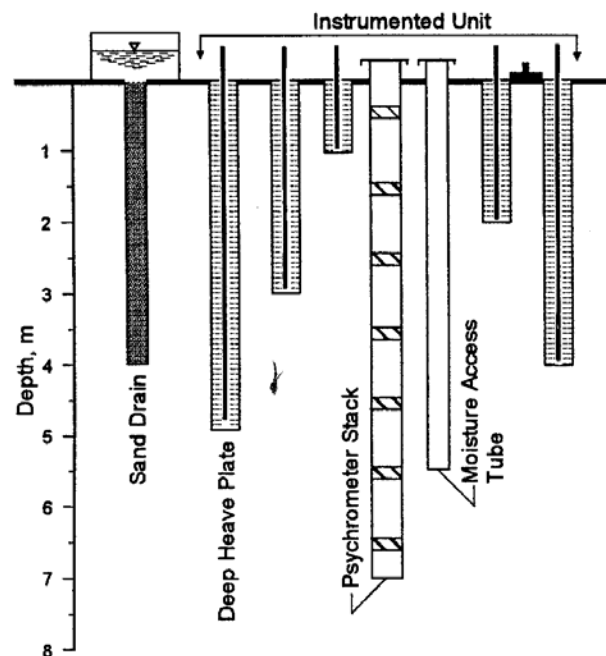


Figure 3.16 – Field Instrumentation for Heave Measurements (from: Al-Shamrani and Dhowian,2003)

Only the vertical swell and the changes in suction and moisture content were measured over the course of about one year. The initial values of soil suction over the depth of investigation ranged from 4,500 to 5,500 kPa. The average moisture content increase during this study was about six percent (6%); and though lateral swell pressures were not measured, the ultimate suction values of 800 to 1,500 kPa and the time-dependent trend of suction decrease obtained is similar to those observed in other laboratory and field studies and will be useful in subsequent discussions. These data are shown in Figure 3.17.

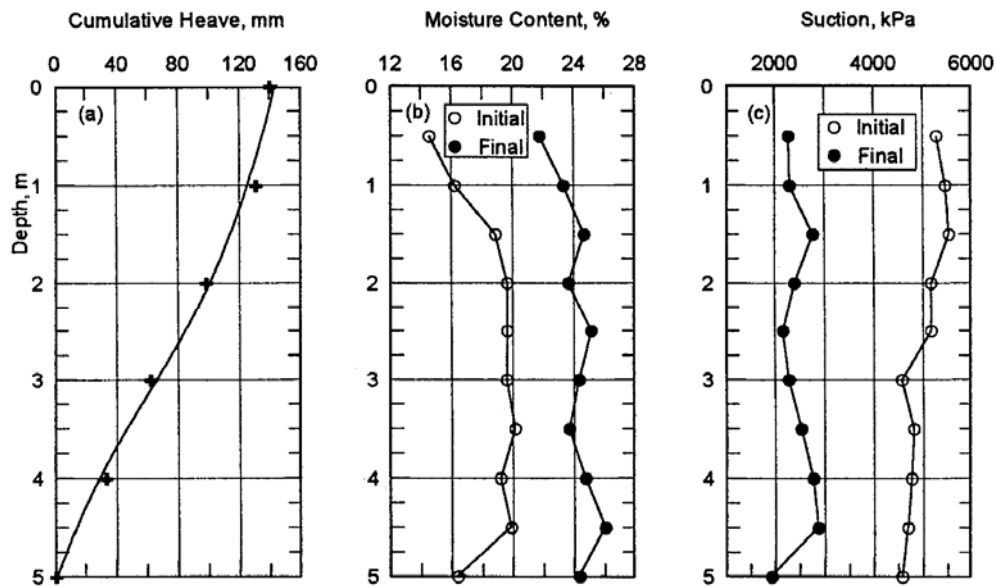


Figure 3.17 – Test Site Measured Data. Vertical Swell, Moisture Content and Suction Changes (from: Al-Shamrani and Dhowian,2003)

3.3.2 In situ Test Apparatus

Only one paper of practical significance to this study was found describing an in situ instrument and method for determining lateral swell pressures resulting from increasing soil water content (Ofer et al., 1983). This method incorporates a pressure

transducer within an instrument that is inserted into soils with as little disturbance as possible.

The In Situ Swelling Pressure Probe (ISP) developed by Ofer et al., is a cylindrical steel probe with an outside diameter 90 mm and a height of 200mm and consists of 4 major components: a pressure transducer, porous wetting rings, a cutting edge, and a connection head. The pressure transducer is a cylinder which has an airtight chamber at mid-height. A portion of the outer wall of the chamber is only 0.8 mm thick to which a circumferential strain gage is cemented. Holes are provided to allow connection of tubes from an air pressure system and to allow passage of electric leads from the strain gage to a strain indicator. A photograph of the principal components of the system is shown in Figure 3.18; and Figure 3.19 shows a detail of the wetting ring configuration.

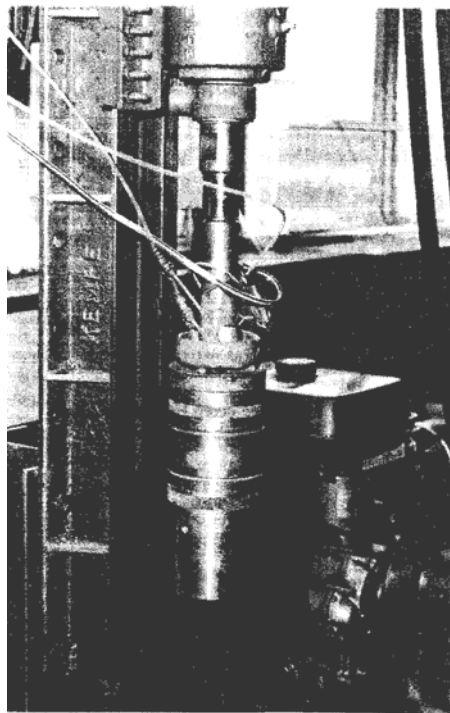


Figure 3.18 – In situ Swelling Pressure Probe MK II System (from: Ofer et al., 1983)

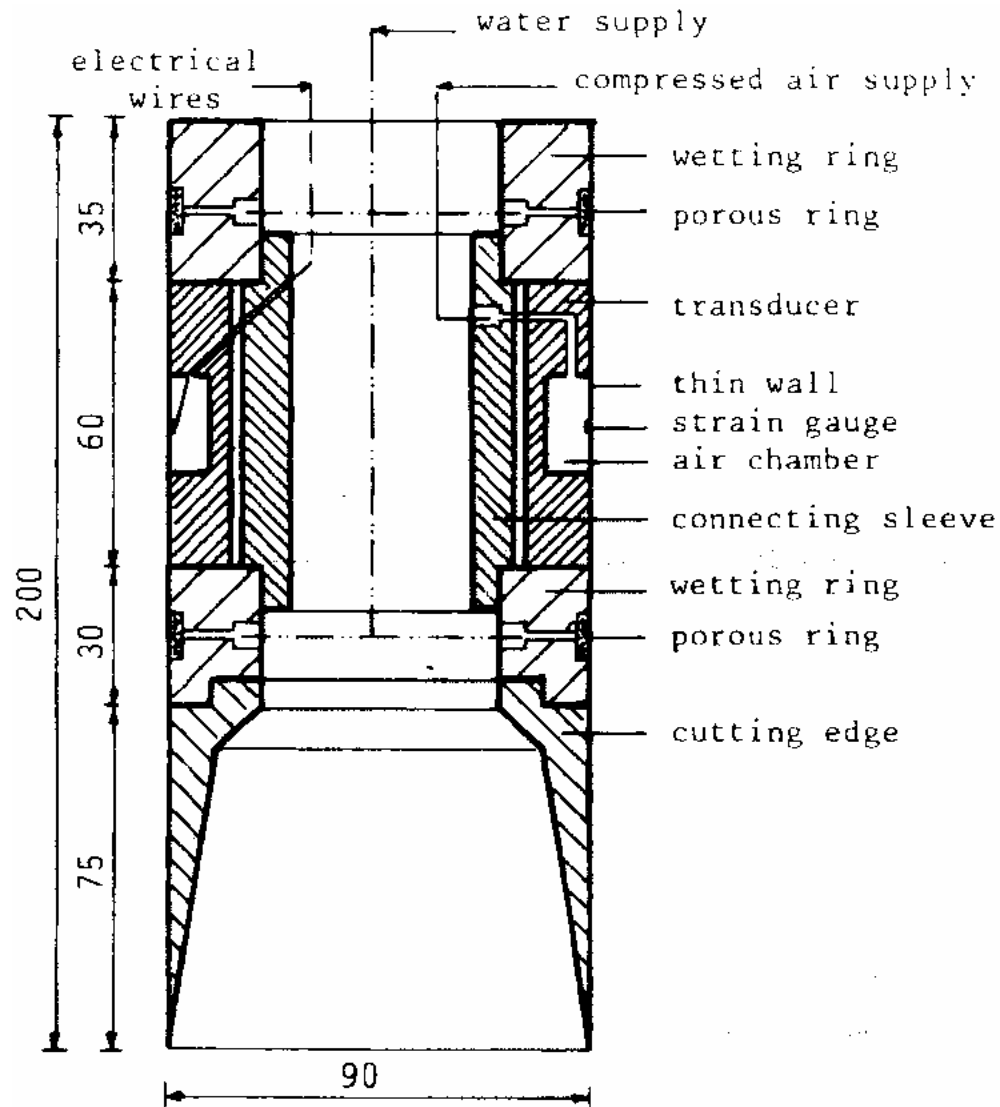


Figure 3.19 – In situ Swelling Pressure Probe MK II (from: Ofer et al., 1983)

The transducer is calibrated in the laboratory in two ways, both using a calibration cylinder placed over the probe that can form an airtight seal around the probe. In the first calibration, air pressure is introduced between the calibration cylinder and the probe, simulating applied soil pressure, and recording the strain gage response. The second calibration is based on the null principle, where air is simultaneously introduced into both

the pressure transducer chamber and into the annulus between the probe and the calibration cylinder so that the measured strain of the thin-walled portion of the chamber remains zero. The coefficients of variation for both correlations was greater than 0.999. Porous wetting rings are located on either side of the transducer and connected to a water supply. As the soil moisture is increased, the resulting pressure changes are measured and recorded in real time.

Field tests were conducted at two different depths: 0.6 m and 2.0 m. For each test an oversized hole (100 mm diameter) was drilled using dry auger methods to about 250 mm short of the target depth. A slightly undersized core barrel (85 mm diameter) was then used to drill to the target depth. After drilling, the 90 mm diameter ISP was placed in the hole and pushed to the target depth with the cutting edge shaving the sidewalls of the slightly undersized test interval, ensuring a tight probe fit with minimal disturbance. The lateral soil pressures in both tests exhibited an initial sudden decrease followed by a steady increase to a peak value followed by a reduction in pressure which eventually stabilized to a constant value, though the magnitudes of the lateral pressures measured were not stated. The pattern of increase to a peak pressure then a reduction to a stable level is similar to those observed in the laboratory and other field studies described above and below. However, the initial lateral pressure decrease observed is thought to represent stress release or redistribution around the probe developed during insertion.

3.3.3 Large-scale Study

Katti et al., (1983) conducted large-scale experiments investigating lateral swell pressure development on retaining structures with and without use of non-swelling clay materials (cohesive non-swelling materials, or CNS) both atop high-plasticity expansive

clay fill, and between the structure and the clay fill. These studies built on research published by Katti et al, and Kate and Katti dating from the late 1960's (1967, 1969, 1975, 1980, 1981, 1982). The experiments were conducted on sand, CNS and expansive clay soils layer-compacted into a reinforced frame with dimensions adjustable up to about 4 feet wide, 8 feet deep and 12 feet tall. One of the four vertical walls of the experiment frame was instrumented and equipped to restrain horizontal deflections. By maintaining zero deflections along the vertical length of wall after fill compaction was complete, the lateral swelling pressures generated after both compaction and saturation could be measured. Saturation for each test increment was conducted for a period of 60 days, though the means of saturation were not explicit. The overall experimental setup is shown in Figure 3.20.

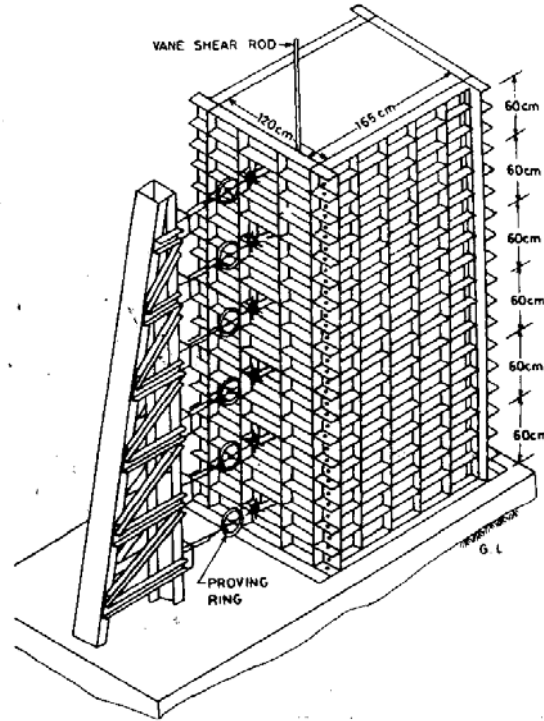


Figure 3.20 – Large-scale Experiment Setup (from: Katti et al., 1983)

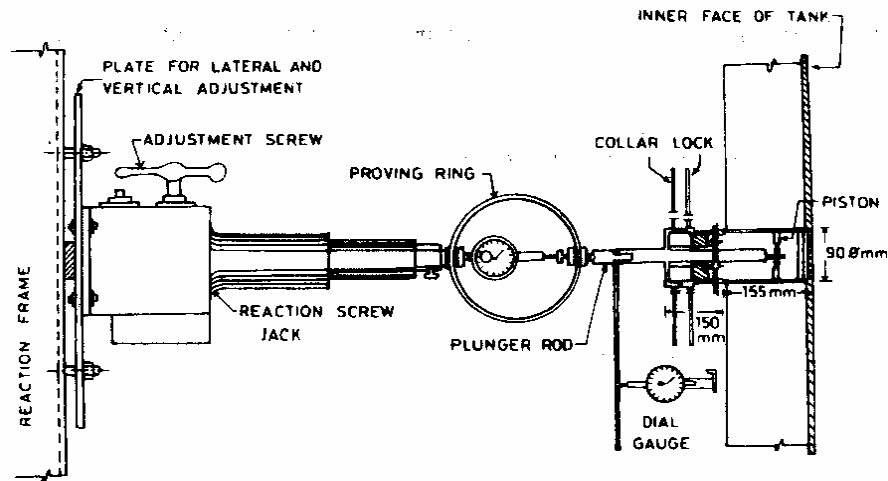


Figure 3.21 – Large-scale Experiment Instrumentation (from: Katti et al., 1983)

Four types of tests were conducted: Case 1.) Evaluation of lateral pressures developed with depth for granular materials (sand), CNS and expansive clay soils in loose dry, compacted dry and compacted saturated conditions; Case 2.) Evaluation of lateral pressures developed with depth of expansive clay fill having varying thicknesses of CNS inserted between the wall and the expansive clay fill; Case 3.) Evaluation of lateral pressures developed with depth of expansive clay fill with varying thicknesses of CNS placed and compacted atop the expansive fill; and Case 4.) Evaluation of lateral pressures developed with depth of the expansive clay fill having CNS both placed between the wall and the expansive fill, and atop the fill.

For the Case 1 experiments, the authors observed a linear relationship of lateral pressure with depth for the loose dry conditions of all three materials in close agreement with K_0 values obtained from Jaky's equation: $K_0 = 1 - \sin\phi$. For the compacted dry condition, the observed lateral pressure relationships were also linear with depth, but the calculated values for K_0 were all in excess of 1, with the sand exhibiting the highest

values (e.g. 2.33 at 1 m depth). These high values are attributed to the addition of impact loads during compaction imparted to the self-weight of the fill at a given depth. Similarly, for the compacted saturated condition of the sand and the CNS, a linear relationship of lateral pressure with depth was observed. Compacted saturated expansive clay materials, however, exhibited a completely different behavior in this study; though it should be noted that these soils had been compacted in an air-dried condition prior to saturation.

For the compacted saturated condition of the expansive clay in the current experimental setup, the lateral pressures against the wall increase rapidly with depth to about 1.5 m, then increase at a lesser rate below that depth. At 1.5 m depth the developed lateral pressures were measured to be about 230 kPa (~4800 psf). Calculations of the lateral pressures generated by the buoyant weight of soil, the water and the impact loads during compaction only amount to about 19 kPa (~400 psf) at that depth. The difference is taken to be the magnitude of lateral swell pressure generated by the absorption/adsorption of water into the crystal structure of the clay minerals (predominately a smectite type clay). Figure 3.22 is a graphic illustration of the measured data.

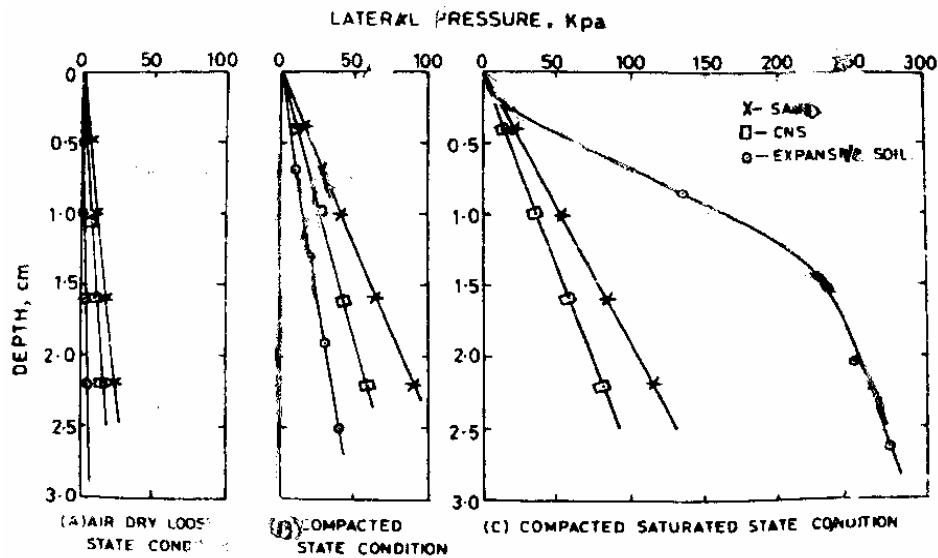


Figure 3.22 – Lateral Pressure Development versus Depth (from: Katti et al., 1983)

In each of the above cases, the maximum lateral pressures developed were observed to decrease with time.

The data developed from Cases 2 through 4 have important implications for the design of retaining structures using expansive cohesive backfill, but detailed assessment and treatment of these aspects of lateral pressure generation are beyond the scope of this current research. However, Figure 3.23 illustrates some of the beneficial impacts of using CNS backings (Case 2), in that lateral swell pressures applied to the back of the wall face are decreased with increased thicknesses of non-expansive backfill placed between the wall face and the expansive retained or reinforced backfill.

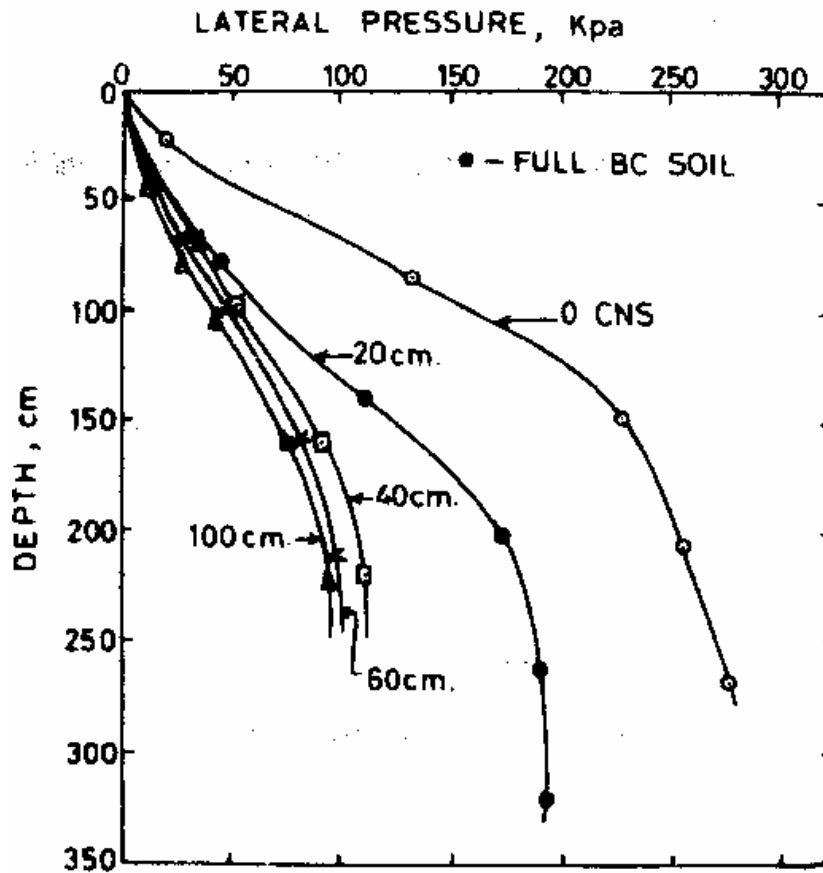


Figure 3.23 – Lateral Swell Pressure versus Depth Using CNS Backing
(from: Katti et al., 1983)

Aytekin et al., (1993) used the data from preceding Katti et al., and Kate and Katti research to develop a finite element model to simulate the observed results. This effort employed the given soil parameters and incorporated assumed suction data for the given soils based on suction compressibility and strain equations proposed by McKeen (1977 and 1980). The numerical analysis correlates well with the experimental observations and the resulting lateral pressure distribution obtained is very similar to that shown in the original research. By assuming some small unreported wall displacement at the top of the wall, the numerical results generated were almost identical to the original observations. The authors note that even minute lateral wall displacements result in a

very large relief of lateral swelling pressure. They further stress the importance of the suction parameter in the numerical model, which is a function of the bulk clay content and mineralogy (and hence, related to the particle size distribution and PI of the soil mass).

In a published response to Xin and Ling (1991), Aytekin (1992) reiterates the validity of the resultant lateral pressure distribution observed by Katti et al, (1983) and further indicates similar findings by Sudhindra and Moza (1987) (not referenced in the response article).

3.3.4 Pilot-scale Study

Clayton et al., (1991) investigated lateral swell pressure development in high plasticity clays used as backfill against retaining structures in a pilot-scale study at the Transport and Roadway Research Laboratory in England. The purposes of this study were threefold: 1.) To investigate the development of lateral soil pressures on the structure from fill placement, compaction and burial; 2.) To investigate the dissipation with time of lateral soil pressures generated due to compaction, etc.; and 3.) To investigate the lateral soil pressures developed as soil moistures increase after compaction is complete. This last point is of primary interest to this present research.

In this study an experimental “trough” structure 3 m deep and 20 m long and 5 m wide was constructed of rigid concrete. 6 m of the center of one side the concrete is replaced by a moveable, yet rigid, metal wall in three 2 m x 2 m sections. This central metal panel is instrumented with three vertical profiles each containing six horizontal earth pressure cells and is supported with two vertical and four horizontal load cells to record total thrusts. For the third part of the study a 2 m square, similar to the moveable

panel, is inset into the opposite “rigid” wall. This segment of the wall was instrumented full-height with pneumatic, hydraulic, and vibrating wire cells.

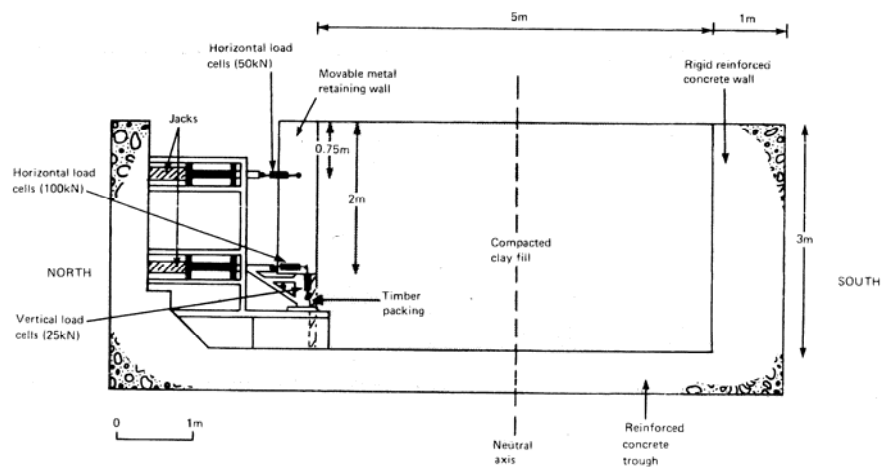


Figure 3.24 – Experimental Retaining Wall (from: Clayton et al., 1991)

High-plasticity London Clay ($W_L = 78$, $PI = 49$) was placed into the trough structure and layer-compacted to about 5-inch lifts. Field density measurements were conducted throughout fill construction. Fill moisture contents were determined to range from about 27% to 30%, slightly dry of the Plastic Limit. Average dry density was determined to be about 93% of Standard Proctor, corresponding to an air void content of about 6% to 8%. It should be noted that the soils used contained clods up to about eight inches in diameter and the moisture contents indicated are near the optimum moisture content.

During the study, pressure measurements were recorded from all instrumentation during three defined stages of the test. Stage 1, the fill placement and compaction, extended from day 1 through day 13. Stage 2 was from the end of fill construction to day 40, when measured lateral pressure reductions had stabilized sufficiently. Stage 3 began on day 69 after the installation of a pattern of sand drains to expedite soil wetting. A free

water surface at the top of the fill was maintained throughout the duration of the test. Stage 3 extended through day 692.

It was found that the maximum average lateral pressure increase along the instrumented rigid concrete section was about 100 kPa (~ 2100 psf), with individual cells measuring pressure increases of up to 150 kPa (~3100 psf). These maxima at each location were all recorded at sensor depths between about 1 and 1.5 m (about 3 to 5-foot depth). Estimates of lateral pressure increases based on traditional equivalent fluid pressure calculations yield values of only about 8 kPa (~170 psf). Again, it should be noted that the compaction moisture contents were slightly below the plastic limit. Corresponding measurements from the instrumented moveable metal wall indicated lesser pressure increases; however, on day 172 this segment was allowed to move outward very slightly (about 0.5 mm) to prevent possible instrument damage resulting from the high lateral thrusts generated by that time. This outward deflection dramatically decreased the exerted lateral pressure temporarily and allowed the test to continue. After the deflection was permitted, the measured lateral swell pressure maxima were recorded on day 210, nearly five months after wetting began. Depending on the type of instrumentation, these maxima were found to be about 2 to 3 times the lateral pressures initially generated by compaction only. However, had deflection not been allowed to occur, these maxima would have been much greater. After reaching maximum values, the measured lateral swell pressures were observed to slowly decline at all depths, but the values recorded at the end of the study were still considerably higher than the pressures developed as a result of the initial compaction efforts.

Further observations revealed that vertical swell was continuing through the end of the study, suggesting that even after 20 months the fill soils had not reached moisture equilibrium. A summary of the measured data is presented in Table 3.3.

Table 3.3 – Average Lateral Swell Pressure Developed During Pilot-scale Test (from: Clayton et al., 1991)

Day	Average total pressure (kPa)						
	Concrete wall			Metal wall			
	Hydraulic cells	Pneumatic cells	Vibrating wire cells	Hydraulic cells	Pneumatic cells centre profile	Pneumatic cells (eastern profile)	Horizontal load cells
13 (end of stage 1)	49	61	26	28	34	28	27
40 (end of stage 2)	39	56	25	25	32	33	23
210 (during stage 3)	96	105	91	73	76	61	65
692 (end of stage 3)	57	78	70	53	56	57	51

In their conclusions the authors suggest that for well-compacted clay materials of PI less than about 30, lateral swelling pressures generated by the fill will likely be less than the lateral pressures developed immediately following placement and compaction. For high PI clays, they suggest that lateral swelling pressures may be zero if the fills are placed at moisture contents at or above a critical value as shown in Figure 3.25.

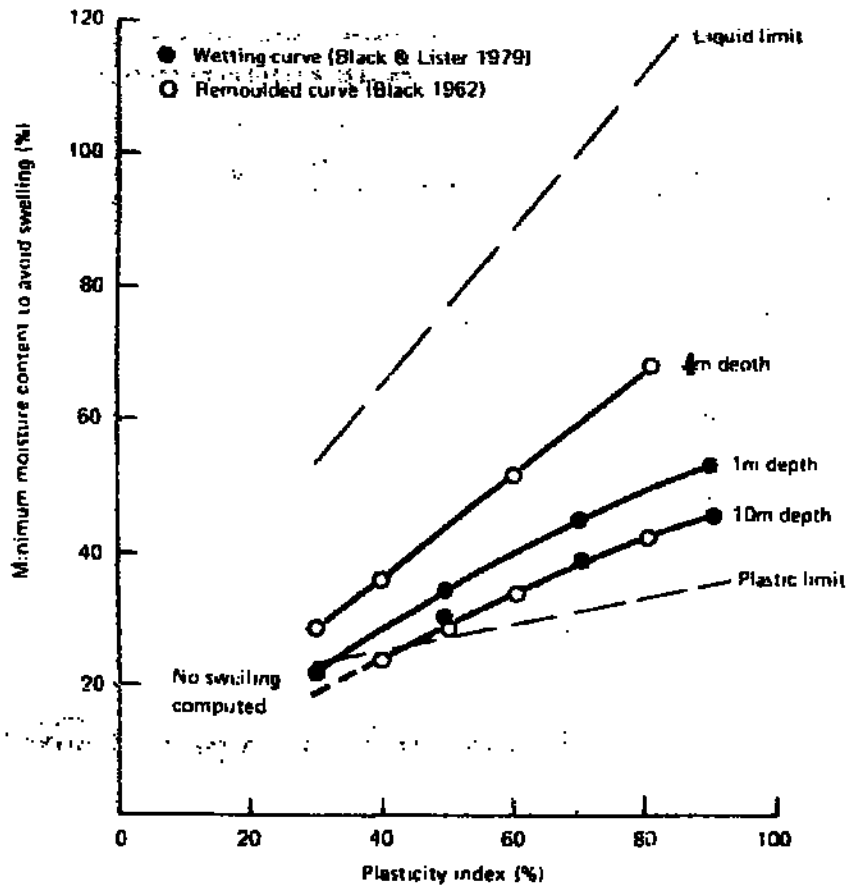


Figure 3.25 – Minimum Moisture Content to Avoid Swelling versus PI (from: Clayton et al., 1991- adapted from Black and Lister, 1979)

The data indicate that the compaction moisture contents above the PL required to prevent swelling increase with increasing PI, and the increase shows to be greater for shallow fills than for deeper fills. However, the authors suggest that for clays with PI above 40, the critical moisture condition required to prevent significant lateral (or vertical) swelling may perhaps result in such a reduction of soil shear strength as to be barely trafficable to construction equipment (MC 10% or more above PL for clays with PI = 60). They suggest that allowing some small wall deflections could permit use of lower moisture fill (the deflections would dissipate the tendency for increased lateral

swell pressures arising from lower initial moistures). They conclude that further studies are necessary to fully evaluate these relationships.

3.4 Comparisons of Laboratory and Field Measurements

The foregoing research presented illustrates that the conventional and more widely used methods employed for the prediction of various parameters of swell (one-dimensional oedometer-type swell tests) are not representative of the actual earth responses observed in nature or in field studies. Published literature indicates that these types of measurements typically overestimate the vertical swell observed by something on the order of a factor of three. However, no investigations along these lines are found that consider the impact or relationships of differing of bulk clay mineralogies on these estimates. Further, the research considered indicates that specialized types of triaxial three-dimensional testing are required to reasonably estimate the lateral components of swell.

Though all laboratory and field studies incorporate some measure of conditions or aspects in their construction that are not representative of in situ conditions, it is clear that the data developed from the various triaxial systems discussed compares most closely with the various field observations described.

Typically the magnitude of the measurements of lateral swell pressure (and the other parameters of swell) obtained from field, large-scale or pilot-scale studies are less than those obtained from laboratory studies, even those laboratory triaxial studies mentioned. This discrepancy may possibly be attributed, in large part, to differing boundary conditions existing in the small diameters of the sample test specimen rings. It is believed that these boundary issues are eliminated as the size of the experimental

apparatus increases and as the distance of the apparatus boundaries from the instrumented areas increase. At present, this author believes that the overall results of lateral swell pressures measured in the large and pilot-scale tests may be reliably used in developing a method for predicting the lateral swell pressures that could be developed when using expansive clay materials for retaining structure backfill or where retaining structures must be placed against expansive soil strata.

3.5 Summary of Literature Review Findings

The primary purpose of the preceding literature review was to assess the findings of all accessible previous research relevant to the topic of determining the magnitude of lateral swell pressure, and to highlight pertinent information from those studies which might lead to the development of methods incorporating reasonable estimates of lateral swell pressure into the design of earth retaining structures using on-site cohesive expansive backfill materials.

Two ancillary purposes of this study are to convey an appreciation of the complexities of the behavior of expansive clay materials when used as retaining structure backfill materials, and to illuminate the lack of concerted previous research into the topic of lateral swell pressure exerted by expansive clay soils against those structures.

The primary conclusions that can be drawn from the limited available published studies in the area of lateral swell pressure of expansive cohesive soils are summarized in the Table 3.4 below:

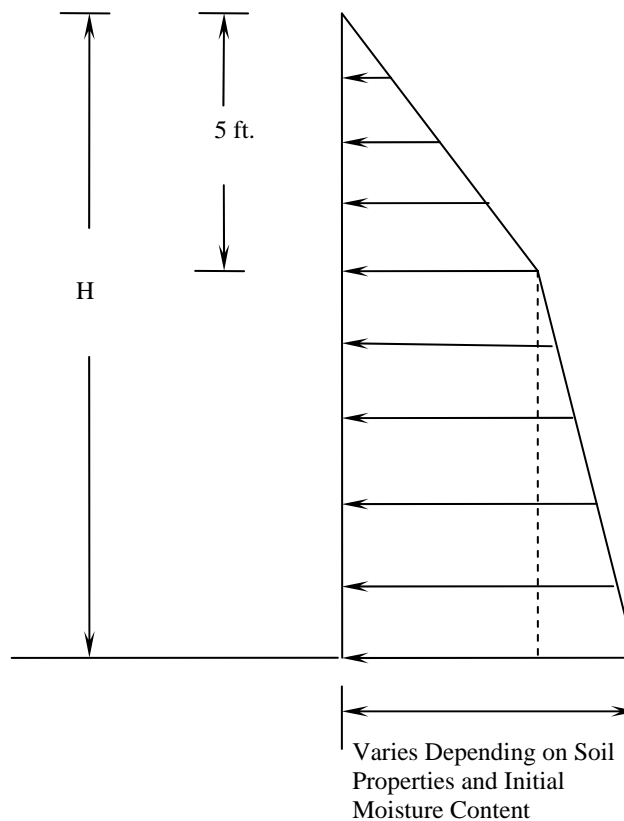
Table 3.4 - Literature Review Conclusions

Number	Conclusion
1	Conventional 1-dimensional laboratory tests overestimate swell strain by about a factor of 3. Triaxial tests results compare more favorably with field measurements.
2	The LSP MkII triaxial setup (Ofer, 1981) can be used to simulate the effects of wall yielding. The Wattanasanticharoen et al. (2007) setup may be modified to investigate the impact of varying suction changes.
3	Small wall deflections result in greatly reduced applied lateral swell pressures. This reduction can also be accomplished by placing a non-expansive material between the structure and the expansive backfill.
4	Applied lateral pressures due to swelling may exceed 5 times the vertical overburden pressure. This difference increases with increasing surcharge.
5	Well-compacted materials generate higher lateral swell pressures than less compacted materials. Maximum observed pressures occur at optimum moisture content and 100% density.
6	Increased compaction moisture content results in decreased suction and decreased lateral swell pressure generated for a given material.
7	Materials with similar mineralogical composition and bulk physical properties and characteristics exhibit similar swelling characteristics, regardless of origin or depositional history.

By using the data developed from these previous studies, it should be possible to develop an initial process for making reasonable predictive estimates of retaining wall

stability when using expansive cohesive clays as backfill, or when placing retaining structures against such naturally occurring materials. Further, in view of the general patterns of those results obtained in those studies and in conjunction with notable limitations in the samples, preparations and procedures, among others, a clear path forward for further research into this topic is now evident.

Based on the available research reviewed, a composite triangular pressure distribution for lateral swell pressure development will be considered in subsequent analyses in this work, as shown in Figure 3.26. Since soil strains follow the path of least resistance, strains at and near unburdened surfaces will be vertical. Hence, lateral swell pressures equal zero at the surface.



**Figure 3.26 – Interpreted Lateral Swell Pressure Distribution
(based on: Katti et al., 1983; Clayton et al., 1991)**

CHAPTER 4

TRADITIONAL RETAINING WALL DESIGN

4.1 Introduction

Designs for most retaining walls constructed with a foundation, both rigid and flexible, specify the use of granular materials (sand and/or gravel) as the backfill materials to be used behind those structures, primarily because the methods for calculating earth pressures on the walls are relatively simple and well established (Coulomb, 1776; Rankine, 1857). This simplicity is due, in part, to the relatively inert nature of granular materials, i.e., the particles do not appreciably interact chemically with each other, with the surrounding soil particles, or with water. Additionally, the shear strength of these materials is due to interparticle contact and is entirely dependent on the effective angle of internal friction (ϕ'), as the materials are assumed to drain water quickly and not develop increased pore water pressures when subjected to increased loading. Hence the resulting active and passive pressures used in the traditional design methodologies are only dependent on this single independent soil parameter, though the Coulomb method is a bit more involved in that it considers the backslope angle of the fill and wall-soil interface friction in the calculations of applied lateral earth pressure. Typical rigid and flexible retaining structure profiles are shown in Figure 4.1 below.

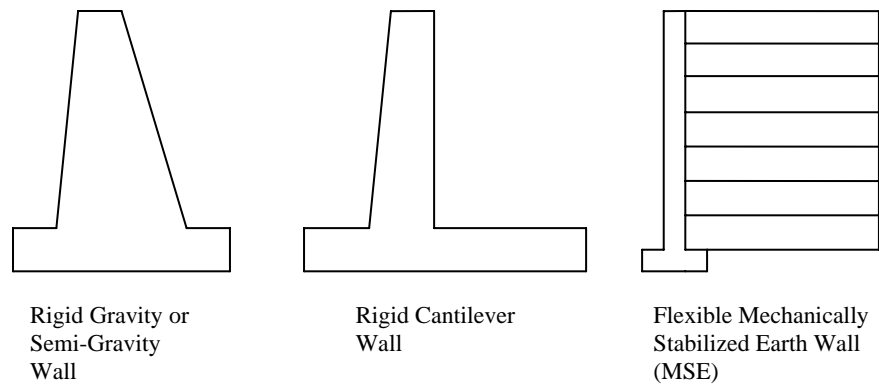


Figure 4.1 – Common Types of Retaining Walls

In contrast to granular soils, cohesive soils (clays and silts), are much more reactive chemically, particularly with water (especially clay soils), and they possess an additional component of shear strength due to particle cohesion (c or c'). Furthermore, cohesive soil mass reactions with water are time-dependent, which adds another degree of complexity to any analysis of retaining wall stability when cohesive materials are present behind the structure.

4.2 Basic Concepts

Since lateral forces applied to retaining structures are primarily directed so as to destabilize the structure (driving forces), determination of the magnitude and orientation of these forces are crucial to the development of a safe and economic design to resist those driving forces and also to incorporate an acceptable Factor of Safety into the overall design. In traditional design methodologies, these lateral forces are generated from three sources: the backfill soil itself, water in the backfill, and surcharge loads atop the backfill in proximity to the wall as illustrated in Figure 4.2. The moist unit weight of soil (γ_m) is considered in the computations above the water table and the submerged unit weight (γ_{sat}) is considered below that depth.

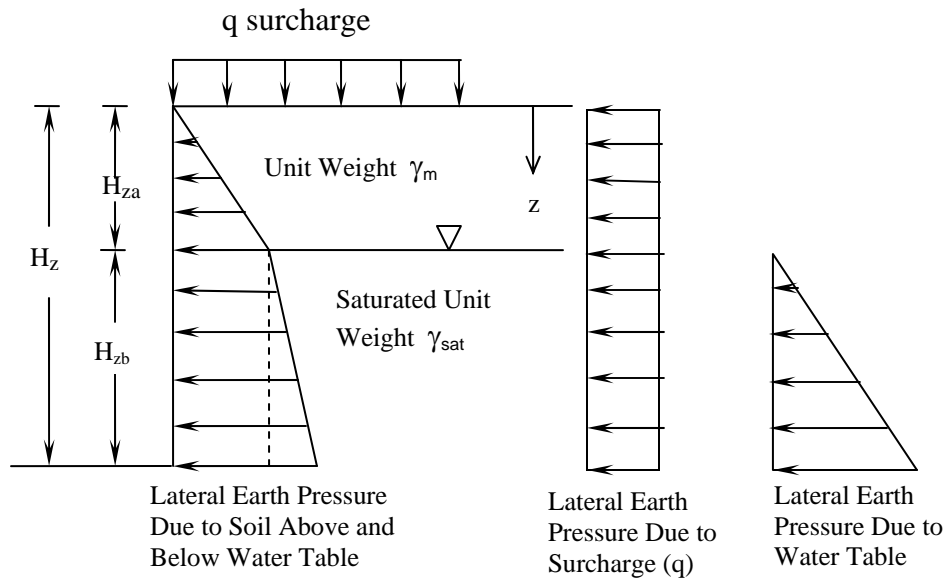


Figure 4.2 – Lateral Earth Pressures From the 3 Main Pressure Components: Soil, Surcharge and Water

Vertical stresses existing in a soil mass at a given depth z below the ground surface is the sum of two components: the self weight of the soil(s) above z , and any surcharge loads. This can be written as

$$\sigma_v = \gamma z + q \quad (4.1)$$

Horizontal stresses within that same soil mass and at the same depth z are taken to be some fraction, K , of the effective overburden pressure plus any hydrostatic pore water present. This can be written as

$$\sigma_h = K\sigma'_v + u \quad (4.2)$$

where u = pore water pressure

K = coefficient of lateral earth pressure

Three wall conditions are generally considered during retaining wall design. These are, in order of increasing applied pressure: active, at-rest and passive.

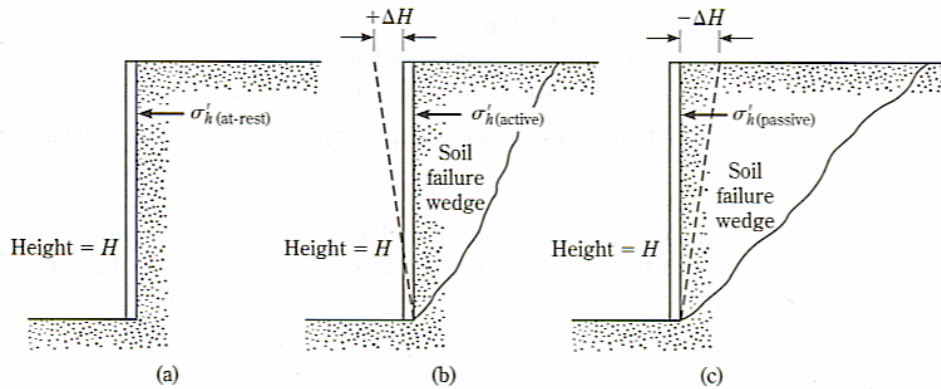


Figure 4.3 – At-Rest (a), Active (b) and Passive (c) Pressures on Retaining Structures (from: Das, 2004)

Though of considerable importance in certain situations (e.g., sheet pile walls), the passive pressure condition has far less application in the analysis and design of typical rigid concrete or mechanically stabilized earth (MSE) retaining wall structures, primarily because: 1) this force is typically small compared to the other forces present, and 2) those forces are resistive to wall movement at the toe of the wall which, over time, may be removed for various reasons (erosion, utility installation, etc.). As such, passive resistance is often ignored in both rigid and flexible wall analyses, resulting in a more conservative design (Das, 2004). When used, the effective cohesion and friction angle (c' and ϕ') of the materials providing the passive resistance are typically reduced to about 2/3 to 3/4 of their measured values in sliding stability calculations.

For at-rest conditions where no movement of the wall is allowed, K is denoted as K_o . Jaky (1944) first suggested that this value be calculated as

$$K_o = 1 - \sin \phi' \quad (4.3)$$

where ϕ' = drained peak friction angle. Other researchers have proposed alternate calculations (e.g., Brooker and Ireland, 1965; Mayne and Kulhawy, 1982). For the sake

of simplicity, the Jaky formula will be considered for the remainder of this present work when at-rest conditions are considered.

For the active condition where some small outward movement of the wall is allowed to occur, the actual lateral active pressure of cohesive soils acting against a wall at a given depth would be

$$\sigma'_a = \sigma'_v K_a - 2c'\sqrt{K_a} \quad (4.4)$$

Therefore, for a wall of height H with no water table, the total lateral active force from cohesive backfill acting upon a unit length of wall is

$$P_a = \frac{1}{2} \gamma H^2 K_a - 2c'H\sqrt{K_a} \quad (4.5)$$

Rankine (1857) proposed that the active pressure coefficient, K_a , for horizontal backfill against a frictionless wall be taken as

$$K_a = \tan^2 \left(45 - \frac{\phi'}{2} \right) \quad (4.6)$$

Note that

$$\tan^2 \left(45 - \frac{\phi'}{2} \right) = \frac{1 - \sin \phi'}{1 + \sin \phi'} \quad (4.7)$$

When inclined backfill is considered, Rankine's active pressure coefficient becomes

$$K_a = \cos \alpha \frac{\cos \alpha - \sqrt{\cos^2 \alpha - \cos^2 \phi'}}{\cos \alpha + \sqrt{\cos^2 \alpha - \cos^2 \phi'}} \quad (4.8)$$

where α is the angle of inclination above the horizontal and ϕ' is the soil friction angle.

When soils also possess appreciable cohesion, the computation of K_a becomes very

complex. In these cases, values of K_a are generally obtained by interpolation from published tables of values calculated for the variables α , ϕ' , and the term $\frac{c'}{\gamma z}$ (e.g. Caquot and Kerisel, 1948).

Because the Coulomb active pressure coefficient considers the backslope angle of the fill (α), the wall angle (β) and the interface soil-wall friction angle (δ), the expression for K_a is also very cumbersome. The calculation for Coulomb's active pressure coefficient is shown in eq. 4.9. For a vertical backface of wall, the value of β is 90° .

$$K_a = \frac{\sin^2(\beta + \phi')}{\sin^2 \beta \sin(\beta - \delta) \left[1 + \sqrt{\frac{\sin(\phi' + \delta) \sin(\phi' - \alpha)}{\sin(\beta - \delta) \sin(\alpha + \beta)}} \right]^2} \quad (4.9)$$

Again, values are generally obtained by interpolation from published tables. The results obtained by Coulomb's methods are generally regarded a more conservative and more reflective of actual conditions. However, for illustration purposes and in the interest of simplicity, Rankine's values and methods will be used for the remainder of this study where appropriate.

The form of the above Rankine equations for the passive condition are similar to those above, but with opposite sign conventions as shown

$$K_p = \tan^2 \left(45 + \frac{\phi'}{2} \right) \text{ and} \quad (4.10)$$

$$P_p = \frac{1}{2} \gamma H^2 K_p + 2c' H \sqrt{K_p} \quad (4.11)$$

It should be noted that for the at-rest condition where no movement of the wall is permitted, and hence, no failure wedge is developed within the backfill, the total lateral force per unit length of wall becomes

$$P_o = \frac{1}{2} \gamma H^2 K_o \quad (4.12)$$

4.3 Rigid Walls

Typical rigid retaining structures or walls consist of longitudinal segments of cast-in-place steel-reinforced concrete that are securely anchored to a foundation, generally either a shallow footing, driven pile or drilled pier, by means of embedded steel dowels protruding from the foundation some distance into the wall stem. Where shallow footings are utilized, the longitudinal segments may be cast monolithically with the footing, or cast separately after the footing has been cast and the concrete achieved sufficient strength. When cast separately, a shear key is often constructed along the line of dowel connections to provide additional structural integrity.

Rigid walls, as the name implies, are designed to be very stiff and relatively inflexible, maintaining their lines of installation at the toe and top of the wall, and points in between, during the life of the wall. For certain types of rigid walls where no outward movement is allowed, such as basement walls, at-rest lateral earth pressure conditions prevail. For other situations, the allowable movements that can be tolerated are generally only those required to develop the lower active earth pressure conditions. Rigid walls are relatively impermeable and are often designed with provisions for positive backfill drainage to prevent the buildup of hydrostatic pressures.

4.3.1 Lateral Earth Pressures Acting on Rigid Walls Using Granular Backfill

In the traditional design methodology for a rigid retaining wall structure using granular backfill materials ($c = 0$) with a horizontal fill surface behind the wall, the distribution of active pressure exerted by backfill on a wall of height H , is considered to be triangular and the total exerted force is expressed in the following form

$$P_a = \frac{1}{2} \gamma H^2 K_a \quad (4.13)$$

Figure 4.4 illustrates the condition where a water table is present. It should be noted that where water is present within the backfill, the hydrostatic water pressure distribution is also taken as triangular. However, surcharge loads are often assumed to be constant with depth, resulting in a rectangular pressure distribution.

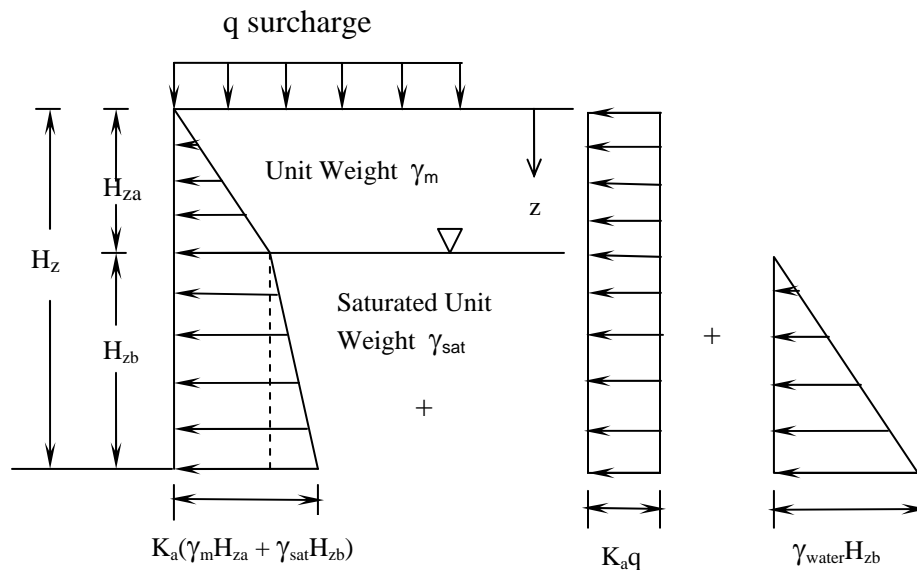


Figure 4.4 – Lateral Earth Pressures on Conventional Rigid or Flexible Walls

The active force is applied per unit length of wall. Where both water and surcharge loads are present, the active force acting per length on the wall becomes

$$P_a = \frac{1}{2} \gamma_m H^2_{za} K_a + \gamma_m K_a H_{za} H_{zb} + \frac{1}{2} \gamma_{sat} H^2_{zb} + \frac{1}{2} \gamma_w H_{zb}^2 + qHK_a \quad (4.14)$$

where H_{zb} is the height of the water above the base of the wall as shown in Figures 4.2 and 4.4. Similar expressions are obtained for the at-rest and passive conditions with the substitution of K_o or K_p for K_a , as appropriate.

The total force per unit length of wall obtained from the above calculations is typically represented graphically as single force vector acting at a particular point. This point is at the backside of the soil wedge above the heel of the structure foundation in the Rankine calculation, and is a point on the backside of the wall in the Coulomb calculation as illustrated in Figures 4.5 and 4.6. Determination of this point of application is required for calculating the potential overturning moment generated on the retaining structure.

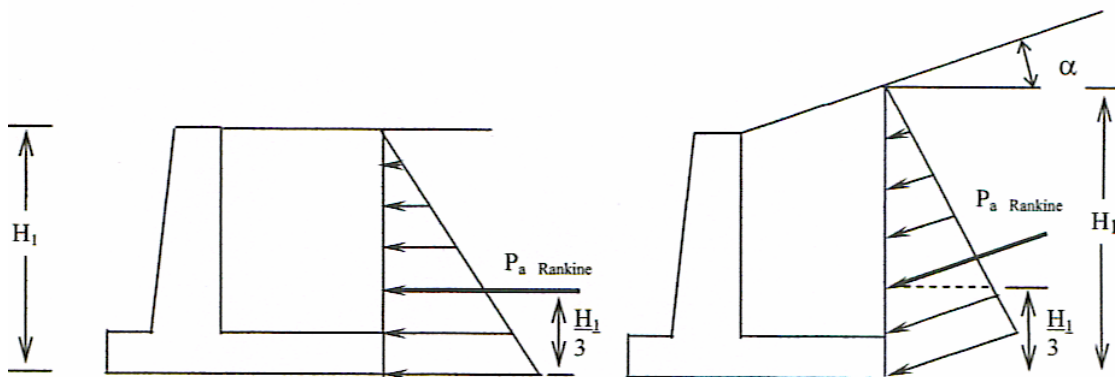


Figure 4.5 –Rankine Active Force (P_a) and Point of Application. Horizontal Backfill (left), Inclined Backfill (right)

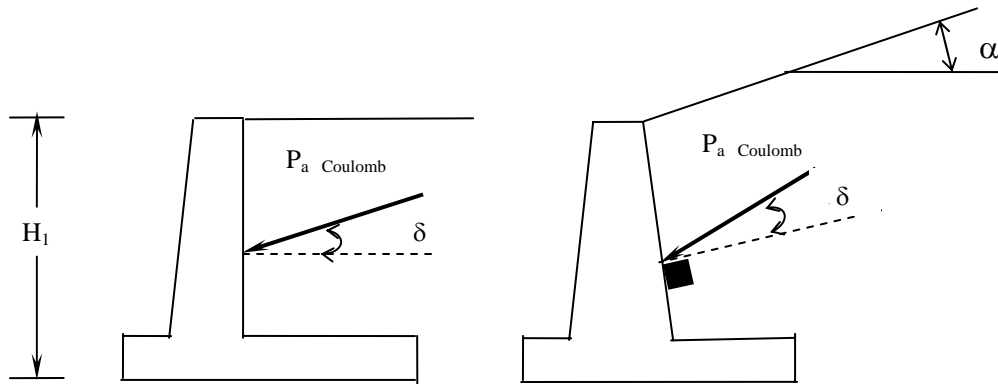


Figure 4.6 – Coulomb Active Force (P_a) and Point of Application. Vertical Wall Face (left), Inclined Wall Face (right)

Adjustments to the calculated values of K_a , due to an inclined backfill surface, can be found in Das (2004). For these cases the resultant forces acting on the wall structure are still applied at the same point on the wall, all else being equal, but the lines of action of those forces are parallel to the slope of the backfill, resulting in both horizontal and vertical components of applied force. In practice in the Dallas-Fort Worth, Texas area, these corrections are usually not employed for slopes less than about 4H:1V.

Casagrande (1973) found that the pressure distribution assumptions commonly employed may be oversimplified and that more complex distributions likely exist in practice. However, for the illustrative purposes of this research, the foregoing pressure distribution assumptions will be considered valid.

4.3.2 Lateral Earth Pressures Acting on Rigid Walls Using Cohesive Backfill

The traditional design methodology for a rigid retaining wall structure using cohesive backfill materials is more complex than that used for the case of granular backfill outlined above. Though the calculation methods for hydrostatic and surcharge loads, and for the point of application of the resultant active lateral pressures are the same

in each case, the presence and the nature of cohesion forces requires more in-depth analysis. As seen from eq. 4.5, above the water table, the Rankine active lateral earth force per unit length of wall equation is

$$P_a = \frac{1}{2} \gamma H^2 K_a - 2c' H \sqrt{K_a} \quad (4.15)$$

Hydrostatic and surcharge loading can be added into this calculation, but no consideration of lateral earth pressures due to lateral swelling pressure of expansive cohesive backfill soils is attempted in either the Rankine or Coulomb model.

In looking at this equation, it is evident that the lateral force applied to the upper part of the wall is actually negative because of the cohesion term as shown in Figure 4.7. This negative value becomes zero at some depth (z_c), which is considered to be the maximum depth of potential tensile crack formation between the soil backfill and the back face of the wall (Das, 2002, 2005). This depth is found by

$$z_c = \frac{2c'}{\gamma \sqrt{K_a}} \quad (4.16)$$

After formation of the crack, no contact exists between the soil and the wall; hence, no earth pressure is applied to the wall above the bottom of the crack. However, hydrostatic pressures will develop above that point should the crack fill with water.

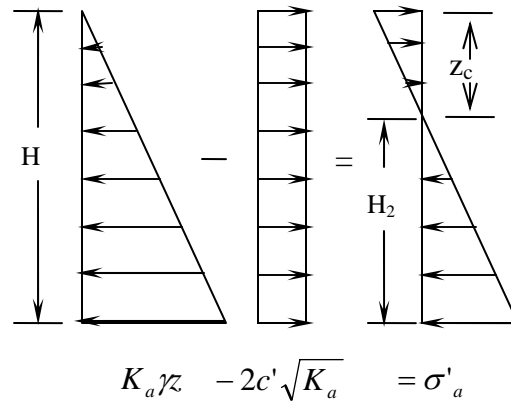


Figure 4.7 – Rankine Lateral Earth Pressure Distribution and the Location of Tensile Crack Development With Cohesive Soil Backfill

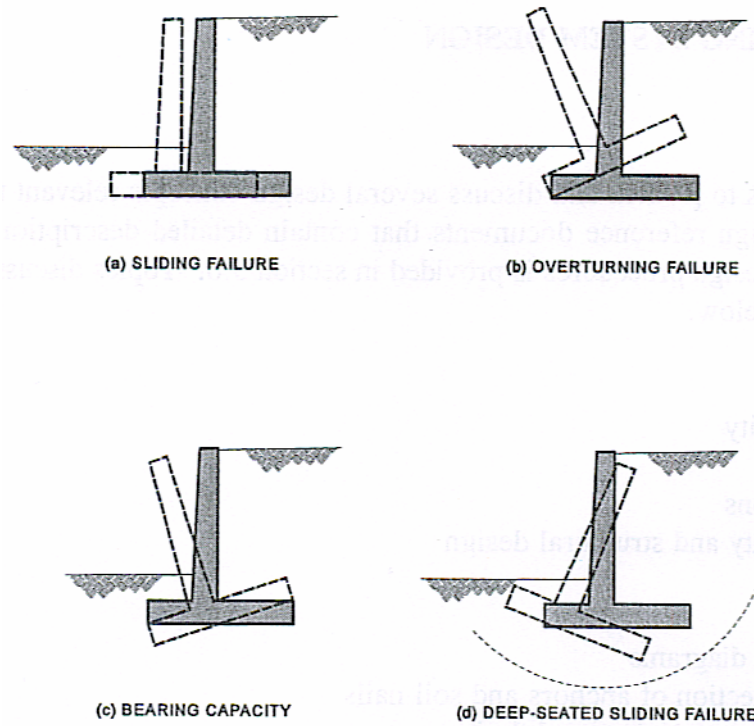
4.3.3 Wall Stability Calculations

For any earth retaining structure, both internal and external stability calculations must be performed to insure that the design will be both safe for people and property. These requirements will determine whether a given design will be economical to construct.

Internal stability checks for rigid retaining structures involve calculations to determine the size and spacing of the concrete wall stem reinforcing steel required to resist the applied moments and shear forces exerted by the retained earth. Details of these checks are not considered in this work, except to mention that the reinforcing required is entirely dependent on the magnitude of the applied force, P_a or P_o , and that reinforcement is then proportioned accordingly.

External stability checks for rigid retaining structures involve calculations assessing the ability of the wall system as a whole to resist movement. Four different external stability calculations (potential modes of failure) are routinely performed for the design of any retaining structure: Overturning Stability, Sliding Stability, Bearing

Capacity of the foundation soils, and Global Stability. The four principal modes of retaining structure failure are shown in Figure 4.8.



**Figure 4.8 – Four Common Modes of Retaining Structure Failure
(from: FWHA, 1997)**

Lateral earth pressures do not play a significant role in global stability analyses. However, determination of the lateral earth forces (pressures) exerted on retaining structures is of primary importance for the overturning and sliding stability of the structure. Lateral forces also influence the bearing capacity stability of the overall structure due to loading eccentricities developed and transmitted to the wall foundation.

Depending on the application, an acceptable Factor of Safety for overturning, or toppling, ranges from 1.5 to 3 (Das, 2004). For rigid structures, the Federal Highway Administration (1999) recommends a minimum Factor of Safety of 2.0 against overturning for wall footings based in soil and a minimum of 1.5 for wall footings based

in rock. Critical structures such as hospital or nuclear facilities should incorporate higher Factors of Safety. The check for overturning is rather straightforward and can be expressed as

$$FS_{(OT)} = \frac{\sum M_R}{\sum M_O} \quad \text{where,} \quad (4.17)$$

$\sum M_R$ = sum of moments resisting overturning

$\sum M_O$ = sum of driving moments tending to overturn the structure (soil, water and surcharge)

These moments are computed at the toe of the structure foundation at the foundation base. As the driving moments increase, internal wall stability can be increased through additional structural reinforcement. External stability is generally increased by increasing the length of the wall foundation heel. The industry assumption is that a triangular pressure distribution for the backfill soil is correct. With this configuration, the total lateral force per unit length of wall for the soil only is P_a ($P_a \cos \alpha$ for inclined backfill), and this force is applied at a point $\frac{H}{3}$ above the base of the wall. Therefore, the driving moment due to the soil is

$$M_O = P_a \cos \alpha \left(\frac{H}{3} \right) \quad (4.18)$$

and, as noted above, the calculation of P_a is the primary concern. When other loads are present, such as surcharge, free water and swelling, the point of resultant load application can be determined by summing moments of each force about the toe of the structure and dividing by the magnitude of the total force

An acceptable Factor of Safety for sliding is usually 1.5 for most applications (Das, 2004; FHWA, 1999). Similar to the check for overturning, the sliding stability analysis can be expressed as

$$FS_{(SL)} = \frac{\sum F_R}{\sum F_d} \quad \text{where,} \quad (4.19)$$

$\sum F_R$ = sum of horizontal resisting forces

$\sum F_d$ = sum of horizontal driving forces from soil, water and surcharge (P_a or $P_a \cos \alpha$)

Again, as the driving forces increase, internal wall stability can be increased through additional structural reinforcement. External stability is generally increased by increasing the size (heel width) of the wall foundation, or by increasing the foundation depth and calculating the resisting passive forces at the toe and front of the wall. Construction of a shear key at the base of the foundation will also increase sliding stability by taking advantage of the resistive passive forces generated at the front face of the key.

Because of the overturning moments generated on retaining structures, more vertical pressure is applied at the toe of shallow retaining structure foundations (footings) than at the heel. As the applied lateral force increases, the magnitude of maximum vertical pressure exerted on the subgrade soils (at the toe) also increases. Bearing capacity typically requires a Factor of Safety of at least 2 and can be calculated as

$$FS_{(BC)} = \frac{q_u}{q_{\max}} \quad \text{where} \quad (4.20)$$

q_u = Ultimate bearing capacity as determined by the general ultimate bearing capacity equation (ref. Meyerhof, 1963)

q_{max} = Maximum applied pressure at the toe of the structure foundation due to the eccentricity caused by the moments generated.

A deficient computed Factor of Safety for bearing capacity can be resolved by increasing the size of the foundation, decreasing the height of the wall, installing deep foundations or improving the subgrade by some form of soil modification.

For the remainder of this present research, only overturning and sliding stabilities will be considered. An example calculation for overturning and sliding for a typical rigid retaining wall is shown below ($H_z = 15$ feet), based on the generalized case shown in Figure 4.9. H_2 and z_c are not shown in this figure, but are calculated based on eq. 4.16 as illustrated in Figure 4.7. The dimensions and properties shown in Figure 4.9 are defined in Table 4.1, as are the other parameters used in subsequent calculations.

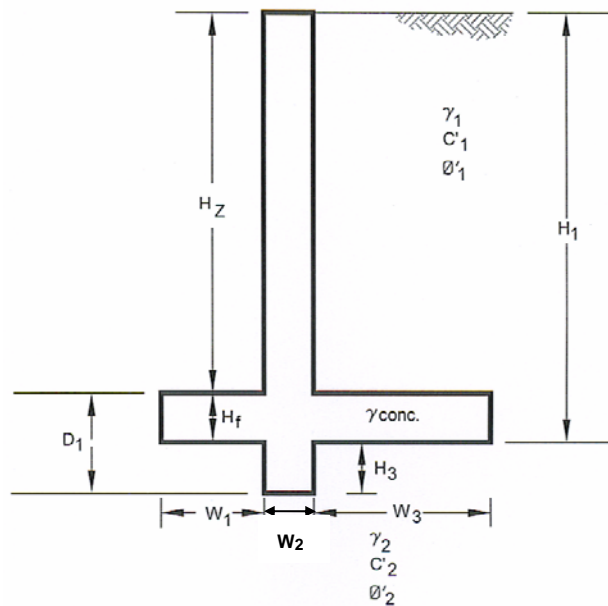


Figure 4.9 – Generalized Rigid Wall Geometry

**Table 4.1 Soil Parameter and Geometric Definitions for Examples
(based on wall geometry shown in Figure 4.9)**

Soil Parameters

γ_{water}	- Unit Weight of Water
γ_1	- Unit Weight of Retained Soil
γ_2	- Unit Weight of Foundation Soil
γ_{conc}	- Unit Weight of Concrete
C'_1	- Effective Cohesion of Retained Soil
C'_2	- Effective Cohesion of Foundation Soil
ϕ'_1	- Effective Friction Angle of Retained Soil
ϕ'_2	- Effective Friction Angle of Foundation Soil
K_a	- Rankine Active Pressure Coefficient
K_p	- Rankine Passive Pressure Coefficient
P_{soil}	- Active Soil Pressure
P_{cohesion}	- Cohesion Soil Pressure
P_{net}	- Net Soil Pressure
P_a	- Net Active Force
P_p	- Net Passive Force
$P_{\text{lat sw}}$	- Net Lateral Swell Force

Geometric Parameters

H_1	- Overall Wall Height
Z_c	- Theoretical Depth of Tension Crack Formation
H_2	- $H_1 - Z_c$
H_Z	- Height of Exposed Wall Facing
H_f	- Wall Footing Thickness
W_1	- Width of Wall Toe
W_2	- Width of Wall Stem
W_3	- Width of Wall Heel
D_1	- Embedment Depth Plus Keyway Depth

In Example 4.1, free water is assumed to extend upward to the theoretical depth of the tension crack, though it is assumed that no soil-wall separation has formed (soil remains in contact with the wall). Lateral swell pressure is not considered at this point.

Example 4.1 - 15-Foot Wall Facing with High Water Table

γ_{water}	62.4	pcf	K_a	0.472		H_z	15.0	ft
γ_1	114	pcf	K_p	2.371		H_f	2.0	ft
γ_2	120	pcf	Z_c	5.34	ft	W_1	4.0	ft
γ_{conc}	150	pcf	H_1	17	ft	W_2	1.5	ft
C'_1	209	psf	H_2	11.66	ft	W_3	15.0	ft
C'_2	200	psf	P_{soil}	915.4	psf	D_1	2.0	ft
ϕ'_1	21	deg	P_{cohesion}	287.3	psf			
ϕ'_2	24	deg	P_{net}	628.1	psf			

Moment

<u>Item</u>	<u>Area</u>	γ	<u>Force</u>	<u>Arm</u>	<u>Moment</u>
P_a			3,663.62	3.89	14,245
P_w		62.4	4,245.43	3.89	16,508
Total Driving			ΣF_{horiz}	7,909.05	ΣM_{drive}
					30,753
A_1	225	114	25,650.00	13.00	333,450
A_2	22.5	150	3,375.00	4.75	16,031
A_3	41	150	6,150.00	10.25	63,038
P_p			0.00		
Total Resisting			ΣF_{vert}	35,175.00	ΣM_{resist}
					412,519

OVERTURNING

$$FS = \frac{\Sigma M_{\text{resist}}}{\Sigma M_{\text{drive}}} = 13.41$$

SLIDING

$$FS = \frac{\Sigma F_{\text{vert}}}{\Sigma F_{\text{horiz}}} = 1.83$$

Following the above calculations, Table 4.2 presents the computed Factors of Safety for a variety of wall heights and footing heel widths for a given set of soil conditions. The assumed parameters are conservative and typical for the expansive near surface soils found in North Texas. It should be noted that the computations for Tables 4.2 and 4.3 assume a rather high water table, which significantly reduces the calculated Factors. Analyses using reduced water levels are presented in Table 4.4 for comparison.

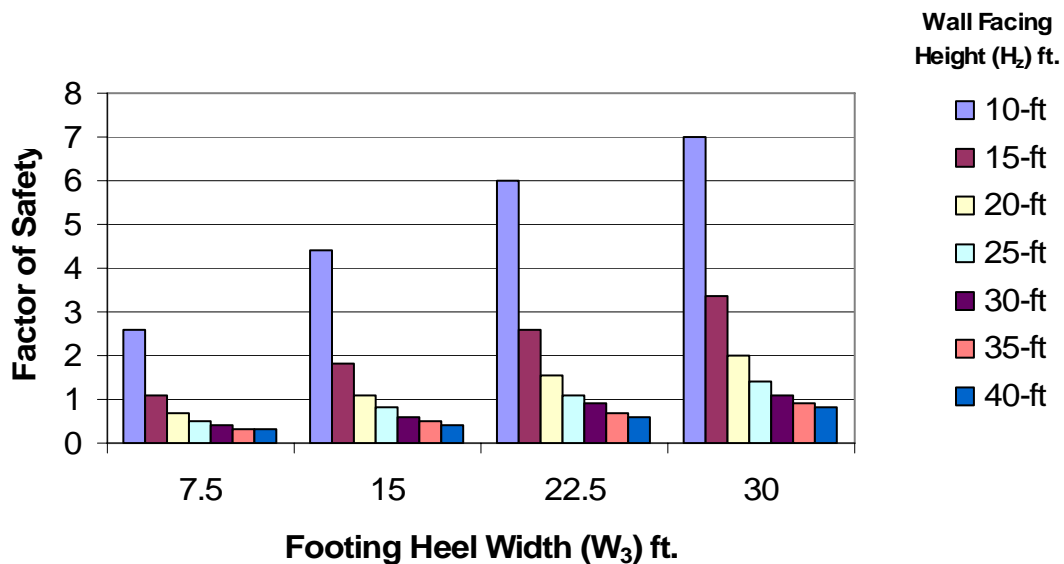
**Table 4.2 - Factors of Safety versus Wall Height and Footing Heel Width
(Assumes High Water Table)**

H _z , ft.	W ₃ = 7.5 ft.		W ₃ = 15 ft.		W ₃ = 22.5 ft.		W ₃ = 30 ft.	
	FS _{OT}	FS _{SL}	FS _{OT}	FS _{SL}	FS _{OT}	FS _{SL}	FS _{OT}	FS _{SL}
10	20.07	2.61	>50	4.40	>90	>6	>150	>7
15	5.20	1.07	>13	1.83	>25	2.60	>40	3.36
20	2.29	<0.7	5.90	1.09	>11	1.55	>17	2.01
25	1.27	<0.5	3.28	<0.8	6.18	1.08	9.99	1.41
30	<0.8	<0.4	2.07	<0.6	3.92	<0.9	6.33	1.07
35	<0.6	<0.3	1.43	<0.5	2.70	<0.7	4.36	<0.9
40	<0.4	<0.3	1.04	<0.4	1.97	<0.6	3.18	<0.8

It can be seen that as wall or structure heights increase, both the overturning and sliding stabilities decrease for a given footing width, as evidenced by the lower computed

Factors of Safety. These Factors are increased by increasing the footing heel width, as illustrated above.

According to Table 4.2, sliding stability is the controlling condition for the assumed given soil and geometric parameters. It is interesting to note that required heel widths to maintain a Factor of Safety greater than or equal to 1.5, increase faster than the wall heights increase. For the given parameters, it was found that when wall heights reach about 18 feet in height, the required heel is also 18 feet to achieve a Factor of Safety equal to 1.5. For walls taller than 18 feet, the required heel width is greater than the wall height. These trends are illustrated graphically in the chart below as Figure 4.10.



**Figure 4.10 – Factors of Safety With Respect to Sliding
(Based on Data From Table 4.1)**

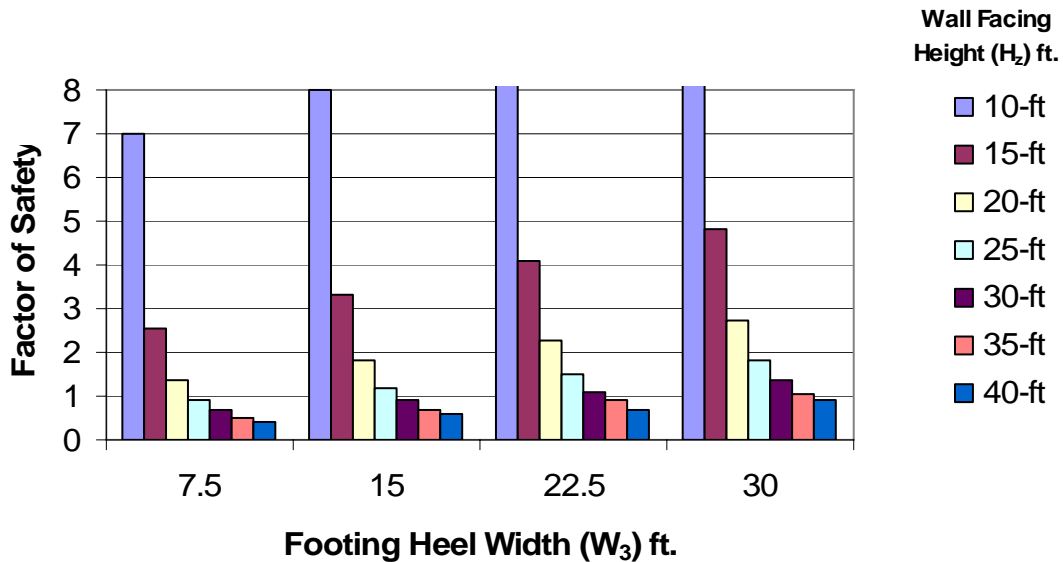
To improve sliding resistance and/or to reduce retaining structure footing widths, a keyway may be constructed at the base of the footing to mobilize the passive resistance of the foundation soils, thereby increasing the Factor of Safety against sliding. Table 4.3

below presents the same FS_{Sliding} data as in Table 4.2 , but incorporates the effect of the addition of a 4-foot deep keyway below the base of the footing (6 feet below top of footing). This assumes that all soils in front of the structure below the top of footing elevation will remain intact throughout the design life of the structure.

Table 4.3. Comparisons of Factors of Safety Against Sliding With and Without 4-foot Deep Keyway Below Base of Footing (Assumes High Water Table)

H_z , ft.	$W_3 = 7.5$ ft.		$W_3 = 15$ ft.		$W_3 = 22.5$ ft.		$W_3 = 30$ ft.	
	Without Keyway	With Keyway	Without Keyway	With Keyway	Without Keyway	With Keyway	Without Keyway	With Keyway
10	2.61	>7	4.40	>8	>6	>10	>7	>12
15	1.07	2.55	1.83	3.31	2.60	4.07	3.36	4.83
20	<0.7	1.36	1.09	1.82	1.55	2.28	2.01	2.74
25	<0.5	<0.9	<0.8	1.19	1.08	1.51	1.41	1.84
30	<0.4	<0.7	<0.6	<0.9	<0.9	1.11	1.07	1.35
35	<0.3	<0.5	<0.5	<0.7	<0.7	<0.9	<0.9	1.06
40	<0.3	<0.4	<0.4	<0.6	<0.6	<0.7	<0.8	<0.9

The above data for Factors for Safety with a keyway are illustrated graphically in the chart in Figure 4.11 below.



**Figure 4.11 – Factors of Safety With Respect to Sliding Using a Keyway
(Based on Data From Table 4.2)**

Increasing the keyway depth an additional 2 feet improves the calculated Factor of Safety about 20 to 40 percent for the range of geometries analyzed. As expected intuitively, the percentage of improvement increases with decreased H_z heights.

Depending on the specific situation to be considered, the assumed water level incorporated into the preceding calculations may not reflect the conditions found in actual practice. In residential, and perhaps some commercial areas, where landscaping irrigation may be heavy to excessive at certain times of the year, high water conditions as modeled may occasionally occur. However, retaining structures in these areas rarely exceed 10 to 15 feet in height. The following tabulation is provided to examine the effect of a lower, and perhaps more realistic, groundwater level on retaining structure sliding stability as would likely be encountered in a non-irrigated environment. To reinforce the validity of these analyses, any practical retaining structure design using expansive soil

backfill will certainly require some means of free water drainage behind such structure. The details of these measures need not be scrutinized here, but the gross effect of such measures will likely be to effectively lower the hydrostatic head acting against said structure. The computations performed for the following tabulated Factors of Safety assume a static groundwater level equal to half the distance from the base of the footing to the theoretical depth of tension crack development H_2 , or a minimum of 5 feet above the base of the footing, whichever is greater.

Table 4.4 - Comparison of Factors of Safety Against Sliding With Differing Water Levels (Assumes 4-foot Deep Keyway Below Base of Footing)

H_z , ft.	$W_3 = 7.5$ ft.		$W_3 = 15$ ft.		$W_3 = 22.5$ ft.		$W_3 = 30$ ft.	
	High Water Level	Moderate Water Level	High Water Level	Moderate Water Level	High Water Level	Moderate Water Level	High Water Level	Moderate Water Level
10	>7	>9	>8	>11	>10	>14	>12	>16
15	2.55	4.27	3.31	>5	4.07	>6	4.83	>8
20	1.36	2.27	1.82	3.04	2.28	3.81	2.74	4.58
25	<0.9	1.45	1.19	1.99	1.51	2.53	1.84	3.07
30	<0.7	1.03	<0.9	1.44	1.11	1.86	1.35	2.27
35	<0.5	<0.8	<0.7	1.11	<0.9	1.45	1.06	1.78
40	<0.4	<0.7	<0.6	<0.9	<0.7	1.18	<0.9	1.45

The chart in Figure 4.12 illustrates graphically the computed Factors of Safety against sliding for the data in Table 4.4 assuming a moderate water level. Figure 4.13 compares Factors of Safety for a 25-foot high wall using the data from Tables 4.2 through 4.4.

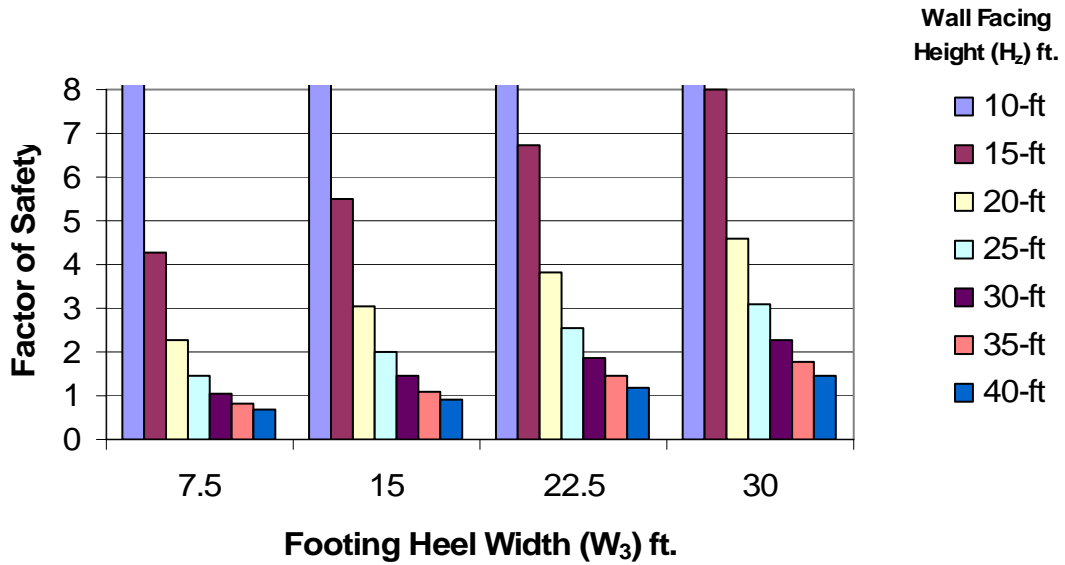


Figure 4.12 – Factors of Safety With Respect to Sliding Using a Keyway and Assuming a Moderate Water Table (Based on Data From Table 4.3)

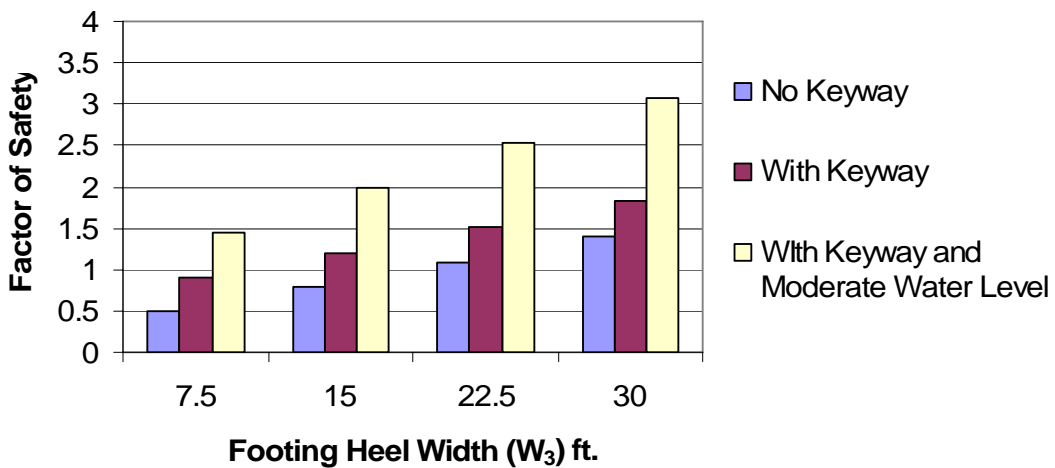


Figure 4.13 – Comparison of Factors of Safety With Respect to Sliding for a 25-foot Tall Wall (Based on Data From Tables 4.1 through 4.3)

4.4 Flexible (MSE) Walls

Flexible retaining walls, or mechanically stabilized earth walls (MSE walls), typically consist of a block (wedge) of reinforced soil backfill faced with relatively small pre-cast concrete wall segments or panels that are integrally connected to each other (not mortared together), or may simply just rest atop each other with staggered overlap. The wall facing segments are available in a wide variety of shapes to suit virtually any architectural or aesthetic purpose. The segments rest on a shallow footing, leveling pad or grade beam and are not attached to the foundation as is the case with a rigid wall system. Two typical forms of MSE walls are shown in Figure 4.14. The horizontal lines behind the wall section represent regularly spaced reinforcing elements that are physically connected to the wall facing blocks. These elements commonly consist of geotextiles, geogrids, metal strips, or can be a combination of elements.

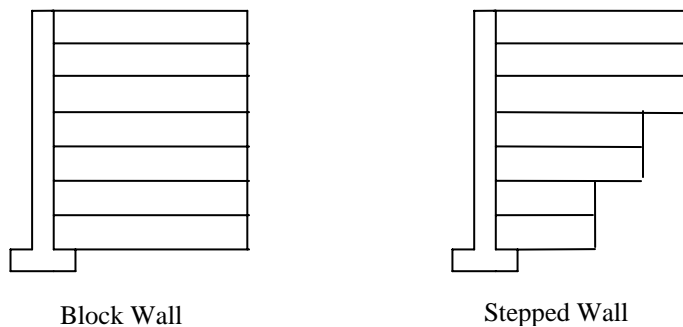


Figure 4.14 – Block and Stepped MSE Walls

The stepped form in Figure 4.14 is sometimes used on tall walls as a cost savings since much of the reinforcement lengths in the lower portions of the wall are behind the

theoretical failure plane in excess of requirements. Determination of this failure plane will be discussed later.

Flexible walls, in contrast to rigid walls, are designed to allow small movements throughout the height and length of the wall without compromising the stability and integrity of the wall system. In addition, the segmental nature of the wall facing blocks can allow water that enters the backfill to drain through the wall facing. Depending on the backfill materials used, this aspect may preclude the necessity of a backfill drainage system behind the wall.

4.4.1 Lateral Earth Pressures Acting on Flexible Walls Using Granular Backfill

Because MSE walls are flexible and free to move somewhat, lateral earth pressures acting on flexible walls always achieve the active pressure condition. For an MSE wall system, internal wall / soil wedge stability analyses are performed first to determine reinforced section geometry; then external analyses are performed to verify stability. If these checks produce unacceptable results, the internal reinforcement is modified and all stability checks are recalculated.

Also, MSE wall segments are unmortared thus, any water that enters the backfill can drain through the wall facing at the segment joints; and with a free-draining granular backfill, hydrostatic pressures should not develop behind the wall. Therefore the maximum force per unit width of wall is the sum of the lateral loads due to the restrained earth and any applied permanent surcharge (eq. 4.21) as shown in Figure 4.15.

$$P_a = \frac{1}{2} \gamma H^2 K_a + qHK_a \quad (4.21)$$

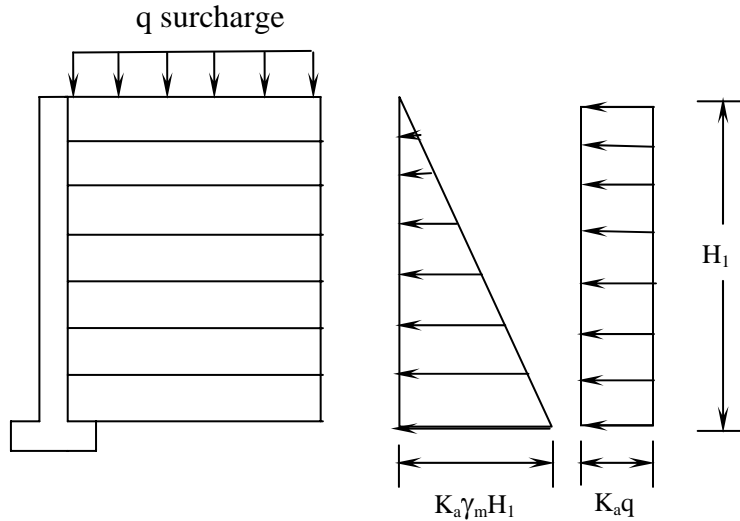


Figure 4.15 – Lateral Earth Pressure on MSE Wall. Soil and Surcharge Only

4.4.2 Lateral Earth Pressures Acting on Flexible Walls Using Cohesive Backfill

Due to the low angle of internal friction exhibited by clay soils, as compared to granular soils, much higher lateral earth pressures result when cohesive soils are used for wall backfill. In addition, since cohesive soils are not free-draining like granular soils, hydrostatic pressures are also exerted on the walls. As a result of these facts, together with the overall complexity of predicting the actual lateral earth pressures exerted by cohesive soils on retaining structures, no established method currently exists for designing MSE retaining walls using cohesive backfill.

In the next Chapter, we will investigate the possibility for using cohesive materials in both rigid and flexible wall systems, and explore the process(es) by which such a design may be reasonably accomplished.

4.4.3 Wall Stability for Flexible Walls

In order to develop a stable wall / soil block geometry for a specified MSE wall height, internal wall stability checks are needed. Internal wall stability checks for MSE walls involve the determinations of soil wedge reinforcement (tie) spacing and length, which controls the dimensions of the reinforced block or wedge of soil. Since the reinforcing elements are in intimate contact with the retained soil, the soil properties have a direct impact on the restraint capacity of those elements. Though a comprehensive treatment of internal stability calculations using cohesive backfill is beyond the scope of this research, the general internal stability check process is illustrated in subsequent paragraphs, followed by some general comments regarding possible measures that may be implemented to compensate for the reduced friction angle of clays versus granular soils.

Internal soil block / wedge stability is achieved through the optimal spacing and length of reinforcing elements, whether geosynthetic materials (GS) or metallic strips. These parameters are computed based on the predetermined force per unit width of wall section, P_a , and assuming a linear potential failure plane extending from the toe of the wall upward equal to an angle of

$$\psi = 45 + \frac{\phi'}{2} \quad (4.22)$$

as shown in figure 4.16.

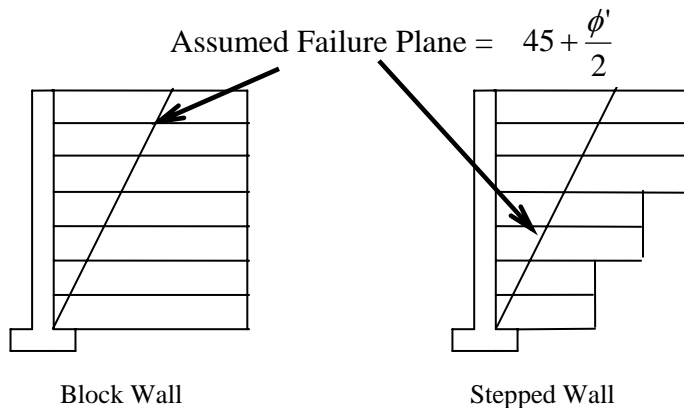


Figure 4.16 – Failure Plane for MSE Wall Reinforcement Length Determination

This failure zone is known as the Rankine active failure zone (FHWA, 1999; Das, 2004). It should be noted that the FHWA Reference Manual (1999) recommends that this failure surface be considered for extensible geosynthetic reinforcements (GS) such as geotextiles or geogrids, and further recommends that inextensible reinforcements such as metallic strips should use a bilinear failure surface as shown in Figure 4.17. For the purposes of this study, we will only consider use of the classical Rankine active failure zone, ψ .

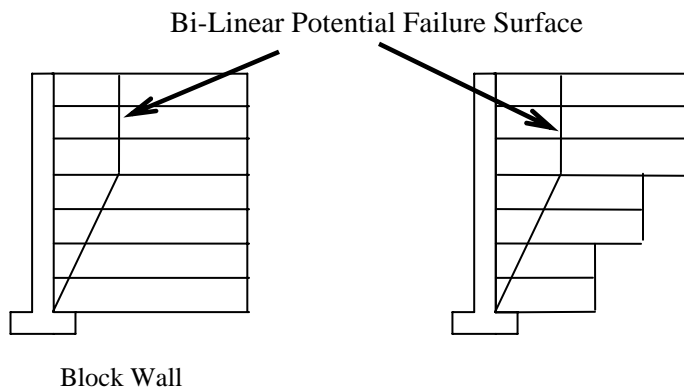


Figure 4.17 - Bi-Linear Potential Failure Plane for Inextensible Reinforcements

The possible modes of failure for any reinforcement are tie breaking (including tie connection) and tie pullout. The first step in determining these parameters is the calculation of the lateral loading due to the soil, and to permanent surcharge and live load, if present (P_a or $P_a \cos \alpha$). This value is determined in the same manner as noted previously. Second, the ultimate tensile strength of the tie material is required. For geosynthetic materials, this is the manufacturer's stated ultimate tensile strength. For metallic reinforcement, this value is calculated by the following equation:

$$T_{ult} = wtf_y ; \text{ where} \quad (4.23)$$

w = width of tie

t = thickness of tie, and

f_y = yield strength of tie material

The ultimate tensile strength is then converted to an allowable tensile strength (T_{all}) for use in further calculations by a series of reduction factors for GS (installation damage, creep, degradation, etc.), and then employing an appropriate Factor of Safety (FS), typically 1.4 or greater. For metallic strip reinforcement, a Factor of Safety of about 2.5 to 3 compared to the ultimate tensile strength is generally considered acceptable.

Once lateral loading and allowable tensile strengths have been determined, the vertical reinforcement spacing of elements, S_v , can be determined by

$$S_v = \frac{T_{all}}{S_h P_a FS} \quad (4.23)$$

where S_h = the horizontal reinforcement spacing

It should be intuitive that the resistance to the driving lateral forces is only developed at some distance behind the determined failure plane. The tie length required

behind the failure plane to resist pullout is known as the effective length, l_e . The tie length in front of the failure plane provides no resistance to pullout and is known as l_r , or the length within the Rankine active zone. The resistance available on a reinforcing element is simply a form of the general friction equation or, more specifically, the general shear strength equation

$$\tau = c' + \gamma z \tan \phi', \text{ where} \quad (4.24)$$

τ = shear strength

c' = effective cohesion

γz = vertical overburden pressure at depth z ; and

ϕ' = effective soil friction angle

Since each element has two (2) sides on which friction is developed, the required effective tie length can be determined by

$$l_e = \frac{S_v S_h P_a F S}{c' + \gamma z \tan \phi'} \quad (4.25)$$

It can be seen that, with decreasing depth, z , the total length of reinforcing elements must increase, not only because l_r increases, but also because l_e increases due to reduced applied friction from the reduced normal force γz . For very tall retaining structures, project economics may suggest a variable vertical reinforcement spacing as in Figure 4.18. This may also result in a “stair-stepped” soil block configuration.

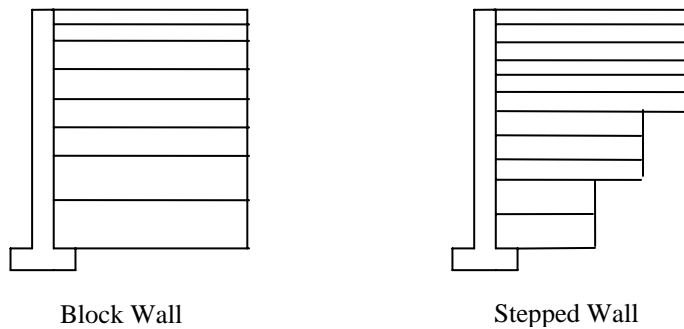


Figure 4.18 – Variable Vertical Reinforcement Spacing

Once the reinforcement spacing and lengths are determined for an MSE structure, the soil block/wedge geometry is then finalized, and the various external stability checks can be performed in like manner as to those described in the previous rigid wall sections. For MSE walls, FHWA (1999) recommends a minimum Factor of Safety of 2.0 against overturning and a minimum of 1.5 against sliding.

It should also be noted that the required effective length to resist lateral driving forces increases with a decrease in backfill soil effective friction angle. In other words, the pullout resistance for a given reinforced system decreases as the effective friction angle decreases. Since expansive cohesive soils have much lower effective friction angle than do granular soils, the internal stability of reinforced cohesive backfills is lower than for granular backfills.

Two methods to compensate for this condition are suggested. Both rely on the development of passive resistance within the reinforced soils beyond the presumed plane of failure. The first could apply to both metallic strips of geosynthetics and involves the use of small plates at the ends of reinforcing elements. Sizing and spacing would need to

be determined during the internal stability analysis. The second would primarily apply to geosynthetics, but could also apply to appropriately fabricated metallic strips. This method involves placement of materials that possess an effective 3rd dimension. Materials currently in use today are, in effect, just two-dimensional materials, having length and width only. By adding a height component of sufficient rigidity or tensile capacity, this author believes that considerable passive forces could be mobilized in the reinforced soils. Depending on the final analyses, this dimension might possibly be as small as 1/8 inch on either side of the horizontal plane. Utilization of such elements could more than compensate for the reduction in resistance due to decreased effective friction angle. However, as the required vertical dimensions increase, the manufacture, transport and installation of such materials would become increasingly difficult.

CHAPTER 5

EFFECTS OF LATERAL SWELL PRESSURE ON CALCULATED FACTORS OF SAFETY

5.1 Introduction

As costs for the importation of granular backfill materials continues to increase due to depletion of these materials in certain areas, and to the ever-increasing costs for material transportation, appropriate design methodologies for using on-site materials, cohesive or otherwise, are required to investigate the most economical retaining structure design considering all cost factors, including wall and backfill materials, and construction scheduling-related cost. This chapter explores the analysis and determination of the magnitude of lateral swelling forces that must be incorporated in retaining structure design when cohesive backfill materials are considered as backfill materials.

5.2 Lateral Swell Pressure Effects on External Stability Calculations

Depending on the moisture condition and compaction of the backfill soils, the lateral swell pressures developed by hydrating expansive soils can vary greatly. Close scrutiny of the large scale and pilot scale studies available for analysis reveals that the moisture conditions of the backfill and restrained soils were either dry or near the Proctor optimum moisture content. The data developed from these previous studies indicates that very large lateral swell pressures are generated when compacted expansive soils hydrate.

These pressures, as presented and considered in lateral earth pressure distribution calculations, exceed the combined pressures exerted by the active soil and the hydrostatic pressure. This condition worsens with depth and surcharge pressure.

However, knowing that increased moisture conditions decrease the magnitude of potential lateral swell pressure, and that even very small structure deflections will result in a greatly reduced sustained applied lateral swell pressure, it is conceivable that prudently conservative retaining structure designs may be developed using expansive cohesive backfill materials, provided that these materials are placed at sufficiently high moisture contents and proper compaction levels. This current research suggests that moisture contents from 2 to 10 percent above optimum moisture content, depending on bulk soil characteristics, and compaction levels between 93 and 98 percent of Standard Proctor will limit lateral swell pressure development to less than 100 psf at 5-foot depth and an additional 40 psf per foot of depth below 5-foot depth. Calculations similar to those in Chapter 4, but including lateral swell pressures as noted, are given below. The lateral swell pressure distribution shown in Figure 3.26 is repeated as Figure 5.1; and the geometry shown in Figure 4.9 and utilized in the foregoing analyses is also repeated as Figure 5.2 for convenience. Table 4.1 defines the various soil and geometric parameters.

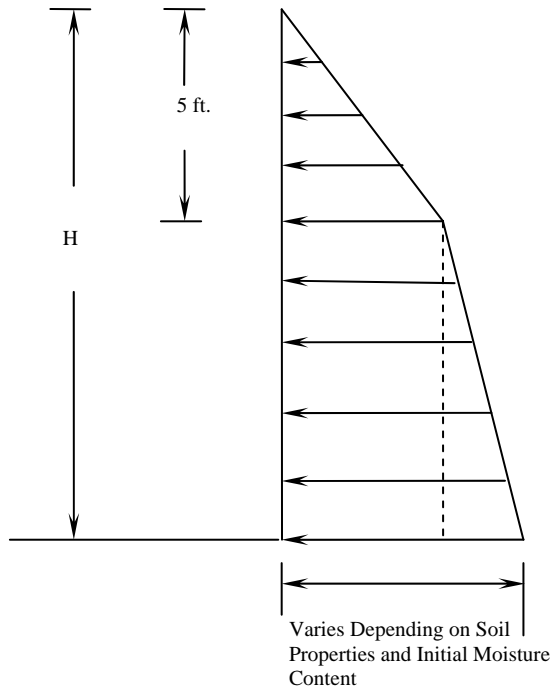


Figure 5.1 – Interpreted Lateral Swell Pressure Distribution

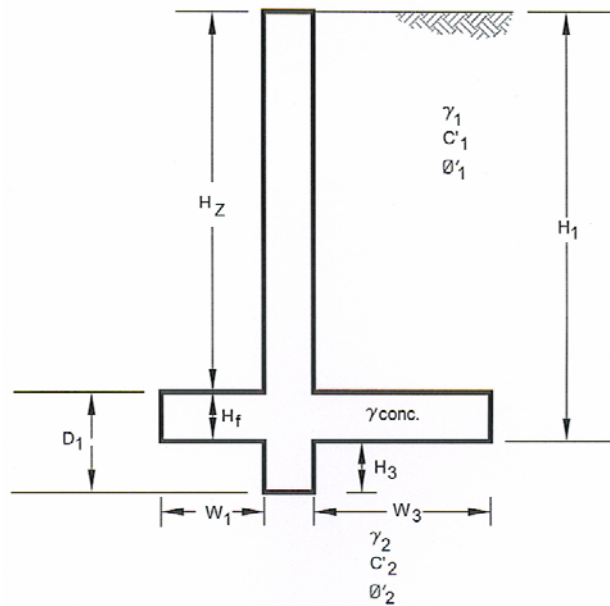


Figure 5.2 – Generalized Retaining Structure Geometry

Example 5.1 - 15- Foot Wall Facing with Lateral Swell Pressure, Moderate Water Table and 4-foot Keyway

1	62.4	pcf	K _a	0.472		H _z	15.0	ft
γ ₁	114	pcf	K _p	2.371		H _f	2.0	ft
γ ₂	120	pcf	Z _c	5.34	ft	W ₁	4.0	ft
γ _{conc}	150	pcf	H ₁	17	ft	W ₂	1.5	ft
C' ₁	209	psf	H ₂	11.66	ft	W ₃	15.0	ft
C' ₂	200	psf	P _{soil}	915.4	psf	D ₁	6.0	ft
φ' ₁	21	deg	P _{cohesion}	287.3	psf			
φ' ₂	24	deg	P _{net}	628.1	psf			

			Moment		
<u>Item</u>	<u>Area</u>	<u>γ</u>	<u>Force</u>	<u>Arm</u>	<u>Moment</u>
P _a			3,663.62	3.89	14,245
P _w		62.4	1,061.36	1.94	2,063
P _{lat sw}			8,126.3	5.31	43,151
Total Driving		ΣF _{horiz}	12,851.28	ΣM _{drive}	59,459
A ₁	225	114	25,650.00	13.00	333,450
A ₂	22.5	150	3,375.00	4.75	16,031
A ₃	41	150	6,150.00	10.25	63,038
P _p			8,817.43		
Total Resisting		ΣF _{vert}	43,992.43	ΣM _{resist}	412,519

OVERTURNING

$$FS = \frac{\Sigma M_{resist}}{\Sigma M_{drive}} = 6.94$$

SLIDING

$$FS = \frac{\Sigma F_{vert}}{\Sigma F_{horiz}} = 2.04$$

Following the above calculations, Table 5.1 presents the computed Factors of Safety for the same range of wall / footing geometries and soil conditions analyzed in Chapter 4. The following computations assume a mid-height water level and a 4-foot

deep keyway below the base of the footing as described in Chapter 4. These data are shown graphically in Figure 5.3.

Table 5.1 - Factors of Safety vs. Wall Height and Footing Heel Width (Assumes Mid-height Water Level, 4-foot Deep Keyway and 100psf/40psf Lateral Swell Pressure)

H _z , ft.	W ₃ = 7.5 ft.		W ₃ = 15 ft.		W ₃ = 22.5 ft.		W ₃ = 30 ft.	
	FS _{OT}	FS _{SL}	FS _{OT}	FS _{SL}	FS _{OT}	FS _{SL}	FS _{OT}	FS _{SL}
10	6.80	2.99	>17	3.74	>32	4.49	>53	>5
15	2.69	1.57	6.93	2.04	>13	2.51	>21	2.98
20	1.41	<1.0	3.64	1.29	6.86	1.62	>11	1.94
25	<0.9	<0.7	2.25	<1.0	4.24	1.17	6.85	1.42
30	<0.6	<0.5	1.53	<0.7	2.89	<1.0	4.66	1.11
35	<0.5	<0.5	1.11	<0.6	2.10	<0.8	3.39	<0.9
40	<0.4	<0.4	<0.9	<0.5	1.59	<0.7	2.57	<0.8

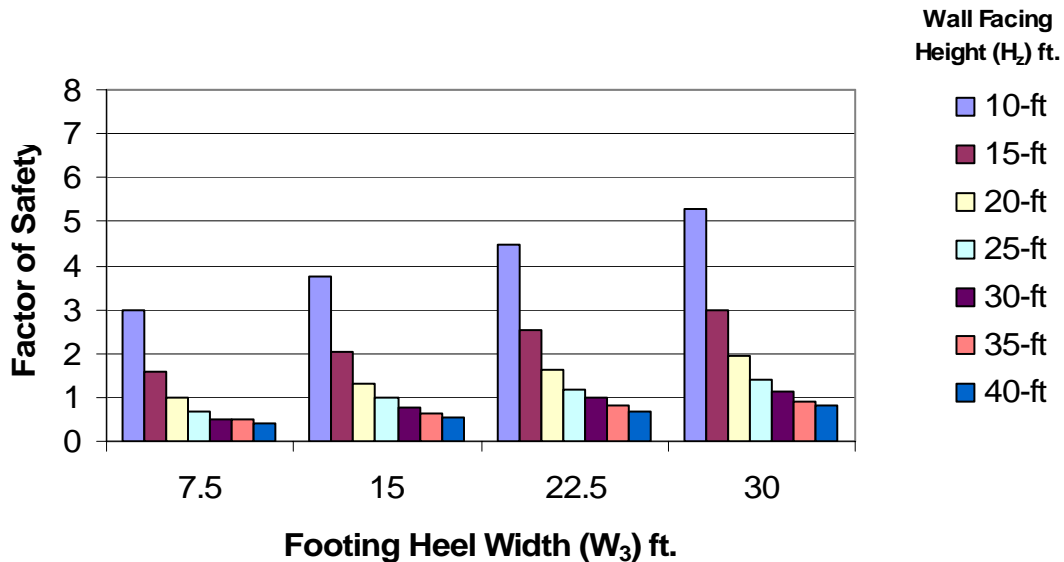


Figure 5.3 –Factors of Safety With Respect to Sliding Using a Keyway, Assuming a Moderate Water Table and Lateral Swell Pressure (Based on Data From Table 5.1)

The considerable reduction in FS for both overturning and sliding when lateral swell pressures are considered can be seen by comparing Figures 4.12 and 5.3. This reduction is illustrated in Figure 5.4 for a 25-foot tall wall. It should be noted that the Factor of Safety for sliding in each case incorporates the effects of a 4-foot deep keyway below the base of the 2-foot thick footing and a lowered permanent groundwater level.

Improvement in the sliding Factor of Safety can be accomplished by replacing the onsite clay subgrade material on which the wall footing and keyway is constructed with a coarse granular material with an effective angle of friction ϕ' of at least 34° . For the conditions illustrated in Example 5.1, the Factor of Safety with respect to sliding increases to 2.42. For the range of geometries investigated, the improvement increase varies from about 10 to 35 percent.

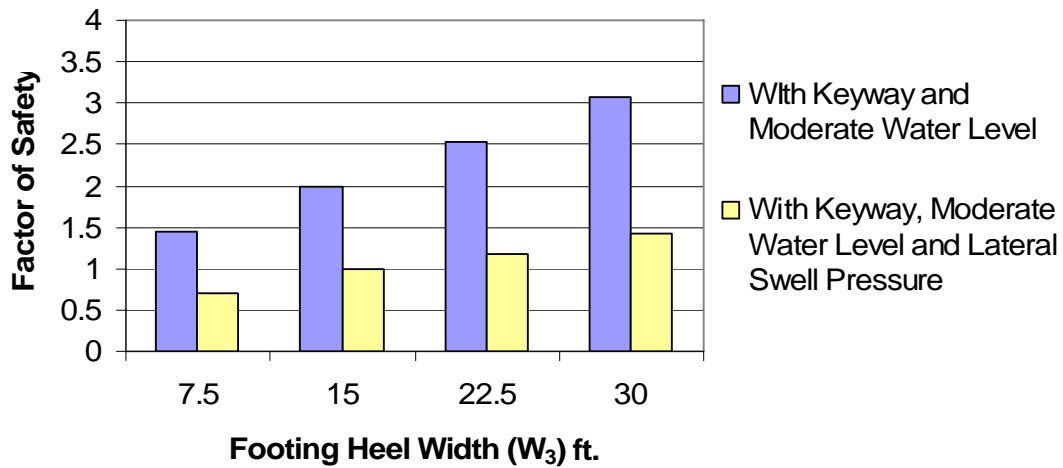


Figure 5.4 – Comparison of Factors of Safety With Respect to Sliding for a 25-foot Tall Wall (Based on Data From Tables 4.3 and 5.1)

As wall heights increase, it can be seen that even with the placement of a basal coarse granular material beneath a rigid wall footing and into which a significant keyway is constructed, the potential for lateral swell pressure generation becomes increasingly difficult to accommodate economically. It should be noted that the preceding calculations assume a “mid-height” groundwater level condition. This is assumed to be a reasonable, but conservative estimate, though in some instances this assumption may exceed reasonably possible worst-case estimates.

The magnitude of potential lateral swell pressure generation incorporated into the above analyses may prove to be excessive for the prudent placement requirements that will likely be specified when using expansive cohesive backfill materials. In other words, at the placement conditions required to minimize potential post-construction soil movements, the potential lateral swell pressure increases may be less than those assumed. Further, slight amounts of allowed wall deflections may reduce these potential lateral

swell pressures to levels much below those assumed. Table 5.2 illustrates the effects on sliding Factors of Safety based on the magnitude of lateral swell pressure development for the given wall geometries and soil parameters considered heretofore. The lateral swell pressures considered include 100, 75 and 45 psf per foot to 5-foot depth with increases of 40, 30 and 18 psf per foot, respectively below 5-foot depth. The computed Factors of Safety tabulated below may be increased by increasing the depth of the keyway, improving the foundation subgrade soils, preventing hydrostatic buildup, or other means.

Table 5.2 - Factors of Safety With Respect to Sliding for Differing Magnitudes of Lateral Swell Pressure Development (Assumes Mid-height Water Level and Keyway)

H _z , ft.	W ₃ = 7.5 ft.			W ₃ = 15 ft.			W ₃ = 22.5 ft.			W ₃ = 30 ft.		
	100/ 40	75/ 30	45/ 18	100/ 40	75/ 30	45/ 18	100/ 40	75/ 30	45/ 18	100/ 40	75/ 30	45/ 18
10	2.99	3.37	4.05	3.74	4.22	>5	4.49	>5	>6	>5	>5	>7
15	1.57	1.80	2.22	2.04	2.34	2.88	2.51	2.87	3.54	2.98	3.41	4.21
20	<1.0	1.10	1.35	1.29	1.48	1.80	1.62	1.85	2.26	1.94	2.22	2.72
25	<0.7	<0.8	<1.0	<1.0	1.05	1.27	1.17	1.33	1.61	1.42	1.61	1.96
30	<0.5	<0.6	<0.7	<0.7	<0.8	<1.0	<1.0	1.03	1.23	1.11	1.25	1.51
35	<0.5	<0.5	<0.6	<0.6	<0.7	<0.8	<0.8	<0.9	<1.0	<0.9	1.02	1.22
40	<0.4	<0.4	<0.5	<0.5	<0.6	<0.7	<0.7	<0.7	<0.9	<0.8	<0.9	1.02

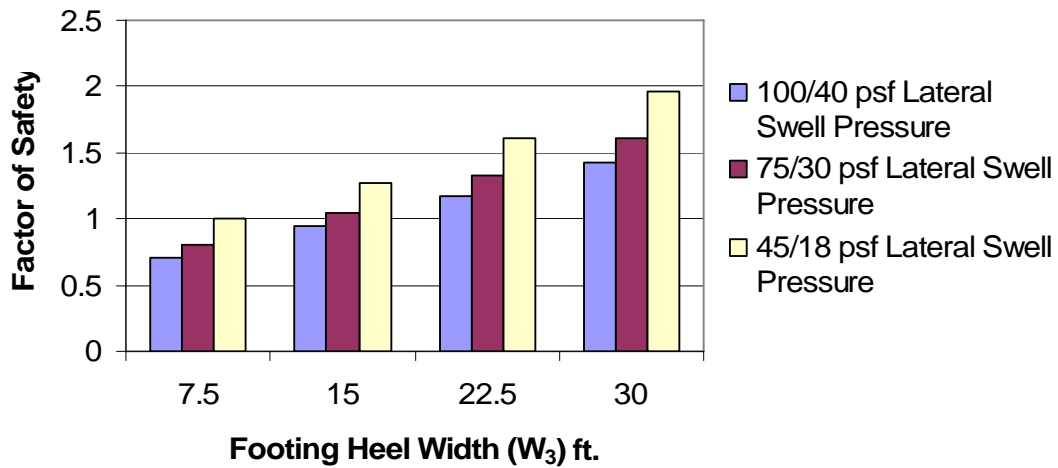


Figure 5.5 – Comparison of Factors of Safety With Respect to Sliding for a 25-foot Tall Wall (Based on Data From Table 5.2)

The above calculations, suggest that rigid retaining structures may indeed be designed using expansive cohesive backfill materials, provided that these materials are placed in such a manner so as to minimize their potential for lateral swell pressure generation. The data indicate that for walls in excess of 30 feet in height using expansive cohesive backfill, additional stabilizing measures noted earlier will need to be incorporated into the design and construction.

To insure the long-term integrity of the structures, precautions must be implemented to prevent the backfill materials from future drying that would result in subsequent increased potential lateral swell pressure development.

5.3 Local Case Study

To illustrate the impact of lateral swell pressure development on an MSE wall, the following background and assumptions, together with computations based on the previously illustrated format, are provided.

An MSE wall constructed along a portion of State Highway 360 in Arlington, Texas failed recently (Figure 5.6).



**Figure 5.6 – Local MSE Wall Failure Due to Sliding
(photograph courtesy of Paul Spraggins, PE, TxDOT Central)**

This failure is believed by some to be due to sliding as a result of lateral swell pressure development in the retained fill that was transmitted through the reinforced section to the wall facing. Prior to photographic availability, wall facing height was estimated to be 20 feet. A 2-foot embedment was assumed in accordance with the widely accepted Texas Department of Transportation (TxDOT), Federal Highway Administration (FHWA) and/or American Association of State Highway Transportation Officials (AASHTO) design guidelines. It was further assumed that the original design included a Factor of

Safety against sliding of about 1.5. Backfill for the reinforced section was assumed to conform to TxDOT minimum effective angle of internal friction equal to 34 degrees, and the reinforced width (W) was assumed to be equal to 0.7H, in accordance with the above guidelines.

Factor of Safety computations based on the assumptions noted and on the simplified geometry shown in Figure 5.7 is presented as Example 5.2.

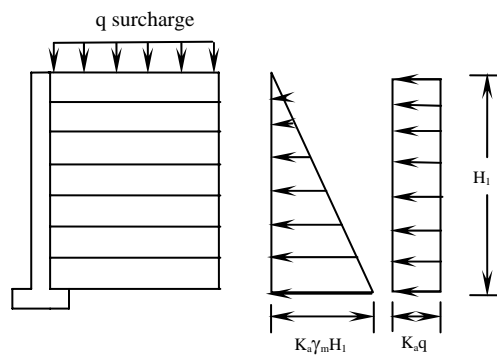


Figure 5.7 – Lateral Earth Pressure on MSE Wall

Example 5.2 – 20-foot MSE Wall Facing w/o Surcharge or Lateral Swell Pressure

γ_{water}	62.4	pcf	K_a	0.283		H_z	20.0	ft
γ_1	130	pcf	K_p	2.371		H_f	2.0	ft
γ_2	120	pcf	Z_c	0.00	ft	W_1	0.0	ft
γ_{conc}	150	pcf	H_1	22	ft	W_2	0.0	ft
C'_1	0	psf	H_2	22.00	ft	W_3	15.4	ft
C'_2	200	psf	P_{soil}	808.6	psf	D_1	2.0	ft
ϕ'_1	34	deg	P_{cohesion}	0.0	psf			
ϕ'_2	24	deg	P_{net}	808.6	psf			

			Moment		
<u>Item</u>	<u>Area</u>	γ	<u>Force</u>	<u>Arm</u>	<u>Moment</u>
P_a			8,894.21	7.33	65,224
q			0.00	0.00	0
$P_{\text{lat sw}}$			0.00	8.36	0
Total Driving		ΣF_{horiz}	8,894.21	ΣM_{drive}	65,224
A_1	308	130	40,040.00	7.70	308,308
A_2	0	150	0.00	0.00	0
A_3	0	150	0.00	7.70	0
P_p			0.00		
Total Resisting		ΣF_{vert}	40,040.00	ΣM_{resist}	308,308

OVERTURNING

$$FS = \frac{\Sigma M_{\text{resist}}}{\Sigma M_{\text{drive}}} = 4.73$$

SLIDING

$$FS = \frac{\Sigma F_{\text{vert}}}{\Sigma F_{\text{horiz}}} = 1.72$$

Without accounting for traffic or backslope surcharge, the Factor of safety against sliding is found to be about 1.72. It should be noted that in this area of North Texas, the foundation soils are residual clays or weathered shales of the Woodbine Formation. As such, an effective angle of internal friction of 24 degrees is considered appropriate for these materials.

When a nominal surcharge (q) of 250 psf is included in the calculations, the computed Factor of Safety is reduced to about the minimum value required for long-term situations as shown in Example 5.3.

Example 5.3 – 20-foot MSE Wall Facing w/Surcharge, w/o Lateral Swell Pressure

γ_{water}	62.4	pcf	K_a	0.283		H_z	20.0	Ft
γ_1	130	pcf	K_p	2.371		H_f	2.0	Ft
γ_2	120	pcf	Z_c	0.00	ft	W_1	0.0	Ft
γ_{conc}	150	pcf	H_1	22	ft	W_2	0.0	Ft
C'_1	0	psf	H_2	22.00	ft	W_3	15.4	Ft
C'_2	200	psf	P_{soil}	808.6	psf	D_1	2.0	Ft
ϕ'_1	34	deg	P_{cohesion}	0.0	psf			
ϕ'_2	24	deg	P_{net}	808.6	psf			

		Moment			
<u>Item</u>	<u>Area</u>	γ	<u>Force</u>	<u>Arm</u>	<u>Moment</u>
P_a			8,894.21	7.33	65,224
q			1,554.93	0.00	17,104
$P_{\text{lat sw}}$			0.00	8.36	0
Total Driving		ΣF_{horiz}	10,449.14	ΣM_{drive}	65,224
A_1	308	130	40,040.00	7.70	308,308
A_2	0	150	0.00	0.00	0
A_3	0	150	0.00	7.70	0
P_p			0.00		
Total Resisting		ΣF_{vert}	40,040.00	ΣM_{resist}	308,308

OVERTURNING

$$FS = \frac{\Sigma M_{\text{resist}}}{\Sigma M_{\text{drive}}} = 3.74$$

SLIDING

$$FS = \frac{\Sigma F_{\text{vert}}}{\Sigma F_{\text{horiz}}} = 1.47$$

When lateral swell pressures are considered, the Factors of Safety against sliding reduce rapidly to values of 1 and below. Example 5.4 illustrates the case for a processed and moisture-conditioned material having a lateral swell potential of about 100 psf per foot to 5-foot depth and about 40 psf below that depth (see Chapters 3 and 5). As described by Katti et al., (1983), the presence of non-expansive fill materials between the wall face and the expansive retained soil will reduce the applied lateral pressures considerably. Despite this reduction, most, if not all retained expansive soils will not be processed during or after construction. Therefore the actual swell potential to be considered in the field will likely be greater than 100/40 psf. Example 5.4 assumes a 70% reduction in applied lateral swell pressure.

Example 5.4 – 20-foot MSE Wall Facing w/Surcharge, and Lateral Swell Pressure

γ_{water}	62.4	pcf	K_a	0.283		H_z	20.0	ft
γ_1	130	pcf	K_p	2.371		H_f	2.0	ft
γ_2	120	pcf	Z_c	0.00	ft	W_1	0.0	ft
γ_{conc}	150	pcf	H_1	22	ft	W_2	0.0	ft
C'_1	0	psf	H_2	22.00	ft	W_3	15.4	ft
C'_2	200	psf	P_{soil}	808.6	psf	D_1	2.0	ft
ϕ'_1	34	deg	P_{cohesion}	0.0	psf			
ϕ'_2	24	deg	P_{net}	808.6	psf			

		Moment			
<u>Item</u>	<u>Area</u>	γ	<u>Force</u>	<u>Arm</u>	<u>Moment</u>
P_a			8,894.21	7.33	65,224
q			1,554.93	11.00	17,104
$P_{\text{lat sw}}$			<u>4,593.00</u>	8.36	<u>38,397</u>
Total Driving		ΣF_{horiz}	15,042.14	ΣM_{drive}	120,726

A ₁	308	130	40,040.00	7.70	308,308
A ₂	0	150	0.00	0.00	0
A ₃	0	150	0.00	7.70	0
P _p			0.00		
Total Resisting		ΣF _{vert}	40,040.00	ΣM _{resist}	308,308

OVERTURNING

$$FS = \frac{\Sigma M_{resist}}{\Sigma M_{drive}} = 2.55$$

SLIDING

$$FS = \frac{\Sigma F_{vert}}{\Sigma F_{horiz}} = 1.02$$

CHAPTER 6

FINDINGS AND CONCLUSIONS

It is clear from the foregoing presentation that a clear and reliable method for estimating lateral swell pressure induced by use of cohesive backfill materials behind retaining structures is not yet available. However, it should also be clear that in order to produce an economical wall design when using these backfill materials, the potential lateral swell pressure generation should be limited to less than 100 psf per foot to 5-foot depth with less than 40 psf per foot increase below that depth for walls a maximum of 15 feet tall. For walls taller than 15 feet, the analyses indicate that lateral swell pressure generation should be limited to much less than the 100 psf / 40 psf considered above.

The analyses of the previous research and contained in this work suggests that the above lateral swell pressure values may be achievable using some combination of increased placement moisture content, reduced placement density and permitting small outward structure deflections to occur. The analyses further suggest that the relatively new, but sophisticated, 3-dimensional laboratory testing techniques now available are quite capable of providing quality lateral swell pressure data for use in future prediction research. These testing protocols should be able to be appropriately modified to investigate the effects of surcharge loading and changing soil suction potential.

Correlation of lateral swell pressure generation with a given suction decrease should greatly facilitate the development of a practical method for estimating lateral swell

pressure potential for cohesive soils based on readily obtainable bulk soil properties (PI, minus 200 sieve, moisture content and clay fraction). A detailed program for future research into this topic is provided in the next Chapter. The anticipated implication to the goal of lateral swell pressure estimation for each respective step in the investigative process is also included.

CHAPTER 7

RECOMMENDATIONS FOR FUTURE RESEARCH

To further the development of a prudent methodology for design of retaining structures using cohesive backfill, the following itemized program is suggested for future lines of research. As a beginning, these items should be addressed individually to develop the correlations (if they exist) unique to each. As the research becomes more sophisticated, two or more aspects should be combined to examine the gross effects of the combined forces in action. The ultimate effort should be to simulate realistic and likely field conditions including as many of these variables as possible.

1. Develop a database of sufficient size based on the experimental results of tests performed on a variety of materials using triaxial testing equipment, or appropriately modified apparatus, capable of measuring the 3-dimensional lateral and axial components of stress and strain in response to a decrease in soil suction potential (increasing moisture content). This database should include a wide variety of naturally occurring soils, blends of soils and artificial soils. The purpose of blended soils is to simulate the actual conditions that often occur on large-scale construction projects, where several subsurface strata are simultaneously excavated and randomly mixed prior to placement as fill.

In addition to the components of stress and strain, the collected data should include normal soil index properties (Atterberg Limits, percent passing a No. 200 sieve and clay fraction), bulk mineralogy, optimum moisture and density relationships (Standard Proctor data), initial and final moisture contents, and initial and final soil suction potentials.

If a reliable correlation between a given suction change to an applied lateral swell pressure proves to be evident, then a powerful predictive tool is available to estimate lateral swell pressure based on simple tests that are routinely conducted. For instance, if it turns out that, regardless of soil type, a suction change from 2,000 kPa to 1,500 kPa always yields a lateral swell pressure of around 5 kPa per foot to 5-foot depth and an additional 2 kPa per additional foot of depth for a given compaction effort and surcharge loading condition, then one should be able to determine the moisture content required to achieve a suction value of 2,000 (or lower) based on the measured bulk physical properties noted, since suction potential is integrally related to those properties and to the moisture content of the sample. An example is illustrated below:

Given: a soil consisting of 70% clay fraction smectite clay with a LL = 105, PI = 67 and 93% material passing a No. 200 sieve. This material may require a moisture content of 50% to achieve a soil suction of 2,000 kPa; whereas a soil consisting of 12% smectite and 68% illite with a LL = 62, PI = 38 and 98% passing a No. 200 sieve may only require a moisture content of 30%, for instance, to achieve the same 2,000 kPa suction desired.

If a correlation does prove to exist, regardless of the threshold number required to limit the magnitude of lateral swell pressure to the values given above, Al-Shamrani and Dhowian (2003) indicate a lower bound of 800 to 1,500 kPa suction potential for artificially saturated soils. It would seem reasonable to expect a lower bound of 1,500 kPa for naturally occurring conditions.

2. Once a database has been developed, or concurrently with its development, Additional laboratory studies should be conducted (3-dimensional) investigating the effects of varying compaction efforts. The data developed during the previous cited research indicates higher developed lateral swell pressures for well-compacted clays placed near the optimum moisture content.

If a “threshold” suction value exists, the moisture content required to achieve that value may be such that the materials would be untrafficable to construction workers and equipment. Evaluating lower compaction densities with simultaneous moisture content reductions may yield an acceptable moisture-density range for limiting lateral swell pressure to design requirements.

3. The insertion of some thickness of non-expansive soil between the structure and the cohesive, expansive backfill appears to greatly reduce the magnitude of lateral swell pressures actually transmitted to the structure(s). Further instrumented laboratory and/or field studies using different “widths” of such non-expansive backfill retaining structures and incorporating more modern “set-ups” and instrumentation are necessary to confirm optimum “widths” and the magnitude of lateral swell pressure reduction. Analyses of said pressure

reductions as functions of depth and/or structure height are also considered necessary.

Though non-expansive materials would likely need to be imported from off-site, the potential to utilize at least some on-site materials would likely be very appealing economically on many projects.

Further, use of a sufficient “width” of non-expansive granular material may provide the additional benefit of eliminating or greatly reducing the hydrostatic pressure applied to the wall. As shown in the external stability calculations in Chapter 4, groundwater (and the associated lateral pressures) was assumed to exist up to the level of potential tension crack development. Should it prove true that hydrostatic pressures are largely reduced through use of some small width of granular material, it may be found that some additional lateral swell pressures could then be accommodated in the design. These increased pressures could arise from a reduction in placement moisture content of the backfill, less allowable wall yielding, greater allowable surcharge and/or other factor(s).

4. The analyses included in this work were limited to conditions of no significant external surcharges in proximity to the retaining structure. The previous research indicates that with increasing surcharge, the resulting lateral swell pressures increase rapidly to well in excess of values calculated by traditional methods.

Further research into this area is warranted to evaluate this phenomenon; first in the laboratory, then possibly in field or large-scale studies. It may prove

that, despite the implementation of efforts to minimize the development of lateral swell pressure as noted in Nos. 1–3 above, surcharge effects would outweigh or overwhelm (for very tall retaining structures) those efforts and render an economical design impractical.

5. Related to Number 4 above, a revised sensitivity analysis of the effect of wall height on external stability Factors of Safety, based on the information developed from the new database would be prudent.
6. Detailed analyses of internal wall stability for MSE walls using cohesive backfill are required. Utilization of modified reinforcement elements as indicated earlier may prove to more than offset the lost resistance resulting from the lower friction angle of cohesive materials compared to those granular materials.
7. Integral to the successful implementation of expansive cohesive backfill behind retaining structures is the long-term maintenance of the installation soil moisture content. Cyclic tests simulating alternating wetting and drying of expansive backfill materials would be invaluable in demonstrating some of the suspected detrimental effects that could arise after properly placed materials are allowed to dry, such as soil shrinkage and possible later development of excessive lateral swell pressures.

Moisture maintenance measures could include covering the top of the backfill surface with some type of geomembrane or poly sheeting, or spraying with an asphaltic emulsion or “tack coat”. For the vertical portions of backfill immediately behind MSE wall facing elements, however, “waterproofing” measures are not viable since any groundwater that may enter the backfill needs

to be able to drain through the backfill (albeit very slowly) at the wall facing. One possibility might be to have some small thickness of granular material between the wall and the backfill, separated with an appropriate geotextile filter fabric.

8. Previous research indicates that when small strains (deflections) are allowed, peak lateral swell pressures dissipate rapidly to sustained values that are a small fraction of the peak magnitude. Further instrumented large-scale laboratory and/or field studies investigating the magnitude of pressure reduction are vital to the completion of reasonable methodologies for structure design when using expansive cohesive backfill materials. This is especially true for MSE walls, where a certain amount of yielding is required to mobilize the internal tensile strength of the reinforcing elements.

REFERENCES

1. Aitchison, G. D., 1965, "Moisture Equilibria and Moisture Changes in Soils beneath Covered Areas," *Australia: Butterworths*, 278 pp.
2. Al-Shamrani, M. A. and Dhowian, A. W., 2003, "Experimental Study of Lateral Restraint Effect on The Potential Heave of Expansive Soils," *Engineering Geology*, Vol. 69, 63-81 pp.
3. Al-Shamrani, M.A., 2004, "Influence of Lateral Restraint on the Swelling Behavior of Expansive Soils," *Geotechnical Engineering*, Vol. 35, No. 3, 101-111 pp.
4. ASTM D 2487, 2004, *Annual Book of ASTM Standards*, Section 4, Construction Vol. 4.08 Soil and Rock, American Society of Testing and Materials, Philadelphia, PA.
5. Atterberg, A., 1911, "The Behavior of Clays with Water, their Limits of Plasticity and their Degrees of Plasticity." *Kungliga Lantbruksakademiens Handlingar och tidskrift*, Vol. 50, No. 2, 132-158 pp
6. Aytekin, M., 1992, "Finite element modeling of lateral swelling pressure distributions behind earth retaining structures," *Doctoral Dissertation*, Texas Tech University, Lubbock, Texas
7. Aytekin, M., Wray, W. K.; Vallabhan, C. V. G., 1992, "Transmitted Swelling Pressures on Retaining Structures," 9th *International Conference on Expansive Soils*, Dallas, Texas, 32-43 pp.
8. Bishop, A. W., and Henkel, D.J., 1962, "The measurement of soil properties in the triaxial test", *Edward Arnold Ltd. London, United Kingdom*.
9. Black, W. P. M. and Lister, N. W., 1979, "The Strength of Clay Fill Subgrades: Its Prediction and Relation to Road Performance," *Proceedings, Institution of Civil Engineers Conference on Clay Fills*, London, 37-48, pp.
10. Brooker, E. W. and Ireland, H. O., 1965, "Earth Pressures at Rest Related to Stress History," *Canadian Geotechnical Journal*, Vol. 2, No. 1, 1-15 pp.

11. Caquot, A. and Kerisel, J., 1948, *Tables for the calculation of Passive Pressure, Active pressure and bearing capacity of Foundations*, Gauthier-Villars, Paris
12. Carder, D. R., 1988, "Earth Pressures on Retaining Walls and Abutments". *Informal discussion, British Geotechnical Society, Institution of Civil Engineers, London England.*
13. Casagrande, A. 1932, "Research on the Atterberg Limits of Soils." *Public Roads*, Vol. 13, No. 8, 121-136 pp.
14. Casagrande, A., 1958, "Notes on the Design of the Liquid Limit Device." *Geotechnique*, Vol. VIII, No. 2, 84-91 pp.
15. Chen, F. H., 1975, *Foundations of Expansive Soils. Development in Geotechnical Engineering* 12, Elsevier Scientific Publishing Co., New York, 280 pp.
16. Chen, F. H., 1988, "Foundations on Expansive Soils", *2nd Edition*, Amsterdam: Elsevier, 463 pp.
17. Clayton, C. R. I., Symons, I. F., and Hiedra-Coco, J. C. 1991, "*Pressure of Clay Backfill against Retaining Structures*," *Canadian Geotechnical Journal*, Vol. 28, No. 2, 282-297 pp.
18. Coulomb, C. A., 1776, Essai sur une application des règles de maximis et Minimis à quelques problèmes de statique, relatifs à l'architecture. *Mémoires de Mathématique et de Physique présentés à l'Académie Royale des Sciences*, Paris, Vol.7, 343-382 pp.
20. Crilly, M. S., Driscoll, R. M., and Chandler, R. J., 1992, "Seasonal ground and water movement observations from an expansive clay site in the UK." *Proceedings, 7th International Conference on Expansive Soils*, Dallas, Texas, USA, 313-318 pp.
21. Cronney, D. and Coleman, J. D., 1948, "Soil structure in relation to soil suction (pF)," *Journal of Soil Science*, Vol. 5, No. 1, 75-84 pp.
22. Das, 2004, *Principles of Foundation Engineering*, 5th Ed., Brooks/Cole - Thomson Learning, Pacific Grove, CA, USA, 743 pp.
23. Das, B. M., 2002, *Principles of Geotechnical Engineering*. Thomson Learning Inc., South Bank, Victoria, Australia, 589 pp.

24. Dhawan, P. K., Mathur, R., and Lal, N. B., 1982, "Effect of Lateral Confinement on Swell Pressure in Expansive Soil," *Highway Research Bulletin, New Delhi*, No. 17, 49-60, pp.
25. Edil, T. B. and Alanazy, A. S., 1992, "Lateral Swelling Pressures", *Proceedings 7th International Conference on Expansive Soils*, Dallas, Texas, 227-232 pp.
26. Edlefsen, N. E. and Anderson, A. B. C., 1943, "Thermodynamics of Soil Moisture", *Hilgardia*, Vol. 15, 31-298 pp.
27. Erol, A. O., Dhowian A., and Youssef, A., 1987, "Assessment of Oedometer Methods for Heave Prediction", *Proceedings 6th International Conference on Expansive Soils*, New Delhi, India, 99-103 pp.
28. FHWA, 1997, "Earth Retaining Structures," *Geotechnical Engineering Circular No. 2, Publication No. FHWA-SA-96038*.
29. Fourie, A. B., 1989, "Laboratory Evaluation of Lateral Swelling Pressure," *Journal of Geotechnical Engineering*, Vol. 115, No. 10, 1481-1486 pp.
30. Fredlund, D. G. and Rahardjo, H., 1993, *Soil Mechanics for Unsaturated Soils*. John Wiley & Sons, Inc., New York, 517 pp.
31. Holtz, R. D. and Kovacs, W. D. 1981, *An Introduction to Geotechnical Engineering*. Prentice Hall, Upper Saddle River, New Jersey, 733 pp.
32. Hurlbut, C. S. Jr., and Klein, C, 1982, "Manual of Mineralogy", 19th ed., John Wiley & Sons, Inc., New York, 733 pp.
33. Jaky, J., 1944, "The Coefficient of Earth Pressure at Rest", *Journal for the Society of Hungarian Architects and Engineers*, Vol. 78, No. 22, 355-358 pp.
34. Kate, J. M. and Katti, R. K. 1980, "Effects of cohesive nonswelling soil layer on The behavior of underlying expansive soil media-An experimental study," *Indian Geotechnical Journal*, Vol. 10, No. 4, 281-305 pp.
35. Kate, J. M. and Katti, R. K., 1975, "Role of microparticles in interaction between cohesive nonswelling soil layer and underlying expansive soil media," *Proceedings of the Fifth Asian Regional Conference on Soil mechanics and Foundation Engineering*, Bangalore, Pakistan, Vol. 1, 15-18 pp.
36. Kate, J. M. and Katti, R. K., 1981, "Experimental studies on the combined effects of cohesive non-swelling soil layer and surcharge load on the behavior of underlying expansive soil," *Indian Geotechnical Journal*, Vol. 11, No. 2, 153-176 pp.

37. Katti, R. K. and Kulkarni, S.K., 1967, "Studies on nonswelling soil layer as a means to resist swelling pressure of expansive soil system," *Proceedings of South East Asian Regional Conference on Soil Engineering*, Bangkok, Thailand, 147-157 pp.
38. Katti, R. K., Bhangale, E. S., and Moza, K. K., 1982, "Lateral pressure in Expansive soil with and without a cohesive non-swelling soil layer, Application to earth pressures on cross drainage structures in canals and key walls in dams", *Final Report Part-I, Submitted to Central Board of Irrigation and Power*, New Delhi, Vol. 110, No. 21, 1-303 pp.
39. Katti, R. K., Bhangale, E. S., and Moza, K. K., 1982, "Lateral pressure of expansive soil with and without a cohesive non-swelling soil layer, Applications to earth pressures of cross drainage structures of canals and key walls in dams," *Final Report Part-I Submitted to Central Board of Irrigation and Power*, New Delhi, Vol. 110, No. 21, 1-303 pp.
40. Katti, R. K., Kulkarni U. V., Bhangale, E. E., and Divshikar, D. G., 1980, "Shear strength development in expansive black cotton soil media with and without a cohesive non-swelling soil surcharge, Application to stability of canals in cuts and embankments," *Technical Report No. 28, Central Board of Irrigation and Power*, New Delhi, 142 pp.
41. Katti, R. K., Kulkarni, S. K., and Kate, J. M., 1969a, "Experimental investigation on cohesive non-swelling soil layer as an intercepting media for footing on expansive soil," *Proceedings of the Second International Research and Engineering Conference on Expansive Clay Soils*, College Station, Texas, 327-333 pp.
42. Kormornik, A. and Zeitlen J. G., 1965, "An Apparatus for Measuring Lateral Soil Swelling Pressure in the Laboratory," *Proceedings of the 6th International Conference on Soil Mechanics and Foundation Engineering*, Vol. 1, Toronto, 278-281 pp.
43. Lal, N. B. and Palit, R. M., 1969, "A New Dimension to the Measurement of Swell Pressure in Expansive Soils," *Proc. Of Symposium on "Characteristics of and Construction Techniques in Black Cotton Soil"* held at College of Military Engg. Poona.
44. Marsh, E. T. and Walsh, R. K. 1996, "Common Causes of retaining-Wall Distress: Case Study," *Journal of Performance of Constructed Facilities*, 35-38 pp.

45. Mayne, P. W. and Kulhawy, F. H., 1982, "K₀-OCR Relationships in Soil," *Journal of the Geotechnical Engineering Division, ASCE*, Vol. 108, No. GT6, 851-872 pp.
46. McDowell, C, 1956, "Interrelationship of Load, Volume Change, and Layer Thickness of Soils to the Behavior of Engineering Structures," *Highway Research Board, Proceedings of the Thirty Fifth Annual Meetings*, Publication No 426, Transportation Research Board, Washington, D.C., 754-772 pp.
47. McKeen, R. G., 1977, "Characterizing expansive soils for design," Presented at the Joint Meeting of the Texas, New Mexico, and Mexico Sections of the ASCE, Albuquerque, New Mexico, 23 pp.
48. McKeen, R.G., 1980, "A Model for predicting expansive soil behavior," *Proceedings, 7th International Conference on Expansive Soils*, Dallas, Texas, The American Society of Civil Engineers (ASCE), New York, 1-6 pp.
49. Meyerhof, G. G., 1963, "Some Recent Research on the Bearing Capacity of Foundations," *Canadian Geotechnical Journal*, Vol. 1, No. 1, 16-26 pp.
50. Mindlin, R. D., 1936, "Pressure on retaining walls." *Proceedings, 1st International Conference on Soil Mechanics and Foundation Engineering*, Vol. 3, 155-156 pp.
51. Mitchell, J. K., 1993, *Fundamentals of Soil Behavior*, 5th Ed., John Wiley & Sons, Inc., New York
52. Ofer, Z. (1982) "Laboratory K₀ Testing of cohesionless soil," *The Civil Engineer in South Africa*, Vol. 24, No. 10, 533-545 pp.
53. Ofer, Z. and Komornik, A., 1983, "Lateral Swelling Pressure of Compacted Clay", *Proceedings, 7th Asian Regional Conference on Soil Mechanics and Foundation Engineering*, Haifa, Israel, 56-63 pp.
54. Ofer, Z., 1981, "Laboratory Instrument for Measuring Lateral Soil Pressure and Swelling Pressure," *Geotechnical Testing Journal*, Vol. 4, No. 4, 177-182 pp.
55. Rankine, W. M. J., 1857, "On Stability of Loose Earth," *Philosophic Transactions of Royal Society*, London, Part I, 9-27.
56. Richards, B.G., 1977, "Pressures on a Retaining Wall by an Expansive Clay," *Proceedings 9th International Conference on Soil Mechanics and Foundation Engineering*, 705-710 pp.

57. Richards, B.G.; Kurzeme, M., 1973, "Observations of Earth Pressures on a Retaining Wall at Gouger Street Mail exchange, Adelaide," *Australian Geomechanics Journal*, Vol. G3, No. 1, , 21-26 pp.
58. Seed, H. B., Mitchell, J. K., and Chan, C. K., 1961, "Swell Pressure Characteristics of Compacted Clay." *Highway Research Board bulletin 313, National Research Council, Washington, D.C.*, 12-39 pp.
59. Simpson, W. E., 1934, "Foundation experiences with clay in Texas", *Civ. Eng.*, Vol. 4, 581-584 pp.
60. Skempton, A. W., 1953, "The Colloidal Activity of Clays," in *Proceedings of the 3rd International Conference on Soil Mechanics and Foundation Engineering*, Vol. I, Imprimerie Berichthaus Zurich, Zurich, 1953, pp. 57-61.
61. Sridharan, A., Rao, A. S., and Sivapullaiah, P.V, 1986, "Swelling pressure of clays," *Geotechnical Testing Journal*, Vol 9, No. 1, 24-33 pp.
62. Sudhindra and Moza, 1987, cited but not referenced.
63. Wattanasanticharoen, E., Puppala, A. J., and Hoyos, L. R., 2007, Publication Pending, "Evaluations of Heaving Behavior of Expansive Soil Under Anisotropic Stress State Conditions", *Geotechnical Testing Journal*.
64. Guralnik, D. B., ed., Webster's New World Dictionary of the American Language, Second College Edition, 1982, Simon and Schuster, New York, 1728 pp.
65. Windal, T. and Shahrour, I., 2002, "Study of the Swelling Behavior of a Compacted Soil Using flexible Odometer", *Mechanics Research Communications*, Vol. 29, No. 5, 375-382, pp.
66. Xin, J. Z. and Ling, Q. X., 1991, "A New Method for Calculating Lateral Swell Pressure in Expansive Soil", *Proceedings 7th International Conference on Expansive Soils*, Dallas, Texas, Vol. 1, 233-238 pp.
67. Yesil, M. M., Pasamehmetoglu, A. G., and Bozdat T., 1993, "A Triaxial Swelling Test Apparatus," *International Journal of Rock Mechanics, Mining Sciences & Geomechanics Abstracts*, Vol. 30, No. 4, 443-450 pp.

BIOGRAPHICAL SKETCH

Mark Gordon Thomas was born on June 26, 1961 in Oshkosh, Wisconsin, USA. He received a Bachelor of Science Degree in geology (Professional Emphasis, and minoring in chemistry) from the University of Wisconsin – Oshkosh in June 1985. After graduation, he worked for 3-1/2 years as a construction materials testing (CMT) engineering technician at an engineering testing company in Dallas, Texas. For the next 15 years he worked as an engineering geologist, sometimes doubling as a senior CMT inspector / technician, for 2 geotechnical consulting firms, also in Dallas. From June, 2004 to April, 2008 he worked for Fugro Consultants, Inc., Dallas, Texas office as a senior engineering geologist / project manager /geotechnical laboratory manager. He accepted a senior level engineering geology / geotechnical engineering position with PB Americas, Inc., to begin mid-April 2008.

In 2003, with the encouragement from family and friends, he decided to return to school to pursue a Masters Degree in Civil Engineering. In January, 2004 he entered the University of Texas at Arlington and by January, 2005 he had completed the required deficiency classes and entered the Graduate School at the University of Texas at Arlington under the tutelage of Dr. Anand J. Puppala. He received his Masters of Science Degree in Civil Engineering from the University of Texas at Arlington in May, 2008.